EMBRY-RIDDLE
Aeronautical University™
SCHOLARLY COMMONS

Spring 4-2020

Constrained Motion Analysis and Control of Spacecraft Asteroid Hovering with Formulation Extension in Geometric Mechanics Framework

Wesley Thomas Stackhouse
Embry-Riddle Aeronautical University

CONSTRAINED MOTION ANALYSIS AND CONTROL OF SPACECRAFT ASTEROID HOVERING WITH FORMULATION EXTENSION IN GEOMETRIC MECHANICS FRAMEWORK

By

Wesley Thomas Stackhouse

A Thesis Submitted to the Faculty of Embry-Riddle Aeronautical University

In Partial Fulfillment of the Requirements for the Degree of

Master of Science in Aerospace Engineering

April 2020

Embry-Riddle Aeronautical University
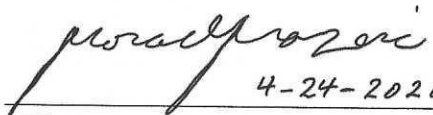
Daytona Beach, Florida

CONSTRAINED MOTION ANALYSIS AND CONTROL OF SPACECRAFT ASTEROID HOVERING WITH FORMULATION EXTENSION IN GEOMETRIC MECHANICS FRAMEWORK
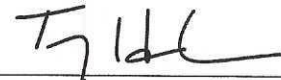
By

Wesley Thomas Stackhouse

This Thesis was prepared under the direction of the candidate's Thesis Committee Chair, Dr. Morad Nazari, Department of Aerospace Engineering, and has been approved by the members of the Thesis Committee. It was submitted to the Office of the Senior Vice President for Academic Affairs and Provost, and was accepted in partial fulfillment of the requirements for the Degree of Master of Science in Aerospace Engineering.

THESIS COMMITTEE

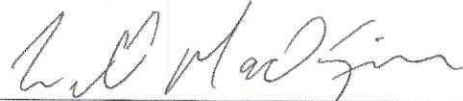4-24-2020

Chairman, Dr. Morad Nazari

Member, Dr. Troy Henderson

Member, Dr. Richard Prazenica

Member, Dr. William MacKunis

Graduate Program Coordinator,
Dr. Magdy Attia

4. 26. 2020

Date

Maj Dean Mirmirani

04.26.2020

Dean of College of Engineering,
Dr. Maj Mirmirani

Date

Christopher Grant

04/27/2020

Associate Provost of Academic Support,
Dr. Christopher Grant

Date

ACKNOWLEDGEMENTS

ABSTRACT

This thesis studies the constrained motion for a spacecraft hovering over an asteroid, where the Udwadia-Kalaba (UK) formulation is applied for nominal control, and an adaptive controller is developed to account for unknowns in the dynamics. Then, the formulation is extended in the geometric mechanics framework to account for rigid body spacecraft asteroid hovering. Constraints are developed and applied for fully constrained and under-constrained asteroid hovering.

The fully constrained solutions provided by the UK fundamental equation are compared to an optimal linear quadratic regulator. An adaptive controller is designed using the UK fundamental equation as a basis in the form of a model reference adaptive controller. The controller is proven to have asymptotic tracking of the reference system designed by the desired constraints on the spacecraft. The convergence of the tracking error dynamics is studied using the Lyapunov's direct method. It is shown that the controller, with accurate estimation of the unknown parameters, results in the minimum required control response due to its basis on the UK equation. The parameters are successfully estimated using a finite-time estimation method.

Furthermore, the extension of the UK formulation into the geometric mechanics framework is developed to account for rigid-body spacecraft, where the formulation also allows orientation constraints to be applied on the spacecraft. Constraints with a basis on the Lie algebra of special Euclidean group $\mathsf{SE}(3)$ are developed to fully constrain a spacecraft's position and orientation for hovering over an asteroid. The geometric mechanics UK formulation successfully gives the required angular

and translational accelerations to maintain the desired configuration (pose) of the rigid-body spacecraft. The developments above are discussed for a spacecraft hovering over the asteroid Bennu and the closed-loop response of the system, control inputs, and control efforts are provided and discussed.

TABLE OF CONTENTS

LIST OF FIGURES

ABBREVIATIONS

ACAF	Asteroid-centered asteroid-fixed
ACI	Asteroid-centered inertial
ARE	Algebraic Riccati equation
GMUK	Geometric mechanics Udwadia-Kalaba
LQR	Linear quadratic regulator
MP	Moore-Penrose
MRAC	Model reference adaptive control
NCE	Non-certainty equivalence
PE	Persistence of excitation
SCB	Spacecraft body
SVD	Singular value decomposition
UK	Udwadia-Kalaba

SYMBOLS

$(\cdot)^+$	Moore-Penrose generalized inverse
$(\cdot)^\times$	Mapping from $\mathbb{R}^3 \to \mathfrak{so}(3)$
$(\cdot)^\vee$	Mapping from $\mathbb{R}^6 \to \mathfrak{se}(3)$
A	$m \times n$ matrix developed from differentiating the constraints and used in the UK equation
$\mathbf{a}$	Unconstrained acceleration a system
$\mathbf{a}_c$	Accelerations applied on a system due to a set of constraints
$\mathbf{b}$	m vector of resulting terms from differentiating the constraints and used in the UK equation
C_{20}	Spherical harmonic constant of the asteroid
C_{22}	Spherical harmonic constant of the asteroid
$\mathbf{e}$	Error between the states of a system and the reference states
g	$\mathsf{SE}(3)$ matrix containing the rotation matrix and position vector of a rigid body
$\mathbb{I}$	Inertia tensor of a rigid body containing the moment of inertia matrix and the diagonal mass matrix
J	Moment of inertia matrix for a rigid body
M	$3n \times 3n$ diagonal mass matrix of n particles
$m_{\mathcal{A}}$	Mass of the asteroid
m_b	Mass of a rigid-body
$\mathbf{q}$	Set of generalized position vectors for n particles
R	Rotation matrix from a body's reference frame to the inertial frame
$\mathbf{r}$	Position vector of the spacecraft
$\mathbf{r}^*$	Desired position expressed in the ACAF frame
r_0	Reference radius of the asteroid

$\mathsf{SE}(3)$	Special Euclidean group describing the rotation and position of a rigid body
$\mathsf{SO}(3)$	Special Orthogonal group describing the rotation of a rigid body
$\mathfrak{se}(3)$	Lie algebra of $\mathsf{SE}(3)$
$\mathfrak{so}(3)$	Lie algebra of $\mathsf{SO}(3)$, the set of all skew-symmetric matrices
U	Gravitational potential of a body
$\mathbf{u}$	Control input
V	Lyapunov function
$\mathbb{V}$	Augmented velocity vector containing the angular and translational velocities
$\mathbf{v}$	Translational velocity of a rigid body
$\mathbf{x}$	Vector describing the state space of a system
$\boldsymbol{\Theta}$	Vector of unknown parameters
$\hat{\boldsymbol{\Theta}}$	Adaptive estimates of the unknown parameters
$\tilde{\boldsymbol{\Theta}}$	Error between the adaptive estimates and the unknown parameters
μ	Gravitational parameter of the asteroid
$\boldsymbol{\Phi}$	Set of m constraints on a system
$\boldsymbol{\Omega}$	Angular velocity vector of the asteroid
$\boldsymbol{\omega}$	Angular velocity of a rigid body

1. Introduction

Spacecraft operations over asteroids or small bodies are crucial for the opportunities they present such as scientific observation, sample retrieval, and/or asteroid mining. These missions will require the spacecraft to orbit or hover over the surface, and/or do various other proximity operations about the asteroid. Depending on the mission objectives, the spacecraft will be required to hover in a fixed or non-fixed position. Asteroids are often irregularly shaped which affects the gravitational field about them. Due to this fact, the dynamics analysis and control design are complex. Typically, the objective of asteroid missions is to gather data about the asteroid. In some cases, there are limited data available about the asteroid, such as uncertainties about its mass, size, or shape. In these situations, it is still necessary for the spacecraft to be able to perform maneuvers and conduct operations without this information.

Some asteroid missions are currently underway. OSIRIS-REx is currently on mission about the asteroid of Bennu with the ultimate goal of a sample return (Lauretta et al., 2017). The OSIRIS-REx spacecraft successfully entered into a stable orbit about the asteroid on December 31, 2018, and it continues to perform its maneuvers in preparation for the sample acquisition and return (Wibben et al., 2019). The Hyabusa 2 spacecraft is on mission at the asteroid Ryugu and successfully landed on February 22, 2019 (Kikuchi et al., 2019). It is also on a sample return mission and collected the sample when it was landing. Asteroid operations will not stop with the above missions, but will continue with even more complex missions than those such as mining the asteroids in lieu of small samples.

1.1. Asteroid Hovering and Proximity Operations

As shown with the current ongoing asteroid missions, various control schemes and methods have been formulated and proven effective in asteroid operations with and without unknowns in the system models. Hyabusa 2 used a passive reflective marker along with an optics based controller to land within 3 meters of the desired

landing site to avoid the boulder-strewn landscape of the asteroid Ryugu (Kikuchi et al., 2019). Nazari et al. (2014) used an extended Kalman filter for the estimation of gravitational parameters by utilizing ground stations on the asteroid. In addition to that observer, optimal controllers were designed using a time-varying linear quadratic regulator and Floquet theory to control a spacecraft to hover over a tumbling asteroid. Gui and de Ruiter (2017) showed an extended state observer with position-only measurements to design a controller for spacecraft asteroid hovering that also rejects disturbances. The controller implemented velocity-free hovering control by driving a full state feedback controller with the estimates from the observer. Furfaro (2015) utilized higher-order sliding mode control theory to design a two-sliding controller to control a spacecraft to hover about an asteroid. Their controller was proven effective in maintaining the hover despite perturbing accelerations.

1.2. Adaptive Control Methods

Adaptive control methods are often used to account for uncertain/unknown parameters, unmodeled dynamics, disturbances, and/or noise. Adaptive control methods have been commonly included when there are uncertainties and unknowns in the system model. In general, adaptive control methods can be split into two groups known as direct adaptive control and indirect adaptive control. Direct adaptive control typically takes the form of directly adapting a feedback gain that is added to the controller to account for the disturbance or unknowns, whereas indirect adaptive control methods use adaptive parameters within the feedback gains or controller to account for the disturbances and/or unknowns (Kaufman et al., 1998). Some examples of various adaptive control methods are adaptive regulation, disturbance accommodating control, adaptive output feedback regulation, model reference adaptive control (MRAC), or combinations of these.

MRAC utilizes adaptive techniques to control a system to follow a known desired reference model despite the system having disturbances and/or unknowns

(Nguyen, 2018). A nonlinear adaptive controller using MRAC techniques was developed to track reference orbits around asteroids with unknown gravitational parameters (Tiwari et al., 2020). Lee and Vukovich (2015) developed an adaptive sliding mode controller for asteroid hovering with uncertainties in the parameters as well as disturbances. This method defined a sliding surface for relative position and velocity between the asteroid and spacecraft to be achieved, while using adaptive update laws for the uncertain parameter and disturbance estimations. Zhang et al. (2019) used terminal sliding-mode control theory to develop a system where only a saturation on the input was considered. An adaptive law was developed for the controller to estimate the unknown upper bounds of the disturbances due to asteroid irregularity and external forces, so that the controller can provide an appropriate response to maintain hovering. Vukovich and Gui (2017) utilized dual quaternions to develop a tracking controller for the coupled rotational and translational dynamics for asteroid proximity missions such as hovering and landing. Then, they introduced an adaptive algorithm to account for uncertainties and disturbances in the model.

A method called the non-certainty equivalence (NCE) principle was proposed by Seo (2015) for pose-tracking using dual quaternions and applied multiple filters to estimate unknown parameters in the dynamics. The NCE method was capable of adaptively estimate the parameters over time. Adetola and Guay (2008) developed a finite-time parameter identification technique to estimate unknown parameters in finite time, where a filter with dynamics that relies on the known system dynamics was used. The proposed estimation method was used alongside an adaptive controller for nonlinear systems and resulted in accurate estimation of the parameters as long as an excitation condition was satisfied by the model.

1.3. Constrained Motion Analysis

A new constrained motion analysis technique was proposed in 1992 by Udwadia and Kalaba (1992) to calculate the exact accelerations applied on a

system for a given set of constraints (Udwadia & Kalaba, 2008). Their method is capable of handling most equality constraints as long as they are differentiable and linear in the accelerations terms after differentiation. The Udwadia-Kalaba (UK) formulation can be used in nonlinear systems just as conveniently as linear systems. The UK equations of constrained motion have been applied to some aerospace missions so far. Lam (2006) used the UK framework applied to a spacecraft orbiting an oblate body, in order to maintain a circular orbit and a constant inclination. Cho and Udwadia (2010) used the UK formulation to find the explicit solution to satellite formation keeping. The UK formulation was used along with coulomb forces to control two charged spacecraft to maintain formation in an elliptic orbit (Memon et al., 2019). The results with and without the coulomb effects were compared to those obtained by the use of near-optimal control schemes designed to achieve the same formation. The UK formulation was applied for spacecraft station keeping in an unstable Lagrange point in the Sun-Earth-spacecraft circular restricted three body problem (Patel et al., 2019).

1.4. Rigid Body Control and Analysis Using Geometric Mechanics

Control of spacecraft (and other aerospace vehicles), has to also account for the rigid body of the vehicle in addition to just its position. However, the attitude of the spacecraft is coupled with its orbital motion and thus the dynamics of both are coupled. The geometric mechanics framework accounts for this coupling. Bullo and Murray (1995) developed proportional derivative control methods on both the Special Orthogonal group $SO(3)$ for rigid body rotational motion and the Special Euclidean group $SE(3)$ for the combined rotational and translational motion. Nazari et al. (2018) developed an almost asymptotically stable controller on $SE(3)$ to control both the rotation and translation of a rigid body simultaneously. Seo and Nazari (2019) developed a NCE adaptive controller designed to control a rigid body and used the NCE principle to reduce the effects of uncertain parameters. Constraints were tested to see how they were satisfied through Munthe-Kaas

integration in multibody systems when using the Lie group of $\mathsf{SE}(3)$, and concluded that the integrator yielded perfect constraint satisfaction (Müller & Terze, 2014a; Müller & Terze, 2014b). Udwadia and Schutte (2012) applied the UK formulation to quaternions in order to develop the control torques required for rigid body rotational dynamics.

1.5. Objectives

In this thesis first the required control inputs are obtained from the UK formulation for spacecraft asteroid hovering for the cases of body-fixed asteroid hovering and hovering in a desired trajectory above the asteroid with the spacecraft modeled as a point mass. The control accelerations for the fixed hovering position are compared to an optimal controller formed by an LQR. Next, the UK equations are used as a basis of an adaptive controller to hover over an asteroid with unknown gravitational parameters. Then, the UK formulation is extended and used in the lie algebra, $\mathfrak{se}(3)$, of $\mathsf{SE}(3)$ and applied to the geometric mechanics framework to study dynamics and control of a rigid body spacecraft constrained motion above the asteroid to achieve and maintain a desired hover configuration (position and orientation) of the spacecraft.

2. Theoretical Background and Preliminary Formulation

The background on the UK constrained motion analysis technique and problem dynamics are discussed here. The basis of the UK formulation is presented along with how they solve a set a constraints. The reference frames and dynamics of a spacecraft about of rotating body are studied.

2.1. Constrained Motion Analysis

The accelerations of a system with constraints will deviate from the accelerations of the same system with no constraints applied. The underlying issue in analyzing these systems is being able to determine the deviation caused by the constraints in the system. Udwadia and Kalaba developed a method based on Gauss's principle of least constraint to find the constraint accelerations in the constrained motion of a system of particles (Udwadia & Kalaba, 1992; Udwadia & Kalaba, 2008). Their method allows for the analysis of constrained systems and, in control design, for calculating the necessary control accelerations in order to maintain desired constraints.

2.1.1. Udwadia-Kalaba Formulation

The UK formulation follows a consistent algorithm for a system and a set of constraints. Starting with a system of n particles with an impressed force acting on the particles, the unconstrained equations of motion are,

$$\ddot{\mathbf{q}} = M^{-1}\mathbf{F} = \mathbf{a} \tag{2.1}$$

where $\mathbf{q} \in \mathbb{R}^{3n}$ is the generalized position vector of the n particles, with $\ddot{\mathbf{q}}$ being the resulting acceleration vector relative to the reference frame of interest, $M \in \mathbb{R}^{3n \times 3n}$ is the diagonal mass matrix of n particles, $\mathbf{F} \in \mathbb{R}^{3n}$ is the impressed force vector on the particles, and $\mathbf{a}$ is the unconstrained acceleration due to the impressed forces. When a set of m constraints are applied on the system, the new dynamics become,

$$\ddot{\mathbf{q}} = \mathbf{a} + \mathbf{a}_c \tag{2.2}$$

where $\mathbf{a}_c \in \mathbb{R}^{3n}$ is the acceleration applied on the system due to the constraints.

The UK formulation accepts a broad range of constraints of the form,

$$\boldsymbol{\Phi}(\dot{\mathbf{q}}, \mathbf{q}, t) = \mathbf{0} \tag{2.3}$$

where $\boldsymbol{\Phi} \in \mathbb{R}^m$ is a vector of the m constraints. Equation (2.3) consists of both holonomic and nonholonomic constraints without a need for them to be integrable. However, there are some restrictions on the admissible constraints. The constraints must be equality constraints and consistent (meaning the constraints do not violate each other) so there exists a solution of $\mathbf{q}$ and $\dot{\mathbf{q}}$ that satisfies all of them simultaneously. Also, after differentiation, the constraints must be linear with respect to the acceleration terms. Note that while the constraints must not conflict, they do not need to be linearly independent of each other.

The constraints from Equation (2.3) are then differentiated until the acceleration terms appear. This typically entails differentiating twice for holonomic constraints and once for nonholonomic constraints. After the constraints are differentiated they are formulated into the constraint equation form:

$$A(\dot{\mathbf{q}}, \mathbf{q}, t)\ddot{\mathbf{q}} = \mathbf{b}(\dot{\mathbf{q}}, \mathbf{q}, t) \tag{2.4}$$

where $A \in \mathbb{R}^{m \times 3n}$, $\mathrm{rank}(A) = r$, and $\mathbf{b} \in \mathbb{R}^m$ is the remaining term which can be functions of the positions, velocities, and time. Thus, and in general, the UK formulation can be applied for any constraint that can be put into the form of Equation (2.4). Once this constraint equation is found, the constraint accelerations are obtained by the UK fundamental equation:

$$\mathbf{a}_c = M^{-1/2} \left(AM^{-1/2} \right)^+ (\mathbf{b} - A\mathbf{a}) \tag{2.5}$$

where $(\cdot)^+$ is the Moore-Penrose (MP) generalized inverse. For the case of a system with a single particle, $n = 1$, $M = m_p I_3$, where m_p is the mass of the particle and

Equation (2.5) reduces to,

$$\mathbf{a}_c = A^+ \left(\mathbf{b} - A\mathbf{a}\right) \tag{2.6}$$

The constraint accelerations obtained by the UK fundamental equation in Equation (2.5) are those that satisfy Gauss's principle of least constraint. For a fully constrained case $(m = 3n)$, there is only one solution that satisfies the constraints. However, in general, there may be infinitely many solutions that will satisfy the constraints. In Section 2.1.2 the Moore-Penrose inverse of a matrix used in Equations (2.5) and (2.6) is discussed.

2.1.2. Moore-Penrose Generalized Inverse

The UK formulation has a basis on the MP inverse as shown in Equation (2.5). There are some important properties that the MP inverse satisfies similar to the properties of a normal inverse. In this section, A is considered to be an m by n matrix with rank r. Then A^+ is the MP inverse of A if it satisfies four conditions known as the MP conditions:

$$1. \quad AA^+A = A \tag{2.7a}$$

$$2. \quad A^+AA^+ = A^+ \tag{2.7b}$$

$$3. \quad AA^+ = (AA^+)^T \tag{2.7c}$$

$$4. \quad A^+A = (A^+A)^T \tag{2.7d}$$

Thus, if the four conditions above are satisfied by A^+, then it is the MP inverse of A. Other generalized inverses of A exist, but they do not satisfy all four conditions in Equation (2.7).

Two important properties of the MP inverse of a matrix A are that it exists and is unique. The singular value decomposition (SVD) of A can be taken so that,

$$A = W\Lambda V^T \tag{2.8}$$

where $W \in \mathbb{R}^{m \times r}$ is an orthonormal matrix, $\Lambda \in \mathbb{R}^{r \times r}$ is a diagonal positive definite

matrix, and $V \in \mathbb{R}^{n \times r}$ is also an orthonormal matrix. Consider the symmetric positive semi-definite matrix AA^T. The eigenvalues and eigenvectors of AA^T are given by,

$$\Lambda_{AA^T} = \begin{bmatrix} \Lambda^2 & 0_{r \times (m-r)} \\ 0_{(m-r) \times r} & 0_{(m-r) \times (m-r)} \end{bmatrix} \in \mathbb{R}^{m \times m}, \quad W_{AA^T} = \begin{bmatrix} W & \tilde{W} \end{bmatrix} \in \mathbb{R}^{m \times m}$$

where $\tilde{W} \in \mathbb{R}^{m \times (m-r)}$ contains the remaining eigenvectors of AA^T corresponding to the $m - r$ zero eigenvalues, so that the r eigenvectors in W corresponding to the r nonzero eigenvalues in Λ^2 make up the SVD of A, $\Lambda = +\sqrt{(\Lambda^2)}$, and the ith column of V is found by $\mathbf{v}_i = \frac{1}{\lambda_i} A^T \mathbf{w}_i$, $i = 1, 2, ..., r$. Each element of Λ is known as a singular value of A. Thus the MP inverse of A is,

$$A^+ = V \Lambda^{-1} W^T \tag{2.9}$$

This SVD definition of A^+ can easily be shown to satisfy the four MP conditions in Equation (2.7), confirming that it is the MP inverse. Two other important definitions of the MP inverse are:

$$A^+ = A^T \left(AA^T \right)^+ \tag{2.10a}$$

$$A^+ = \left(A^T A \right)^+ A^T \tag{2.10b}$$

When A has a rank of m or n, then Equations (2.10a) and (2.10b) respectively reduce to,

$$\text{rank}(A) = m, \quad A^+ = A^T \left(AA^T \right)^{-1} \tag{2.11a}$$

$$\text{rank}(A) = n, \quad A^+ = \left(A^T A \right)^{-1} A^T \tag{2.11b}$$

By applying the definition of the MP inverse in Equation (2.10a) into the UK equation given by Equation (2.5) the symmetric form of the UK equation is obtained as,

$$\mathbf{a}_c = M^{-1} A^T \left(AM^{-1}A^T \right)^+ (\mathbf{b} - A\mathbf{a}) \tag{2.12}$$

This avoids $M^{-1/2}$ and the MP inverse in this equation also reduces to the regular inverse if rank$(A) = m$.

2.1.2.1. Different Classes of Generalized Inverses and General Solution of a Set of Equations

Let any generalized inverse of A be named the $\{i,j\}$-inverse and denoted by $A^{\{i,j\}}$ if it satisfies the ith and jth MP conditions given in Equation (2.7). Since the MP inverse satisfies each of the MP conditions, then the MP inverse is also a $\{1,3\}$-inverse and a $\{1,4\}$-inverse, and all of those are also $\{1\}$-inverses.

Consider the set of equations:

$$A\mathbf{q} = \mathbf{b} \tag{2.13}$$

where $A \in \mathbb{R}^{m \times n}$, $\mathbf{q} \in \mathbb{R}^n$, and $\mathbf{b} \in \mathbb{R}^m$. If the set of equations given in Equation (2.13) is consistent, the solution $\mathbf{q}$ to this set of equations is given by,

$$\mathbf{q} = A^{\{1\}}\mathbf{b} + (I_n - A^{\{1\}}A)\mathbf{h} \tag{2.14}$$

where $\mathbf{h} \in \mathbb{R}^n$ is an arbitrary vector (Udwadia & Kalaba, 2008). Extending this, the solution given by,

$$\mathbf{q} = A^{\{1,4\}}\mathbf{b} \tag{2.15}$$

minimizes $||\mathbf{q}||$ such that $||\mathbf{q}|| \leq ||A^{\{1\}}\mathbf{b} + (I_n - A^{\{1\}}A)\mathbf{h}||$. Therefore, any $\{1,4\}$-inverse of A provides the unique result of a minimized solution, even though the $\{1,4\}$-inverse of A is not unique itself. Now, consider the case where Equation (2.13) is inconsistent such that there is no solution $\mathbf{q}$ that satisfies all the equations. The solution that minimizes the quantity $||A\mathbf{q} - \mathbf{b}||$ is given by,

$$\mathbf{q} = A^{\{1,3\}}\mathbf{b} + (I_n - A^{\{1,3\}}A)\mathbf{h} \tag{2.16}$$

Therefore, if Equation (2.13) is an inconsistent set of equations, the solution using the MP inverse,

$$\mathbf{q} = A^+\mathbf{b} \tag{2.17}$$

is unique and it minimizes the norm of the solution $||\mathbf{q}||$ while also minimizing $||A\mathbf{q} - \mathbf{b}||$. For further details and proofs of the discussion above refer to Udwadia and Kalaba (2008).

2.1.3. Gauss's Principle of Least Constraint

Now that the MP inverse is studied, Gauss's principle of least constraint can be discussed. Gauss's principle of least constraint states that of all the accelerations that satisfy the constraints, only those that minimize the Gaussian, G, will actually materialize within the system,

$$G(\ddot{\mathbf{q}}) = (\ddot{\mathbf{q}} - \mathbf{a})^T M (\ddot{\mathbf{q}} - \mathbf{a}) = \left(M^{1/2}\ddot{\mathbf{q}} - M^{1/2}\mathbf{a}\right)^T \left(M^{1/2}\ddot{\mathbf{q}} - M^{1/2}\mathbf{a}\right) \qquad (2.18)$$

For a system with constraints of the form of Equation (2.4), the resulting equations of motion of the constrained system are found by applying Equation (2.5) to Equation (2.2):

$$\ddot{\mathbf{q}} = \mathbf{a} + M^{-1/2} \left(AM^{-1/2}\right)^+ (\mathbf{b} - A\mathbf{a}) \qquad (2.19)$$

The resulting accelerations shown above are the accelerations of the system that minimize the Gaussian. As discussed in Section 2.1.1, the constraint accelerations obtained by the UK equation given in Equation (2.5) are those that cause the resulting system accelerations $\ddot{\mathbf{q}}$ given in Equation (2.2) to minimize the Gaussian, G. It can be shown that $\ddot{\mathbf{q}}$ in Equation (2.19) satisfies the constraint equation in Equation (2.4). Now, consider any set of acceleration vectors $\ddot{\mathbf{y}} = \ddot{\mathbf{q}} + \mathbf{z}$. If these new accelerations are also a solution, then they must also satisfy Equation (2.4). It can be shown that the Gaussian of those accelerations, $G(\ddot{\mathbf{y}})$, will always be greater than the Gaussian of Equation (2.19), $G(\ddot{\mathbf{q}})$, for $\mathbf{z} \neq \mathbf{0}$. The details of the proof for the discussion above is given in Appendix A.

2.1.4. Baumgarte's Constraint Stabilization Method

Using the UK formulation discussed in Section 2.1.1, only the accelerations required to maintain a given set of constraints are obtained. The control

accelerations for an arbitrary set of initial conditions that do not satisfy the constraints cannot be obtained using that technique. Thus, new constraints should be created based on the original constraints to account for arbitrary initial conditions when implementing the UK technique. For this purpose, Baumgarte (1972) constraint stabilization method is used. In this method, the desired constraints are applied into the form of a damped oscillator differential equation (Cho & Udwadia, 2010):

$$\ddot{\boldsymbol{\Phi}} + K_\alpha \dot{\boldsymbol{\Phi}} + K_\beta \boldsymbol{\Phi} = \mathbf{0} \tag{2.20}$$

where $K_\alpha, K_\beta \in \mathbb{R}^{m \times m}$. If $K_\alpha > 0$ and $K_\beta > 0$ are positive definite matrices, then $\boldsymbol{\Phi}$ asymptotically approaches zero, thus satisfying the desired constraints. As mentioned above, Equation (2.20) describes a damped oscillator. The damping of the constraints can be controlled through the relationship of K_α and K_β. Let $K_\alpha = \text{diag}\{k_{\alpha 1}, k_{\alpha 2}, ..., k_{\alpha m}\}$, $K_\beta = \text{diag}\{k_{\beta 1}, k_{\beta 2}, ..., k_{\beta m}\}$ and $k_{\alpha i}, k_{\beta i} > 0, i = 1, 2, ..., m$. The solution to the ith differential equation in Equation (2.20) is,

$$\Phi_i(t) = c_{1i} e^{\xi_{1i} t} + c_{2i} e^{\xi_{2i} t}$$

where,

$$\xi_{1i, 2i} = \frac{1}{2} \left(-k_{\alpha i} \pm \sqrt{k_{\alpha i}^2 - 4k_{\beta i}} \right)$$

and c_{1i}, c_{2i} are constants that are obtained from the initial conditions.

Thus by appropriate selection of K_α and K_β the damping of the constraints in Equation (2.20) can be adjusted to be underdamped, overdamped, or critically damped. The three types of damping are achieved by,

$$\text{underdamped}: \quad k_{\alpha i}^2 < 4k_{\beta i} \tag{2.21a}$$

$$\text{overdamped}: \quad k_{\alpha i}^2 > 4k_{\beta i} \tag{2.21b}$$

$$\text{critically damped}: \quad k_{\alpha i}^2 = 4k_{\beta i} \tag{2.21c}$$

Therefore, in addition to satisfying the system constraints, a suitable selection of the values $k_{\alpha i}$ and $k_{\beta i}$ determines how fast the ith constraint is satisfied. This allows each constraint to be satisfied in a different way and time, and it allows for the control effort and settling time to be adjusted for the desired control result. Using the Baumgarte's technique described above allows for arbitrary initial conditions to be used while also guaranteeing that the constraints will be satisfied over time.

2.2. Problem Formulation and Dynamics

Before delving into the application of the UK formulation, the dynamics of the unconstrained system need to be analyzed and modeled. In the application of asteroid hovering, this involves modeling the gravitational acceleration of the asteroid. Since asteroids are typically much smaller bodies than planets or moons, they are often irregularly shaped. This requires a better model than using the general assumption of a point mass or spherical body. In general, the acceleration of a system is obtained by taking the gradient of the potential U, i.e.,

$$\frac{^{\mathcal{N}}d^2\mathbf{r}}{dt^2} = \nabla U \tag{2.22}$$

where $\mathbf{r} \in \mathbb{R}^3$ is the position vector of the point of interest and $^{\mathcal{N}}d(\cdot)/dt$ denotes the time derivative with respect to the inertial frame. In order to obtain the gravitational potential of the asteroid, the reference frames and model of the asteroid are obtained.

2.2.1. Reference Frames and Notation

Two references frames are defined here for the asteroid. The asteroid-centered inertial (ACI) frame is centered at the center of the mass of the asteroid, oriented with the z axis aligned with the orbital angular momentum of the asteroid, non-rotating, and fixed. The asteroid-centered asteroid-fixed (ACAF) frame is also centered at the center of the mass of the asteroid, but is aligned with the axes of the principal moments of inertia of the asteroid, and rotating with the asteroid.

The angular velocity of the asteroid is given as $\mathbf{\Omega}(t)$, and is expressed in the ACAF frame. The angular velocity of the asteroid $\mathbf{\Omega}(\cdot) \in \mathbb{R}^3$ is constant or time periodic depending on whether the asteroid is uniformly rotating or tumbling, respectively. The theoretical formulation in this thesis accounts for a general asteroid whether it is uniformly rotating or tumbling asteroid with a time periodic angular velocity. However, the simulations presented are for a uniformly rotating asteroid.

Now that the reference frames are established, the notation for reference frames and time derivatives is discussed. The notation discussed here holds throughout the rest of this thesis. When taking the time derivative of an expression the derivative will always be taken with respect to the ACI frame. However, the use of the dot notation $\dot{(\cdot)}$ represents the time derivative of $(\cdot)$ with respect to the reference frame that $(\cdot)$ is expressed in. For some expression $(\cdot)$ that is expressed in the $\mathcal{X}$ reference frame, the notation $^{\mathcal{Y}}d(\cdot)/dt$ will be the time derivative of $(\cdot)$ relative to the $\mathcal{Y}$ reference frame, but expressed in the $\mathcal{X}$ reference frame. In the case of asteroid hovering let $\mathbf{r}$ be the position vector of the spacecraft expressed in the ACAF frame. The time derivative of this vector is written as,

$$\frac{^{\mathcal{N}}d\mathbf{r}}{dt} = \dot{\mathbf{r}} + \mathbf{\Omega}(t) \times \mathbf{r}$$

where $\mathcal{N}$ is used to represent the ACI frame, $^{\mathcal{N}}d\mathbf{r}/dt$ is the velocity of the spacecraft relative to the ACI frame, but still expressed in the ACAF frame, and $\dot{\mathbf{r}}$ is the velocity of the spacecraft relative to and expressed in the ACAF frame.

2.2.2. Modeling the Gravitational Potential of the Asteroid

The asteroid is now modeled in order to obtain the gravitational potential of the asteroid. The asteroid is modeled as a tri-axial ellipsoid with major axes L_1, L_2, and L_3 aligned with the principal axes of the asteroid, which correspond to the x, y, and z axes of the ACAF frame, respectively. Figure 2.1 shows the major axes of the asteroid Bennu measured out in order to obtain an ellipsoidal approximation of the asteroid. Thus using the ellipsoidal model, the gravitational potential of
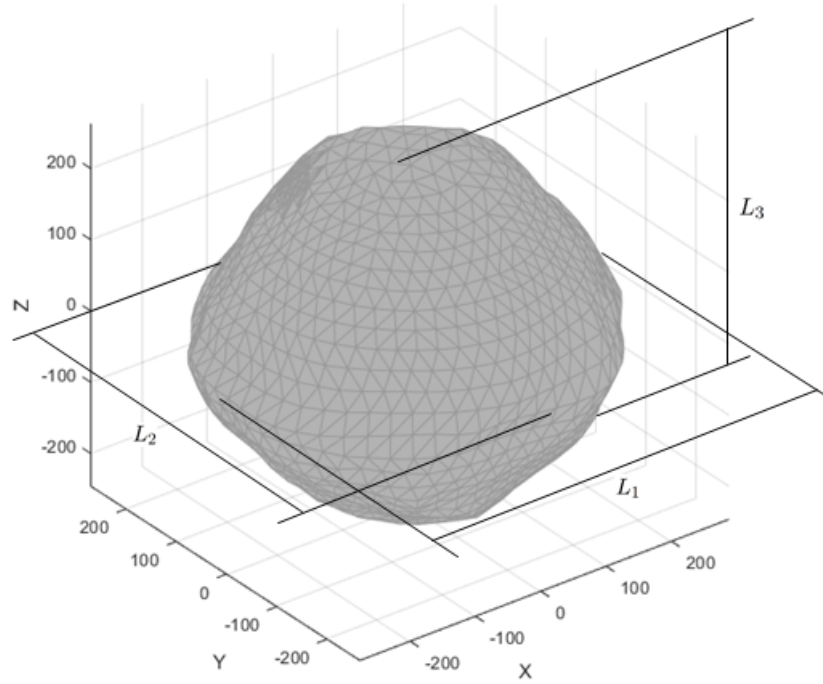
Figure 2.1 The major axes of the asteroid Bennu.

the asteroid experienced by a spacecraft can be modeled by spherical harmonics of second degree and order (Scheeres, 2012):

$$U = \frac{\mu}{r} \left\{ 1 + \left(\frac{r_0}{r} \right)^2 \left[C_{20} \left(1 - \frac{3}{2} \cos^2 \delta \right) + 3 C_{22} \cos^2 \delta \cos(2\lambda) \right] \right\} \qquad (2.23)$$

where $\mu = Gm_\mathcal{A}$ is the gravitational parameter of the asteroid, G is the gravitational constant, $m_\mathcal{A}$ is the mass of the asteroid, r is the magnitude of $\mathbf{r}$, the position vector of the spacecraft, $r_0 = \frac{L_1}{2}$ is the reference radius of the asteroid, set to be the equatorial radius along the x axis of the ACAF frame, and δ and λ are the angles of latitude and longitude, respectively. The spherical harmonic constants of second degree and order are,

$$C_{20} = -J_2 = \frac{1}{5r_0^2} \left(\gamma^2 - \frac{\alpha^2 + \beta^2}{2} \right), \quad C_{22} = \frac{1}{20r_0^2} \left(\alpha^2 - \beta^2 \right) \qquad (2.24)$$

where $\alpha = 1$, $\beta = \frac{L_2}{L_1}$, and $\gamma = \frac{L_3}{L_1}$ are the dimensionless ratios of the major axes of the asteroid.

2.2.3. Spacecraft Dynamics About the Asteroid

The dynamics of the spacecraft motion about the asteroid are modeled through Equation (2.22). Let $\mathbf{r}$ be the position vector of the spacecraft expressed in the ACAF frame. Expanding out the dynamics of a spacecraft about the asteroid via Equation (2.22) along with an added control input and expressed in the ACAF frame yields,

$$\ddot{\mathbf{r}} + \dot{\Omega}^\times(t)\mathbf{r} + 2\Omega^\times(t)\dot{\mathbf{r}} + \Omega^{\times^2}(t)\mathbf{r} = U_\mathbf{r} + \mathbf{u} \tag{2.25}$$

where $U_\mathbf{r} = \nabla U = \frac{\partial U}{\partial \mathbf{r}} \in \mathbb{R}^3$ is the gradient of the gravitational potential with respect to the spacecraft position vector, $\mathbf{u} \in \mathbb{R}^3$ is the control input, and the skew-symmetric mapping $(\cdot)^\times : \mathbb{R}^3 \to \mathfrak{so}(3)$ is defined for a vector $\boldsymbol{w} = [w_1, w_2, w_3]^T \in \mathbb{R}^3$ as,

$$w^\times = \begin{bmatrix} 0 & -w_3 & w_2 \\ w_3 & 0 & -w_1 \\ -w_2 & w_1 & 0 \end{bmatrix} \in \mathfrak{so}(3) \tag{2.26}$$

The latitude and longitude angles are naturally oriented with respect to the ACAF frame. Therefore the trigonometric relations involving the latitude and longitude in Equation (2.23) can be written as,

$$\cos^2 \delta = \frac{\mathbf{r}^T T_\delta \mathbf{r}}{r^2} \tag{2.27a}$$

$$\cos^2 \delta \cos 2\lambda = \frac{\mathbf{r}^T T_\lambda \mathbf{r}}{r^2} \tag{2.27b}$$

where the matrices T_δ and T_λ are,

$$T_\delta = \begin{bmatrix} 1 & 0 & 0 \\ 0 & 1 & 0 \\ 0 & 0 & 0 \end{bmatrix}, \quad T_\lambda = \begin{bmatrix} 1 & 0 & 0 \\ 0 & -1 & 0 \\ 0 & 0 & 0 \end{bmatrix} \tag{2.28}$$

Substituting Equations (2.27) and (2.28) into the expression for the potential

function given in Equation (2.23) and taking the partial derivative with respect to $\mathbf{r}$, the gravitational acceleration acting on the spacecraft due to the asteroid is obtained as,

$$U_{\mathbf{r}} = -\frac{\mu}{r^3} \left[I_3 + \frac{3C_{20}r_0^2}{r^2}F_\delta - \frac{3C_{22}r_0^2}{r^2}F_\lambda \right] \mathbf{r} \tag{2.29}$$

where F_δ and F_λ are

$$F_\delta = \left(I_3 + T_\delta - \frac{5}{2}\hat{\mathbf{r}}^T T_\delta \hat{\mathbf{r}} I_3 \right) \in \mathbb{R}^{3\times3}$$

$$F_\lambda = \left(2T_\lambda - 5\hat{\mathbf{r}}^T T_\lambda \hat{\mathbf{r}} I_3 \right) \in \mathbb{R}^{3\times3}$$

and $\hat{\mathbf{r}} = \frac{1}{r}\mathbf{r}$ is the unit vector in the direction of $\mathbf{r}$. The equations of motion of a spacecraft about the asteroid are now fully defined by Equations (2.25) and (2.29).

3. Nominal Asteroid Hovering Control

In the case of asteroid hovering, the impressed force is the two body problem along with any perturbations added. The UK formulation allows a simple and consistent way to solve constrained motion problems, regardless of whether they are under constrained, fully constrained, or over constrained. In Sections 3.1 and 3.2, the fully constrained and under constrained asteroid hovering scenarios are studied (Stackhouse et al., 2019).

3.1. Fully Constrained Scenario: Body-Fixed Asteriod Hovering

For a spacecraft $(n = 1)$ to hover over an asteroid, $m = 3$ constraints are set in order for the position of the spacecraft to be constant in the ACAF frame. In this case with $m = 3n = 3$, the spacecraft is fully constrained so there is only one solution to the constrained problem, although this problem can be solved through other means.
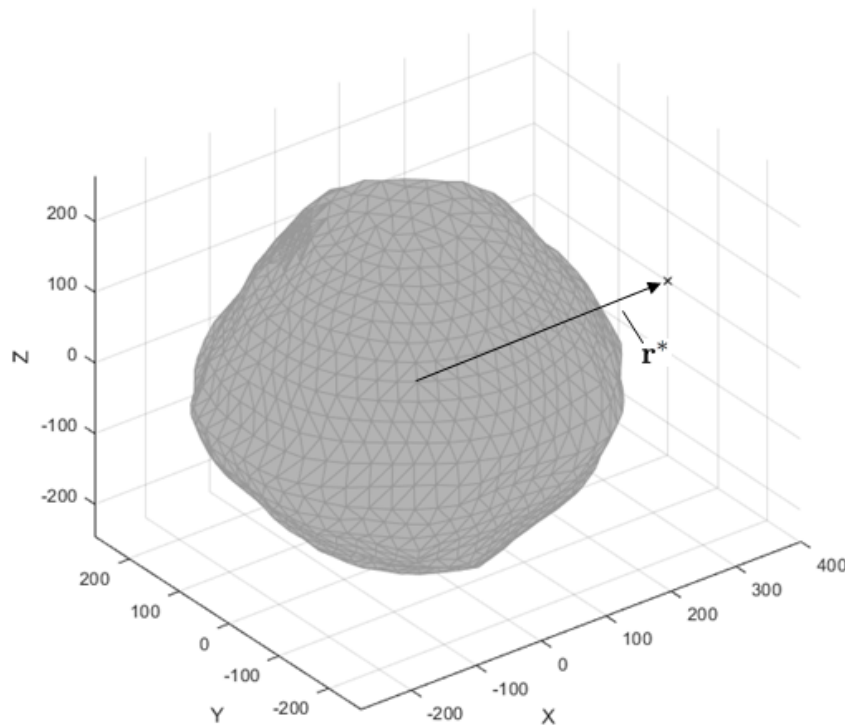
Figure 3.1   The asteroid-fixed hover position displayed in the ACAF frame.

3.1.1. Body-Fixed Asteroid Hovering via the UK Framework

The three constraints selected for the spacecraft to hover over the asteroid are as follows:

$$\mathbf{\Phi} = \mathbf{r} - \mathbf{r}^* = \mathbf{0} \tag{3.1a}$$

where $\mathbf{r}^*$ is the desired hover location expressed in the ACAF frame. Note that the desired hover location is constant in the ACAF frame. Figure 3.1 shows the hovering position over the asteroid Bennu. The three constraints in Equation (3.1a) are now differentiated twice, as they are all holonomic constraints, yielding,

$$\dot{\mathbf{\Phi}} = \dot{\mathbf{r}} + \Omega^\times(t)\left(\mathbf{r} - \mathbf{r}^*\right) = \mathbf{0} \tag{3.1b}$$

$$\ddot{\mathbf{\Phi}} = \ddot{\mathbf{r}} + \dot{\Omega}^\times(t)\left(\mathbf{r} - \mathbf{r}^*\right) + 2\Omega^\times(t)\dot{\mathbf{r}} + \Omega^{\times^2}(t)\left(\mathbf{r} - \mathbf{r}^*\right) = \mathbf{0} \tag{3.1c}$$

Equation (3.1) is then applied to Equation (2.20) and written in the form of the constraint equation given in Equation (2.4):

$$\ddot{\mathbf{r}} = \Omega^{\times^2}(t)(\mathbf{r}^* - \mathbf{r}) + \dot{\Omega}^\times(t)(\mathbf{r}^* - \mathbf{r}) - 2\Omega^\times(t)\dot{\mathbf{r}} - K_\alpha\dot{\mathbf{\Phi}} - K_\beta\mathbf{\Phi} \tag{3.2}$$

This results gives,

$$A = I_3 \tag{3.3a}$$

$$\mathbf{b} = \left(\Omega^{\times^2}(t) + \dot{\Omega}^\times(t) + K_\alpha\Omega^\times(t) + K_\beta\right)(\mathbf{r}^* - \mathbf{r}) - \left(2\Omega^\times(t) + K_\alpha\right)\dot{\mathbf{r}} \tag{3.3b}$$

and $K_\alpha, K_\beta \in \mathbb{R}^{3\times3}$. Since the three constraints on the system explicitly define the the position vector of the spacecraft, the matrix $A = I_3$ is identity. The A matrix in Equation (3.3a) can be applied to the UK equation in Equation (2.6) since $n = 1$, which yields the simple result of:

$$\mathbf{a}_c = \mathbf{b} - \mathbf{a} \tag{3.4}$$

where $\mathbf{a} = \ddot{\mathbf{r}}$ in Equation (2.25) when the control input $\mathbf{u} = \mathbf{0}$:

$$\mathbf{a} = -\dot{\Omega}^{\times}(t)\mathbf{r} - 2\Omega^{\times}(t)\dot{\mathbf{r}} - \Omega^{\times^2}(t)\mathbf{r} + U_{\mathbf{r}} \tag{3.5}$$

which is the unconstrained/ uncontrolled dynamics. Since A is a square matrix, the Moore-Penrose generalized inverse reduces to the normal inverse and, since A is the identity matrix, it is eliminated from the equation altogether. Further applying $\mathbf{b}$ and $\mathbf{a}$, the constraint acceleration becomes (Stackhouse et al., 2019),

$$\mathbf{a}_c = \Omega^{\times^2}(t)\mathbf{r}^* + \dot{\Omega}^{\times}(t)\mathbf{r}^* - U_{\mathbf{r}} + \left(K_\alpha \Omega^{\times}(t) + K_\beta\right)(\mathbf{r}^* - \mathbf{r}) - K_\alpha \dot{\mathbf{r}} \tag{3.6}$$

Over time, the constraint $\boldsymbol{\Phi}$ is guaranteed to converge to $\mathbf{0}$, $\mathbf{r} \rightarrow \mathbf{r}^*$, and $\dot{\mathbf{r}} \rightarrow \mathbf{0}$, so the constraint acceleration settles to the steady state value of maintaining the hover position:

$$\mathbf{a}_{c_{ss}} = \Omega^{\times^2}(t)\mathbf{r}^* + \dot{\Omega}^{\times}(t)\mathbf{r}^* - U_{\mathbf{r}}^* \tag{3.7}$$

where $U_{\mathbf{r}}^* = \lim_{\mathbf{r} \rightarrow \mathbf{r}^*} U_{\mathbf{r}}$ and $U_{\mathbf{r}}$ is given in Equation (2.29). Applying Equation (3.6) as the control will drive the spacecraft from arbitrary initial conditions to the hover position and maintain it.

3.1.2. Body-Fixed Asteroid Hovering via LQR

An optimal control law can be designed to achieve the same hover location. The controller is designed by combining a feedforward controller and a feedback controller (Nazari et al., 2014):

$$\mathbf{u} = \mathbf{u}_{ff} + \mathbf{u}_{fb} \tag{3.8}$$

where $\mathbf{u}_{ff}$ and $\mathbf{u}_{fb}$ are the feedforward and feedback controllers respectively. The feedforward controller is used to maintain the hover position, while the feedback controller is used to account for initial conditions. The feedforward controller for asteroid hovering is set to be the dynamics of the desired hover position. This can

be found, since it is a fully constrained system,

$$\mathbf{u}_{ff} = -U_{\mathbf{r}}^* + \dot{\Omega}^\times(t)\mathbf{r}^* + \Omega^{\times^2}(t)\mathbf{r}^* \tag{3.9}$$

Note that Equation (3.7) is identical to Equation(3.9), thus the control for hover maintenance will be identical between both controllers. This is expected, since there is only a single solution to the constrained problem and the UK solution was simply adding the desired dynamics and taking away the undesired dynamics.

Taking Equation (2.25), converting to state space form and linearizing the system about the desired hovering point yields,

$$\Delta\dot{\mathbf{x}} = A_{\mathbf{r}^*}(t)\Delta\mathbf{x} + B\mathbf{u}_{fb} \tag{3.10}$$

where $\mathbf{x} = [\mathbf{r}^T, \dot{\mathbf{r}}^T]^T$ is the state space vector of the spacecraft's postion and velocity vectors, $\Delta\mathbf{x} = \mathbf{x} - \mathbf{x}^*$ is the linearized state disturbance from the hover state, where,

$$A_{\mathbf{r}^*}(t) = \begin{bmatrix} 0_{3\times3} & I_3 \\ -\dot{\Omega}^\times(t) - \Omega^{\times^2}(t) + U_{\mathbf{rr}}^* & -2\Omega^\times(t) \end{bmatrix} \in \mathbb{R}^{6\times6}, \quad B = \begin{bmatrix} 0_{3\times3} \\ I_3 \end{bmatrix} \in \mathbb{R}^{6\times3} \tag{3.11}$$

$U_{\mathbf{rr}}^* = \frac{\partial^2 U}{\partial \mathbf{r}^2}|_{\mathbf{r}=\mathbf{r}^*} \in \mathbb{R}^{3\times3}$ is the Jacobian of U:

$$\begin{aligned}
U_{\mathbf{rr}}^* = &-\frac{\mu}{r^{*3}}I_3 + \frac{3\mu}{r^{*5}}\mathbf{r}^*\mathbf{r}^{*T} \\
&+ \frac{3C_{20}\mu r_0^2}{r^{*3}}\left[-\frac{3(I_3+T_\delta)}{r^{*2}} + \frac{5(I_3+2T_\delta)}{r^{*4}}\mathbf{r}^*\mathbf{r}^{*T} + \frac{5}{2}\frac{\mathbf{r}^{*T}T_\delta\mathbf{r}^*}{r^{*4}}I_3 - \frac{35}{2}\frac{\mathbf{r}^{*T}T_\delta\mathbf{r}^*}{r^{*6}}\mathbf{r}^*\mathbf{r}^{*T}\right] \\
&- \frac{3C_{22}\mu r_0^2}{r^{*3}}\left[-\frac{2T_\lambda}{r^{*2}} + \frac{20T_\lambda}{r^{*4}}\mathbf{r}^*\mathbf{r}^{*T} + \frac{5\mathbf{r}^{*T}T_\lambda\mathbf{r}^*}{r^{*4}}I_3 - \frac{35\mathbf{r}^{*T}T_\lambda\mathbf{r}^*}{r^{*6}}\mathbf{r}^*\mathbf{r}^{*T}\right]
\end{aligned} \tag{3.12}$$

The feedback controller takes the form of the control law given by the solution of the LQR as,

$$\mathbf{u}_{fb} = -K(t)\Delta\mathbf{x} \tag{3.13}$$

where the gain matrix $K(t)$ is,

$$K(t) = R_c^{-1}(t)B^T P(t) \tag{3.14}$$

where $P(t)$ is the solution to the algebraic Riccati equation (ARE),

$$A_{\mathbf{r}^*}^T(t)P(t) + P(t)A_{\mathbf{r}^*}(t) - P(t)BR_c^{-1}(t)B^T P(t) + Q_c(t) = 0 \tag{3.15}$$

and $Q_c(t) \geq 0$ and $R_c(t) > 0$ are the weight matrices from the cost function, J, which is minimized by $\mathbf{u}_{fb}$,

$$J_c = \frac{1}{2}\int_0^\infty \left(\Delta\mathbf{x}^T Q_c(t)\Delta\mathbf{x} + \mathbf{u}_{fb}^T R_c(t)\mathbf{u}_{fb}\right) dt \tag{3.16}$$

The matrices $A_{\mathbf{r}^*}(t)$, $P(t)$, $K(t)$, $Q_c(t)$, and $R_c(t)$ are shown with a time dependency. This accounts for if the asteroid is tumbling or not. In the case that it is tumbling, the ARE must be solved at all times, and the control gain will be time varying. $Q_c(t)$ and $R_c(t)$ can be selected to be time-varying or not. In the case of a uniformly rotating asteroid with a body-fixed hover position $A_{\mathbf{r}^*}$, P, K, Q_c, and R_c all become constant in time, thus, giving a constant control gain.

3.1.3. Analytical Comparison Between the UK and LQR Control Techniques

Prior to any simulation, there are similarities observed between the UK formulation and the selected optimal controller. The feedforward controller in Equation (3.9), selected for hovering maintenance, is exactly the same as the steady state result obtained by the UK formulation in Equation (3.7). Therefore, there is no difference between the methods for maintaining the hover. The differences appear in the convergence to the hover location from the initial conditions. The UK formulation utilizes an alternate constraint in the form of a critically damped oscillator and the optimal controller utilizes a stabilizing LQR gain matrix applied to a linearized system to regulate the disturbance from the hover position to zero. As these methods are only dealing with the simple case of a body-fixed or constant hover position, the derivation of the dynamics to input in the feedforward controller

is relatively simple. Some more complex hovering scenarios can be observed and achieved using the UK formulation, such as for under constrained hovering.

3.2. Under Constrained Scenario: Hovering in a Desired Trajectory

In some asteroid hovering missions, it may be desired that the spacecraft be moving on a specific trajectory with respect to the body frame rather than in a fixed position. This section deals with the cases where $m < 3n$ so there are still some degrees of freedom remaining. Suppose it is desired for the spacecraft to hover within the vicinity of the desired hover position; this would allow for the spacecraft to have bounded movement. Inequality constraints would give the most ideal results as this would allow for that movement as long as the spacecraft remained within the bounds; however, the UK formulation does not accept inequality constraints. Therefore, some surfaces can be used to still allow some movement about the desired hover potions. The case where the spacecraft has one degree of freedom and is constrained to move on a circle parallel to the surface of the asteroid is studied.

3.2.1. Spacecraft Constrained to Hover in a Circular Trajectory

The first situation where the spacecraft is to remain on a circle can be accomplished by two constraints:

$$\Phi_1 = \frac{\mathbf{r}_c^T}{r_c}(\mathbf{r} - \mathbf{r}_c) = 0 \tag{3.17a}$$

$$\Phi_2 = (\mathbf{r} - \mathbf{r}_c)^T(\mathbf{r} - \mathbf{r}_c) - \rho^2 = 0 \tag{3.17b}$$

where $\mathbf{r}_c$ is the ACAF fixed vector to the center of the circle, r_c is the magnitude of $\mathbf{r}_c$, and ρ is the radius of the circle. Φ_1 constrains $\mathbf{r}$ to remain on the plane roughly parallel to the surface of the asteroid that passes through the end of $\mathbf{r}_c$ and Φ_2 constrains the spacecraft to remain on a sphere centered at the end of $\mathbf{r}_c$. The intersection of these two constraints is where the spacecraft is free to move. Figure 3.2 displays both constraints along with their intersection. Both constraints
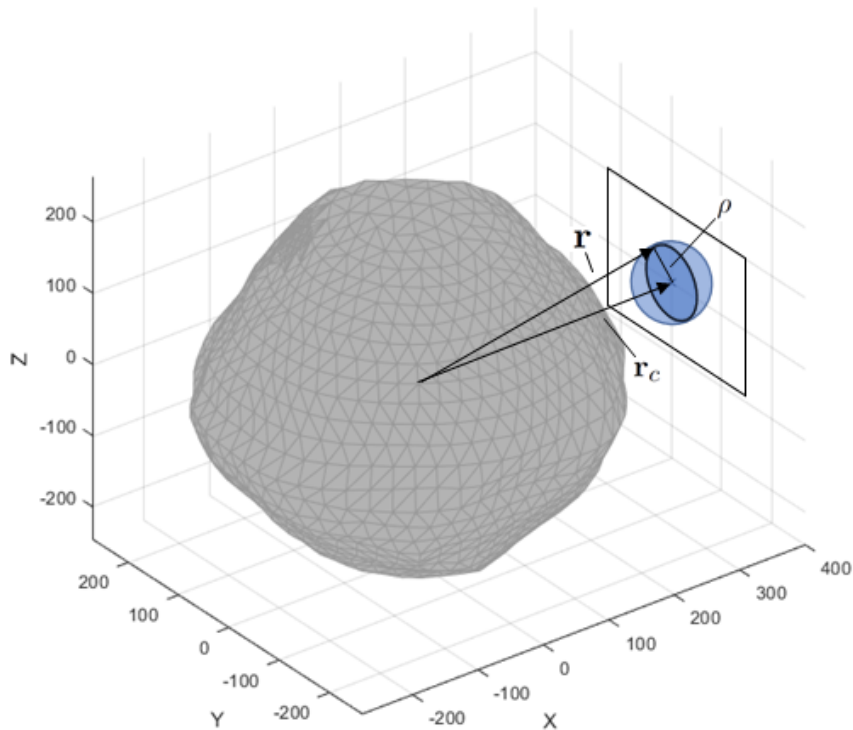
Figure 3.2 Circular trajectory constraints visualized. The intersection of the plane and the sphere defines the circular trajectory of the spacecraft.

together will keep the spacecraft on the circle roughly parallel to the surface of the asteroid. Differentiating the above constraints in Equation (3.17) twice with respect to time, as they are holonomic, results in,

$$\dot{\Phi}_1 = \frac{\mathbf{r}_c^T}{r_c}\dot{\mathbf{r}} = 0 \tag{3.18a}$$

$$\dot{\Phi}_2 = (\mathbf{r} - \mathbf{r}_c)^T \left[\dot{\mathbf{r}} + \Omega^\times(t)(\mathbf{r} - \mathbf{r}_c)\right] = 0 \tag{3.18b}$$

$$\ddot{\Phi}_1 = \frac{\mathbf{r}_c^T}{r_c}\ddot{\mathbf{r}} = 0 \tag{3.19a}$$

$$\ddot{\Phi}_2 = (\mathbf{r} - \mathbf{r}_c)^T\ddot{\mathbf{r}} + \dot{\mathbf{r}}^T\dot{\mathbf{r}} + (\mathbf{r} - \mathbf{r}_c)^T\dot{\Omega}^\times(t)(\mathbf{r} - \mathbf{r}_c) = 0 \tag{3.19b}$$

Applying Equations (3.17), (3.18), and (3.19) to Baumgarte's method, Equation (2.20) and reordering into constraint equation form shown in

Equation (2.4) gives,

$$A = \begin{bmatrix} \frac{\mathbf{r}_c^T}{r_c} \\ (\mathbf{r} - \mathbf{r}_c)^T \end{bmatrix} \tag{3.20a}$$

$$\mathbf{b} = \begin{bmatrix} 0 \\ -\dot{\mathbf{r}}^T \dot{\mathbf{r}} - (\mathbf{r} - \mathbf{r}_c)^T \dot{\Omega}^\times(t)(\mathbf{r} - \mathbf{r}_c) \end{bmatrix} - K_\alpha \begin{bmatrix} \dot{\Phi}_1 \\ \dot{\Phi}_2 \end{bmatrix} - K_\beta \begin{bmatrix} \Phi_1 \\ \Phi_2 \end{bmatrix} \tag{3.20b}$$

where $A \in \mathbb{R}^{2\times3}$, $\mathbf{b} \in \mathbb{R}^2$, and $K_\alpha, K_\beta \in \mathbb{R}^{2\times2}$ since there are only two constraints. By observing the A matrix and $\mathbf{b}$ vector it can be clearly seen that each constraint is represented by each row of A and $\mathbf{b}$. This is useful since constraints can be added or removed without reworking the previous constraints or the dynamics. The A matrix and $\mathbf{b}$ vector found above in Equation (3.20) can be applied to the reduced form of the UK equation shown by Equation (2.6) since there is only one particle. The MP inverse of A can be found using Equation (2.10a), and if A remains full rank, then Equation (2.11a). The symmetric positive semi-definite matrix AA^T is,

$$AA^T = \begin{bmatrix} 1 & \frac{\mathbf{r}_c^T}{r_c}(\mathbf{r} - \mathbf{r}_c) \\ (\mathbf{r} - \mathbf{r}_c)^T \frac{\mathbf{r}_c}{r_c} & (\mathbf{r} - \mathbf{r}_c)^T(\mathbf{r} - \mathbf{r}_c) \end{bmatrix} \tag{3.21}$$

The determinant of AA^T in Equation (3.21) is obtained,

$$\det(AA^T) = (\mathbf{r} - \mathbf{r}_c)^T(\mathbf{r} - \mathbf{r}_c) - \frac{1}{r_c^2}\left[\mathbf{r}_c^T(\mathbf{r} - \mathbf{r}_c)\right]^2 \tag{3.22}$$

The determinant of the matrix AA^T is nonzero if the initial position of the spacecraft is parallel with the vector $\mathbf{r}_c$ i.e. if $\mathbf{r}(0) \times \mathbf{r}_c = \mathbf{0}$. In the case the initial position causes the AA^T matrix to be singular, the MP inverse is required; otherwise, the normal inverse can be used. For appropriate initial conditions,

$$A^+ = A^T(AA^T)^{-1} = \frac{1}{\det(AA^T)}\begin{bmatrix} \frac{\mathbf{r}_c}{r_c} & (\mathbf{r} - \mathbf{r}_c) \end{bmatrix}\begin{bmatrix} (\mathbf{r} - \mathbf{r}_c)^T(\mathbf{r} - \mathbf{r}_c) & -\frac{\mathbf{r}_c^T}{r_c}(\mathbf{r} - \mathbf{r}_c) \\ -(\mathbf{r} - \mathbf{r}_c)^T \frac{\mathbf{r}_c}{r_c} & 1 \end{bmatrix} \tag{3.23}$$

Thus, the required constraint accelerations can be found by applying
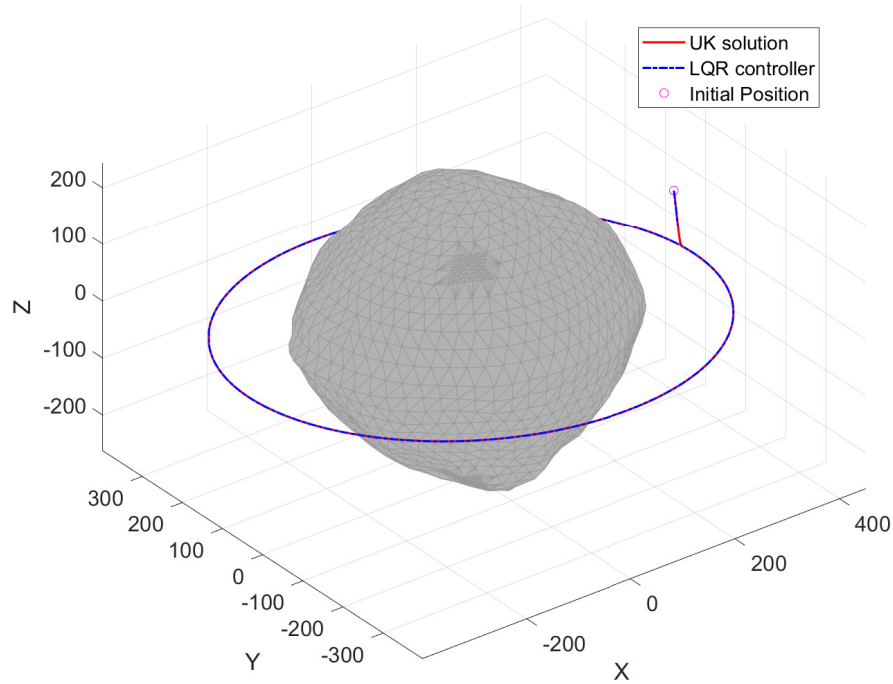
Figure 3.3 Spacecraft trajectory in the ACI frame for an asteroid-fixed hover position. After the initial convergence, the spacecraft moves around the asteroid since the asteroid is rotating relative to the ACI frame.

Equations (3.20) and (3.23) to Equation (2.6).

Since this system is under constrained, there are infinitely many accelerations that can be applied to maintain the desired constraints. The UK equation gives the minimum accelerations required to maintain them. Observing the feedforward and feedback controller previously used for a constant hover position, with these new constraints, it is easily seen that the derivation of the feedforward controller will not be as straightforward as before. Even for the case of a uniformly rotating asteroid, the system will still be time-varying. However, using the UK formulation enables the control accelerations required to maintain those constraints to be obtained conveniently.

3.3. Numerical Simulation Results and Discussion

The control responses discussed previously are applied to a spacecraft to hover over the surface of the asteroid Bennu over one full rotation of the asteroid. Bennu
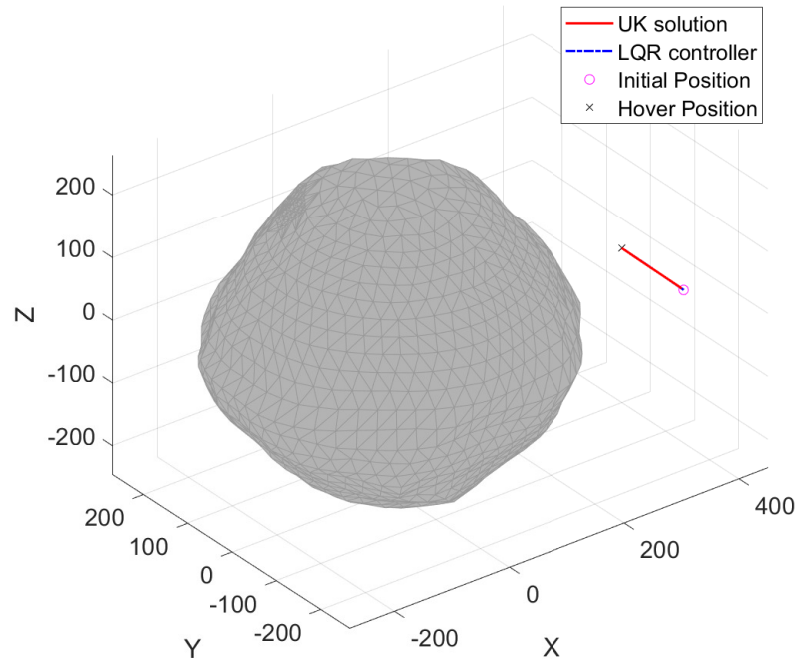
Figure 3.4 Spacecraft trajectory in the ACAF frame for an asteroid-fixed hover position. After convergence to the desired hover position, the spacecraft remains fixed relative to the asteroid.
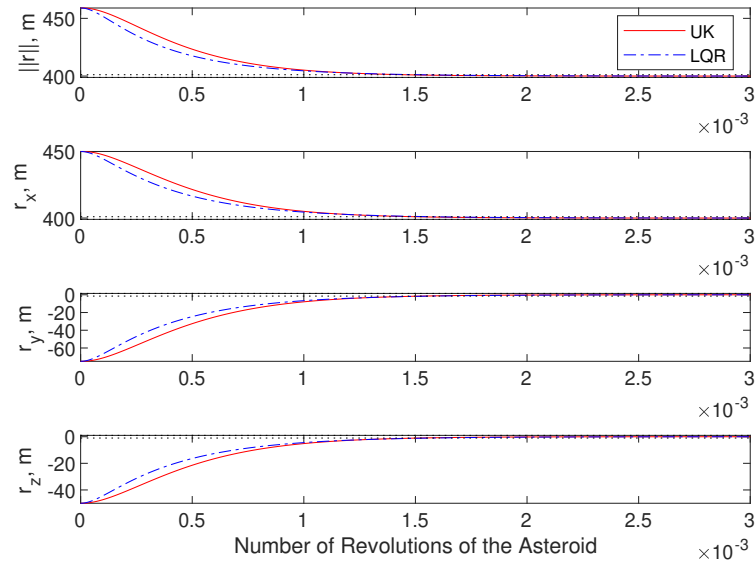
Figure 3.5 Spacecraft position components over time for the asteroid-fixed hover position.

has a gravitational parameter of $\mu = 5.2\ m^3/s^2$ with a density of $\rho = 1.26$ g/cm^3 (Chesley et al., 2014). The shape of Bennu was determined and found to have major axes as $L_1 = 565\ m$, $L_2 = 535\ m$, and $L_3 = 508\ m$, leading to $\beta = 0.9469$, $\gamma = 0.8991$, and $r_0 = 282.5\ m$ (Nolan et al., 2013). From theses values the spherical harmonic constants are found to be $C_{20} = -3.5061 \times 10^{-7}\ m^{-2}$ and $C_{22} = 6.4766 \times 10^{-8}\ m^{-2}$. Bennu has an equatorial inclination of 175 degrees with a constant rotation period of 4.297 hours and rotates about the z axis, meaning Bennu has a retrograde spin with respect to its orbit about the sun (Chesley et al., 2014).

3.3.1. Fully Constrained Asteroid Hovering

First, a simulation is performed for a body-fixed hovering position using the UK formulation results and the optimal controller. The hover location is set as $\mathbf{r}^* = [400, 0, 0]^T$ m. The initial conditions of the spacecraft are set as $\mathbf{r}(0) = [450, -75, -50]^T$ m and $\frac{d\mathbf{r}}{dt}(0) = [0.5, -0.5, -0.2]^T$ m/s in the body frame. The matrices for incorrect initial conditions are selected for critical damping with $K_\alpha = 0.5I_3$ and $K_\beta = K_\alpha^2/4 = 0.0625I_3$. The same initial conditions
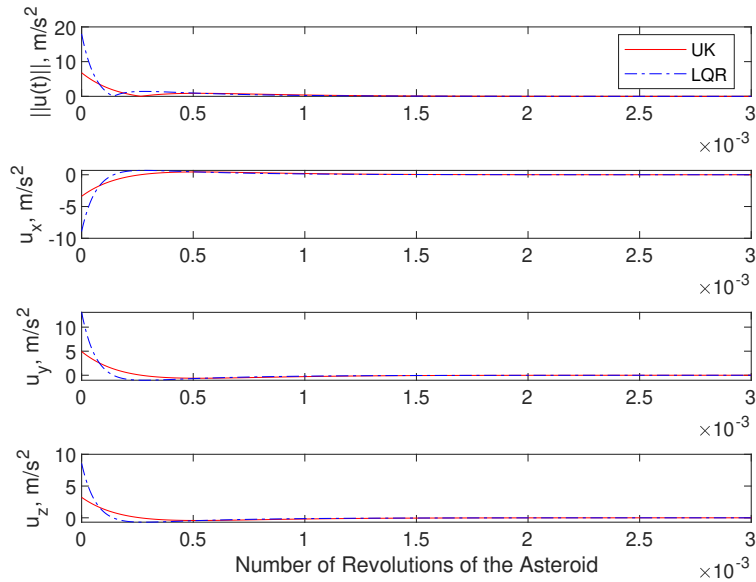
Figure 3.6   The transient control accelerations for asteroid body-fixed hovering.

were used for the simulation of the LQR controller with a selection of $Q_c =$ diag$(1/90^2, 1/90^2, 1/90^2, 1/15^2, 1/15^2, 1/15^2)$ and $R_c = 1/15^2 I_3$.

The spacecraft trajectories in the ACI and ACAF frames are shown in Figures 3.3 and 3.4. In these figures, the convergence of the UK method and the LQR controller only have slightly different paths, but are very close together. The maintenance of the hover position is the same, as the feedforward controller and the steady state UK solutions are identical. Both methods achieve the desired result of a body-fixed hover. Figure 3.5 shows the position components over time for each method. The difference in the paths taken by the UK constraint stabilization method and the LQR controller is more clearly seen here. For this selection of K_α, K_β, Q_c, and R_c both methods cause the spacecraft to converge to 2% of the initial displacement from the hover position in about 0.0015 revolutions or 24 seconds. Each of the position components converges to a constant value, representing each component of the desired hover position.

Figures 3.6 and 3.7 show the transient and steady state control accelerations expressed in the ACAF frame, given by the UK equations and the optimal controller. It can be seen in Figure 3.6, that the transient response of the LQR
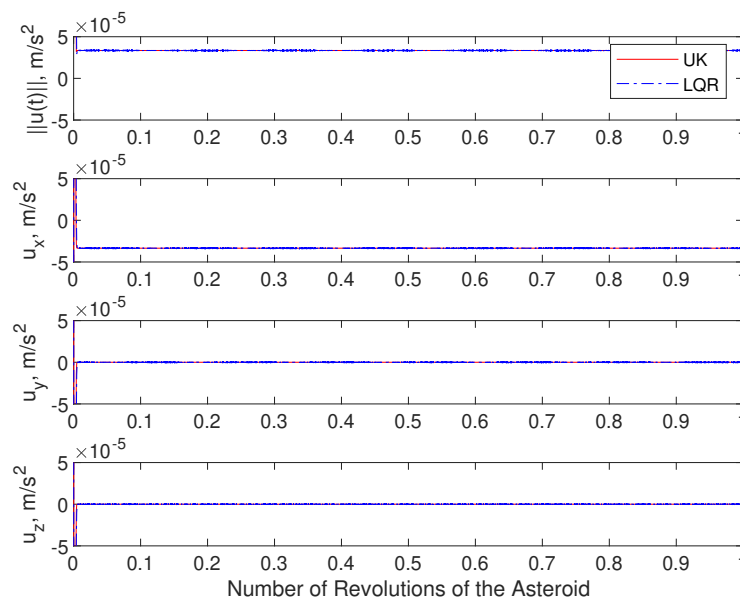
Figure 3.7 The steady state control accelerations for asteroid body-fixed hovering.
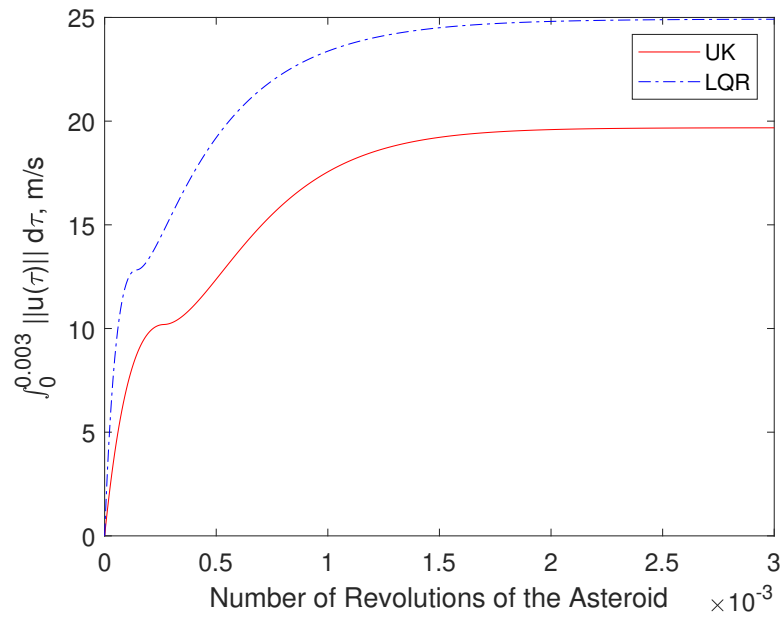
Figure 3.8 The transient integrated control effort to converge to and maintain the hover position.
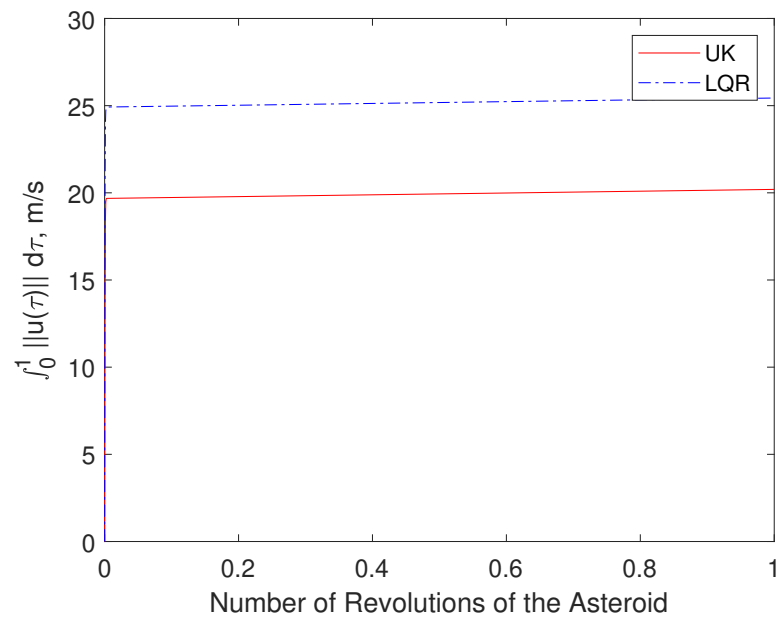
Figure 3.9 The steady state integrated control effort to converge to and maintain the hover position.

starts out with a larger required acceleration, but reduces more quickly than the UK method's accelerations. Both methods then settle down to the maintenance control to remain at the hover position. The maintenance controls are constant in
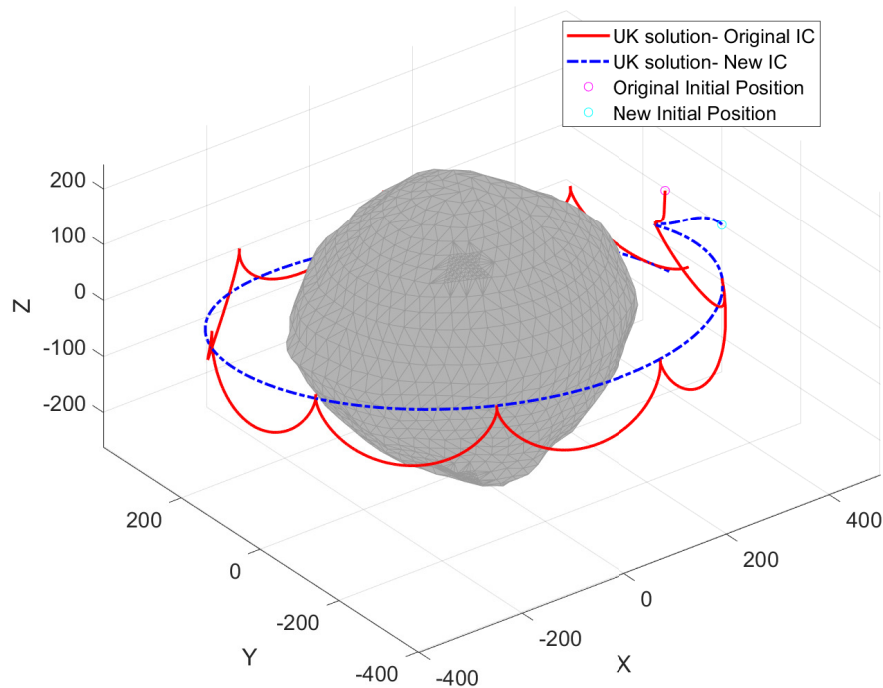
Figure 3.10   Spacecraft trajectory in the ACI frame for a trajectory based hover position for two different initial conditions.

the ACAF frame, as they are both just accounting for gravity of the fixed hover position and the rotation of the asteroid. The integrated control effort over time is shown in Figures 3.8 and 3.9. For the chosen selection of control parameters, the UK equations require a smaller transient integrated control effort of 19.7 m/s, while the LQR controller requires 24.9 m/s. However, in Figure 3.9 the steady state integrated control effort to maintain the hover over one revolution of the asteroid is roughly equivalent at 0.5 m/s for both methods. This is expected since the analytical expressions for the steady state maintenance were shown to be equivalent in Section 3.1.3. Overall, the UK method requires less total control effort for a spacecraft to move to and hover at a body-fixed position.

3.3.2. Under Constrained Asteroid Hovering

In the second case with the trajectory hover position, the vector to the center of the circle is set as $r_c = [400, 0, 0]^T$ m. The radius of the circle the spacecraft
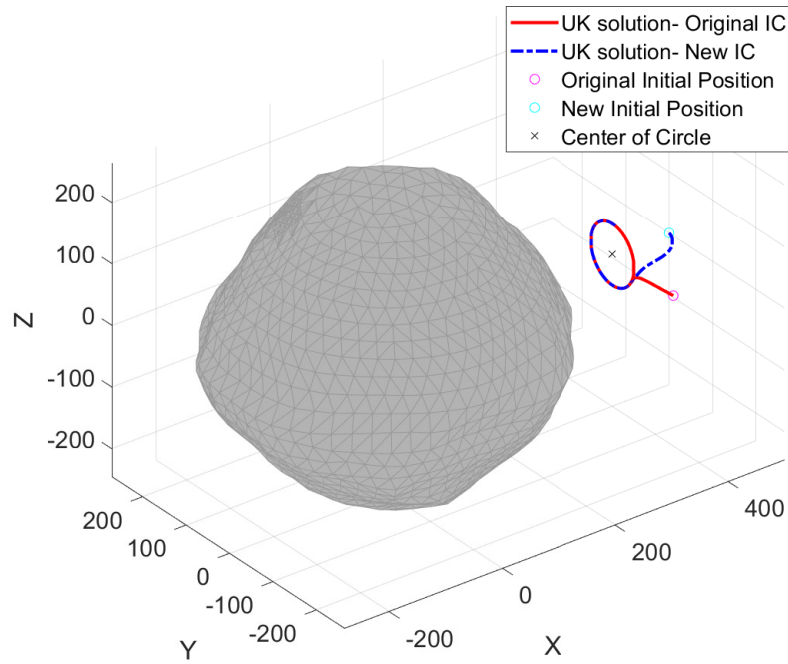
Figure 3.11   Spacecraft trajectory in the ACAF frame for a trajectory based hover position for two different initial conditions.
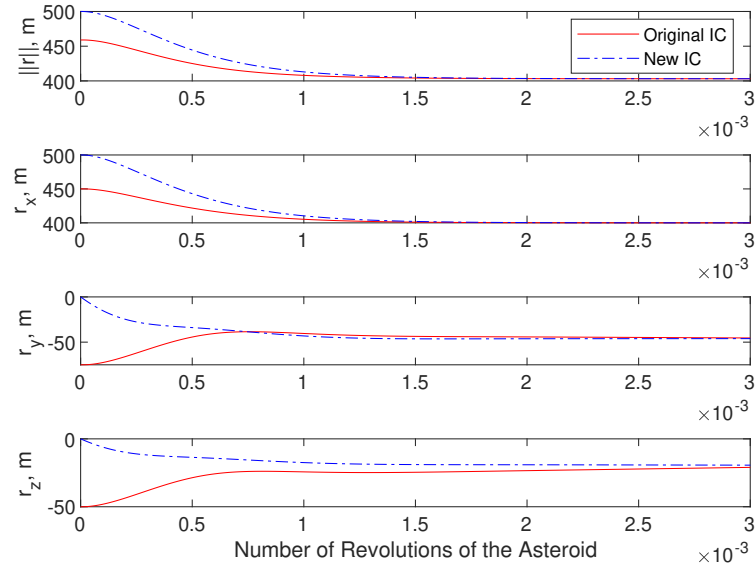
Figure 3.12   The transient position components are plotted over time for the two initial conditions.
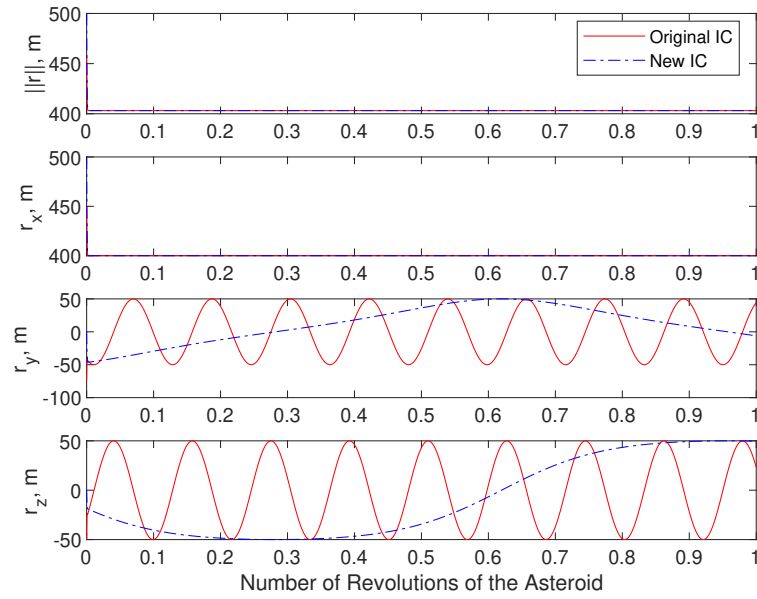
Figure 3.13 The steady state position components are plotted over time for the two initial conditions.
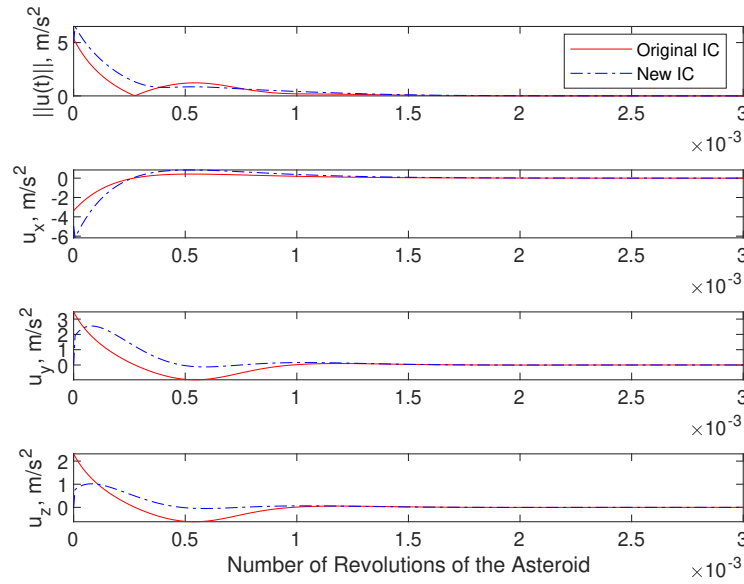
Figure 3.14 The transient control accelerations required for the trajectory hover for each initial condition.

is constrained to is $\rho = 50$ m. The same initial conditions are used as above for the UK formulation. Additionally, the under constrained hovering is given a second initial condition where $\mathbf{r}(0) = [500, 0, 0]^T$ m, which would cause the AA^T matrix to
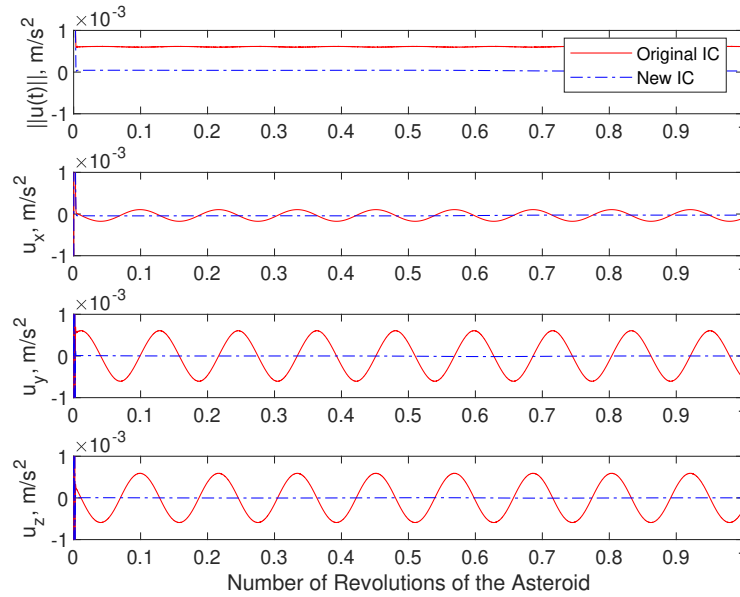
Figure 3.15 The steady state control accelerations required for the trajectory hover for each initial condition.
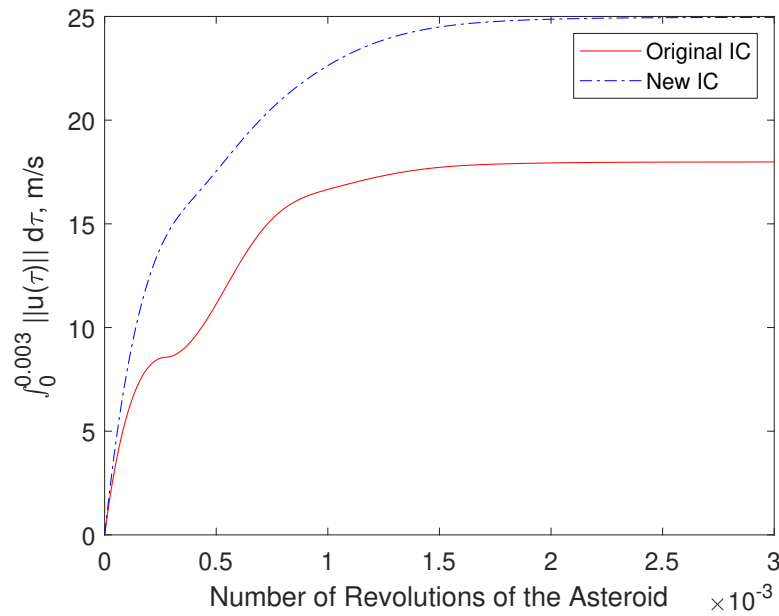
Figure 3.16 The transient integrated control effort for the trajectory hover.

be singular, but the MP inverse allows for this initial condition and UK equations still give the control accelerations for the spacecraft. The matrices for damping of the constraints are again selected for a critically damped case and are set as the same values as in the first simulation, but they are a different size with $K_\alpha = 0.5I_2$
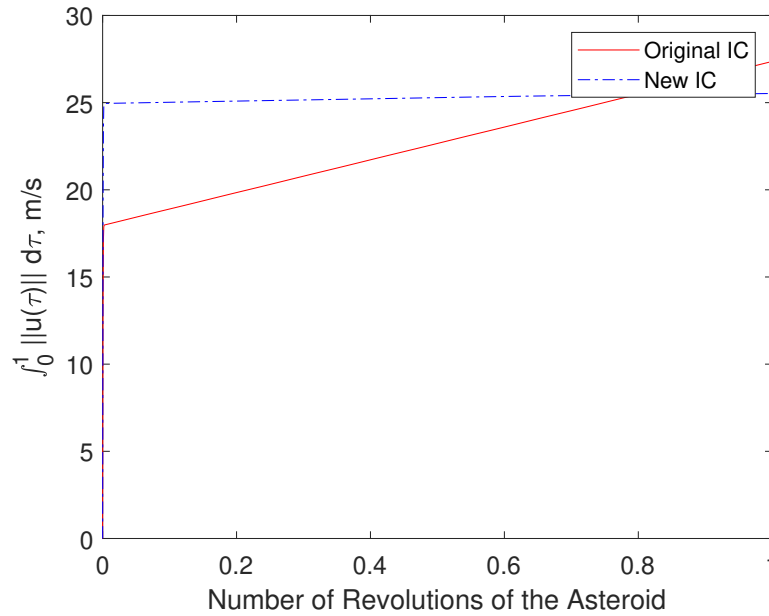
Figure 3.17   The steady state integrated control effort for the trajectory hover.

and $K_\beta = K_\alpha^2/4 = 0.0625 I_2$.

Figures 3.10 and 3.11 show the trajectories in the ACI and ACAF frames respectively. As seen, the spacecraft moves to and remains on the circlular intersection of the two constraints set. However, unlike before, now the spacecraft has to assert additional control to remain on the circle since it is free to move around on the circle. As mentioned before, since this is an under constrained system, the constraints only control the position of the spacecraft, but not how the spacecraft moves on the circle. The two initial conditions shown provide different behaviors once the spacecraft is on the circle. The second initial condition does not cause the spacecraft to move around the circle very quickly as the first initial condition does. Figures 3.12 and 3.13 display the position components of the spacecraft over time for both the transient and steady state response, respectively. The period the spacecraft has as it moves on the circle can be observed in the steady state response of the position. Figures 3.14 and 3.15 show the control accelerations, while Figures 3.16 and 3.17 show the integrated control effort. The second initial condition requires more initial control, but requires much less control

to maintain the constraints, since it ends up moving much slower around the circle. The integrated control effort for the maintenance of the time-varying hover position is larger than for the body-fixed hover. This is due to the spacecraft requiring additional control to account for its non-zero velocity since the spacecraft is applying accelerations to maintain the trajectory as well as to maintain the hover. The more quickly the spacecraft moves about the circular trajectory, maintaining the trajectory requires more input.

3.4. Conclusions

In this chapter, the UK formulation was utilized for a spacecraft to hover over an asteroid. An optimal controller was created using an LQR for a linearized system. The two methods were compared, which showed they had the same maintenance control, but different convergence paths from the initial conditions. A simulation about the asteroid of Bennu showed that, for equivalent settling times, the UK provided a lower total control response than the optimal LQR controller for the given control parameters. The UK formulation was then applied for a spacecraft to maintain a hover trajectory over Bennu.

As shown, the UK formulation can handle time-varying systems just as easily as time-invariant systems. The time-variance may be introduced from a tumbling asteroid or a time dependent hover position. The optimal controller shown here gains complexity when dealing with a tumbling asteroid; however, the feedforward controller incorporated becomes more difficult to derive for more complex hover positions. The UK method does require the dynamics of the system to be known in order to be applied, whereas the optimal controller includes the LQR feedback control law, which has potential to deal with some unmodeled dynamics and/or errors in the modeling. However, altering the uncontrolled system dynamics does not change any of the derivations to do with the constraints and vice versa, which allows for additional constraints, perturbations, or other forces to be accounted for easily in the UK framework.

4. Adaptive Asteroid Hovering Control

As shown in the Section 2.1 and Chapter 3, the UK formulation is a powerful and accurate tool for constrained motion analysis. The dynamics of a spacecraft about the asteroid are modeled in Section 2.2. The UK formulation is shown with its application for asteroid hovering in Chapter 3. However, the system dynamics must be known in order to get accurate results.

The goal of this chapter is to utilize the UK constrained motion analysis technique to control a spacecraft to hover over an asteroid in the presence of unknowns and/or parameter uncertainties in the system. Indirect adaptive control methods are implemented to the UK equations in the form of adaptive estimations. By augmenting those adaptive estimations with the UK technique, an adaptive estimation of the unconstrained dynamics can be obtained. However, in order for this augmented technique to give optimal results, the adaptive parameters need to converge to the actual unknown parameters of the system. Persistence of excitation (PE) is required for the adaptive estimates to converge to the true unknown values. Therefore, excitation is desired within the system to gain enough information from the dynamics of the system to be able to acquire the unknown parameters. The method of finite-time parameter estimation is used to estimate some of the parameters given assuming there is sufficient excitation in the system over a finite period of time. After the parameters are accurately estimated, that excitation is no longer necessary in the system.

4.1. Spacecraft Asteroid Hovering Dynamics with Unknown Gravitational Parameters of the Asteroid

Since it is assumed that the system includes unknown gravitational parameters, the dynamics need to be rewritten. In order to design the controller, the dynamics are first be converted into state space form. In general, the nonlinear dynamics of a system with unknowns can be expressed in state space form as,

$$\dot{\mathbf{x}} = \mathbf{f}(\mathbf{x}, \mathbf{u}, t) + \bar{G}(\mathbf{x}, \mathbf{u}, t)\boldsymbol{\Theta} \tag{4.1}$$

where $\mathbf{x} \in \mathbb{R}^{6n}$ is the state vector, $\mathbf{f}(\mathbf{x}, \mathbf{u}, t) \in \mathbb{R}^{6n}$ and $\bar{G}(\mathbf{x}, \mathbf{u}, t) \in \mathbb{R}^{6n \times s}$ make up the dynamics of the system, and $\boldsymbol{\Theta} \in \mathbb{R}^s$ is a vector of s unknown constants.

In the case of spacecraft asteroid hovering, the gravitational parameters of the asteroid, μ, C_{20}, and C_{22} are considered to be the unknown constants. Initially, it is assumed that only the angular velocity of the asteroid $\boldsymbol{\Omega}(t)$, the reference radius r_0, and an initial guess of μ are known, but the mass and the shape of the asteroid are unknown. Therefore, $\boldsymbol{\Theta}$ in Equation (4.1) takes the form,

$$\boldsymbol{\Theta} = \begin{bmatrix} \mu & C_{20}\mu r_0^2 & C_{22}\mu r_0^2 \end{bmatrix}^T \tag{4.2}$$

Note that the reference radius, although assumed as a known value, is also included in $\boldsymbol{\Theta}$. Therefore, factoring the unknowns out of Equation (2.29) results in,

$$U_{\mathbf{r}} = \bar{g}\boldsymbol{\Theta} \tag{4.3}$$

where,

$$\bar{g} = \begin{bmatrix} -\frac{1}{r^3}\mathbf{r} & -\frac{3}{r^5}F_\delta\mathbf{r} & \frac{3}{r^5}F_\lambda\mathbf{r} \end{bmatrix} \in \mathbb{R}^{3 \times 3} \tag{4.4}$$

is the partitioned matrix of the gravitational acceleration vector.

Assuming the unknowns in the spacecraft asteroid hovering dynamics in Equation (2.25) are given by $\boldsymbol{\Theta}$ in Equation (4.2), Equation (2.25) can be written in nonlinear state space form as in Equation (4.1), i.e.,

$$\dot{\mathbf{x}} = A_0\mathbf{x} + B\mathbf{u} + B\bar{g}\boldsymbol{\Theta} \tag{4.5}$$

where $\mathbf{x} = \begin{bmatrix} \mathbf{r}^T, & \dot{\mathbf{r}}^T \end{bmatrix}^T \in \mathbb{R}^6$ is the state vector of the spacecraft position and velocity in the ACAF frame,

$$A_0 = \begin{bmatrix} 0_{3\times3} & I_3 \\ -\dot{\Omega}^\times(t) - \Omega^{\times 2}(t) & -2\Omega^\times(t) \end{bmatrix} \in \mathbb{R}^{6\times6}, \quad B = \begin{bmatrix} 0_{3\times3} \\ I_3 \end{bmatrix} \in \mathbb{R}^{6\times3}$$

and the nonlinear terms are given by $\bar{g}$ in Equation (4.4).

4.2. Adaptive Control Design

Constrained motion analysis in the UK framework requires the exact dynamics of the system to be known, as they are used to obtain the minimized solution. Since $\boldsymbol{\Theta}$ in Equation (4.2) is unknown, the UK equations cannot be used directly. In order to apply the UK equations despite unknowns in the dynamics, adaptive control techniques are implemented. The adaptive controller developed here uses an indirect adaptive control formation and takes the form of a model reference adaptive controller (MRAC).

4.2.1. Implementation of Adaptive Estimates Into the UK Equation

Let $\hat{\boldsymbol{\Theta}}$ be the adaptive estimate of $\boldsymbol{\Theta}$. Since the unconstrained dynamics in Equation (3.5) contain unknowns due to $\boldsymbol{\Theta}$, an adaptive estimate of the unconstrained acceleration $\hat{\mathbf{a}}$ is developed by replacing the unknowns $\boldsymbol{\Theta}$ with $\hat{\boldsymbol{\Theta}}$ in Equations (4.3) and (3.5), i.e.,

$$U_{\mathbf{r}} = \bar{g}\hat{\boldsymbol{\Theta}} \tag{4.6}$$

$$\hat{\mathbf{a}} = -\dot{\Omega}^{\times}(t)\mathbf{r} - 2\Omega^{\times}(t)\dot{\mathbf{r}} - \Omega^{\times 2}(t)\mathbf{r} + \bar{g}\hat{\boldsymbol{\Theta}} \tag{4.7}$$

Replacing the unconstrained acceleration $\mathbf{a}$ in the point mass UK equation given by Equation (2.6) with the adaptive estimate of the unconstrained acceleration in Equation (4.7), the estimate of the constraint acceleration is obtained as,

$$\hat{\mathbf{a}}_c = A^+ \left(\mathbf{b} - A\hat{\mathbf{a}}\right) \tag{4.8}$$

This result can then be used as part of the control scheme as it replaces the unknowns in the solution obtained by the UK formulation with the adaptive estimates.

4.2.2. Reference System Modeling

Along with the dynamics of the system, a reference system needs to be created. In the case of constrained motion under unknown dynamics, the reference system

will be based on the dynamics required by the constraints. Let $\mathbf{x}_r \in \mathbb{R}^6$ be the state vector for the reference system. The reference system is then modeled as,

$$\dot{\mathbf{x}}_r = A_r \mathbf{x}_r + B\mathbf{u}_r \tag{4.9}$$

where,

$$A_r = \begin{bmatrix} 0_{3\times3} & I_3 \\ 0_{3\times3} & 0_{3\times3} \end{bmatrix} \in \mathbb{R}^{6\times6}$$

and $\mathbf{u}_r \in \mathbb{R}^3$ is the reference control input. In order to apply the same set of constraints on the reference system as the real system, the UK equation, Equation (2.6) is applied so $\mathbf{u}_r = A^+(\mathbf{b} - A\mathbf{a}_r)$. However, the reference system's unconstrained acceleration is $\mathbf{a}_r = \mathbf{0}$. Hence, the reference system becomes,

$$\dot{\mathbf{x}}_r = A_r \mathbf{x}_r + BA^+\mathbf{b} \tag{4.10}$$

4.2.3. Adaptive Control Law

With the reference system defined in Equation (4.10) and the dynamics given in Equation (4.5), the controller is chosen to be in the form of (Stackhouse et al., 2020):

$$\mathbf{u} = \hat{\mathbf{a}}_c - K_r\mathbf{e} = A^+\left(\mathbf{b} - A\hat{\mathbf{a}}\right) - K_r\mathbf{e} \tag{4.11}$$

where $\hat{\mathbf{a}}_c$ is given in Equation (4.8), $K_r \in \mathbb{R}^{3\times6}$ is a feedback gain matrix, and $\mathbf{e} = \mathbf{x} - \mathbf{x_r} \in \mathbb{R}^6$ is the error between the system states and the reference states. This controller is chosen since the UK equations give the minimum accelerations required to maintain a set of constraints. If $\hat{\Theta}$ converges to Θ, this controller provides the minimum accelerations needed to maintain the hover position. However, since Θ is unknown, the estimated UK solution will not be the correct solution as long as the adaptive estimates are not correctly estimated. To account for this error, the additional feedback gain is utilized to keep the system converging to the desired dynamics. Thus, by applying the control law in Equation (4.11) to

the dynamics in Equation (4.5), the closed-loop dynamics are obtained as,

$$\dot{\mathbf{x}} = A_r\mathbf{x} - BK_r\mathbf{e} + BA^+\mathbf{b} + B\mathbf{y} \tag{4.12}$$

where $\mathbf{y} = (\mathbf{a} - A^+A\hat{\mathbf{a}})$.

Pre-multiplying $\mathbf{y}$ in Equation (4.12) by A and using the first MP condition in Equation (2.7a) yields,

$$A\mathbf{y} = A\left(\mathbf{a} - A^+A\hat{\mathbf{a}}\right) = A\mathbf{a} - AA^+A\hat{\mathbf{a}} = A\left(\mathbf{a} - \hat{\mathbf{a}}\right) \tag{4.13a}$$

Applying Equation (3.5) and Equation (4.7) into Equation (4.13a) gives,

$$A\mathbf{y} = \mathbf{z} \tag{4.13b}$$

where $\mathbf{z} = A\bar{g}\tilde{\boldsymbol{\Theta}}$ and $\tilde{\boldsymbol{\Theta}} = \boldsymbol{\Theta} - \hat{\boldsymbol{\Theta}}$ is the difference between the actual unknown parameters and their adaptive estimates. Note that Equation (4.13b) is a consistent equation, and recall from Section 2.1.2.1 that the solution to that equation with minimum norm is:

$$\mathbf{y} = A^{\{1,4\}}\mathbf{z} = A^+\mathbf{z} \tag{4.13c}$$

where the last part in Equation (4.13c) follows since the MP inverse is also a $\{1,4\}$-inverse. According to Equation (4.13c) and the definitions for $\mathbf{z}$ given below Equation (4.13b), it is obtained that,

$$\mathbf{y} = A^+A\bar{g}\tilde{\boldsymbol{\Theta}} \tag{4.13d}$$

Substituting $\mathbf{y}$ from Equation (4.13d) into Equation (4.12) the closed-loop dynamics of the spacecraft over the asteroid are obtained as,

$$\dot{\mathbf{x}} = A_r\mathbf{x} - BK_r\mathbf{e} + BA^+\mathbf{b} + BA^+A\bar{g}\tilde{\boldsymbol{\Theta}} \tag{4.14}$$

Subtracting Equation (4.10) from Equation (4.14) aboves gives the tracking error dynamics as,

$$\dot{\mathbf{e}} = A_c\mathbf{e} + BA^+A\bar{g}\tilde{\boldsymbol{\Theta}} \tag{4.15}$$

where,

$$A_c = A_r - BK_r$$

Observing the error dynamics in Equation (4.15), the feedback gain matrix K_r can be selected. This control gain matrix K_r needs to be selected such that the matrix A_c is Hurwitz. Hence, if $\tilde{\Theta} = \mathbf{0}$, then the error will converge to zero over time. However, there is no guarantee that $\tilde{\Theta}$ converges to zero.

4.2.4. Lyapunov Stability Analysis

Since there is no guarantee that $\tilde{\Theta}$ converges to zero, Lyapunov's direct method is used to study stability of the tracking error dynamics. Let the Lyapunov candidate function be of the form (Stackhouse et al., 2020):

$$V = \mathbf{e}^T S \mathbf{e} + \tilde{\Theta}^T \sigma_\Theta^{-1} \tilde{\Theta} \tag{4.16}$$

where $S \in \mathbb{R}^{6 \times 6}$ and $\sigma_\Theta \in \mathbb{R}^{3 \times 3}$ are symmetric positive definite matrices $(S, \sigma_\Theta > 0)$. Taking the time derivative of the Lyapunov candidate and applying the error dynamics from Equation (4.15) results in,

$$\dot{V} = \mathbf{e}^T \left(A_c^T S + S A_c \right) \mathbf{e} + 2\tilde{\Theta}^T \left(\bar{g}^T A^+ A B^T S \mathbf{e} + \sigma_\Theta^{-1} \dot{\tilde{\Theta}} \right) \tag{4.17}$$

Since A_c is Hurwitz,

$$\forall Q = Q^T > 0 \quad \exists S = S^T > 0 \quad | \quad A_c^T S + S A_c = -Q \tag{4.18}$$

In addition to the second part of Equation (4.17), the adaptation law can be found as,

$$\dot{\tilde{\Theta}} = -\dot{\hat{\Theta}} = \sigma_\Theta \bar{g}^T A^+ A B^T S \mathbf{e} \tag{4.19}$$

This adaptation law causes the second term in $\dot{V}$ to vanish, i.e.,

$$2\tilde{\Theta}^T \left(\bar{g}^T A^+ A B^T S \mathbf{e} + \sigma_\Theta^{-1} \dot{\tilde{\Theta}} \right) = 0$$

Thus, for a selected positive definite matrix $Q = Q^T > 0$ and the adaptation law in

Equation (4.19), Equation (4.17) becomes,

$$\dot{V} = -\mathbf{e}^T Q \mathbf{e} \tag{4.20}$$

which is negative definite. Thus, from Lyapunov, it can be shown that $\mathbf{e}$ is bounded, which means that $\tilde{\Theta}$ is also bounded. Therefore, it is shown that $\dot{V}$ is bounded and $\ddot{V}$ is bounded, meaning $\dot{V}$ is uniformly continuous. According to Barbalat's lemma, this means that $\dot{V} \to 0$ as $t \to \infty$ proving that $\mathbf{e} \to \mathbf{0}$ and $\tilde{\Theta} \to \tilde{\Theta}_{ss}$ as $t \to \infty$ (Nguyen, 2018; Sastry, 1999). This guarantees that the states asymptotically track the reference trajectory, and that the vector of estimated parameters $\hat{\Theta}$ converges to some constant vector. However, the components of that constant vector are not necessarily the actual values of the system parameters Θ. In order for $\hat{\Theta}$ to converge to Θ, there needs to be PE within the system. The problem, however, is that PE is not easily attainable within nonlinear systems. Through a numerical simulation of the adaptive controller designed in this section, it is shown through the natural dynamics of hovering in a constant relative position with respect to the ACAF frame, along with the initial tracking convergence, that μ converges to its actual value. However, as expected, the other values in $\hat{\Theta}$ do not converge to Θ.

After a simulation of hovering over the asteroid for one revolution, the system had enough information in it for the estimated μ to converge to its true value. The other two unknowns, C_{20} and C_{22}, only converged to incorrect constants. The discussion in the next section takes place after the first revolution of the asteroid, and accounts for its new knowledge of μ. The controller is restructured based on this knowledge and a new estimation system is applied.

4.3. Restructuring the Adaptive Controller

Now that $\hat{\mu}$ converges to the actual value of μ of the asteroid via the adaptation law, the controller and dynamics can be restructured to account for the other two unknowns C_{20} and C_{22}. Equations (3.5) and (4.3) are altered for the remaining

unknown terms so that,

$$\mathbf{a}_2 = -\dot{\Omega}^{\times}(t)\mathbf{r} - 2\Omega^{\times}(t)\dot{\mathbf{r}} - \Omega^{\times 2}(t)\mathbf{r} - \frac{\mu}{r^3}\mathbf{r} + \bar{g}_2\boldsymbol{\Theta}_2 \tag{4.21a}$$

$$\bar{g}_2 = \begin{bmatrix} -\frac{3\mu r_0^2}{r^5}F_\delta\mathbf{r} & \frac{3\mu r_0^2}{r^5}F_\lambda\mathbf{r} \end{bmatrix}, \quad \boldsymbol{\Theta}_2 = \begin{bmatrix} C_{20}, & C_{22} \end{bmatrix}^T \tag{4.21b}$$

where $\bar{g}_2 \in \mathbb{R}^{3\times 2}$ is the restructured matrix of $\bar{g}$, $\boldsymbol{\Theta}_2 \in \mathbb{R}^2$ is the new vector of unknown parameters. The traditional equation for an unperturbed orbit $-\frac{\mu}{r^3}\mathbf{r}$ is given in Equation (4.21a), where only the perturbations of the gravitational acceleration due to irregular shape remain inside of the $\bar{g}_2\boldsymbol{\Theta}_2$ term. Note in this restructure of the controller, r_0 is also pulled out of $\boldsymbol{\Theta}_2$ leaving only the spherical harmonic constants C_{20} and C_{22}. Originally, the reference radius r_0 was put into $\boldsymbol{\Theta}$ as it affects the adaptation law. Factoring r_0 out into $\bar{g}_2$ changes how the adaptation law propagates the vector of unknowns for the controller as g is included in the adaptation law. This controller redesign requires that both μ and r_0 are factored out into $\bar{g}_2$.

Continuing with the adaptive controller design, $\hat{\boldsymbol{\Theta}}_2 \in \mathbb{R}^2$ is again the adaptive estimate of $\boldsymbol{\Theta}_2$ so that,

$$\hat{\mathbf{a}}_2 = -\dot{\Omega}^{\times}(t)\mathbf{r} - 2\Omega^{\times}(t)\dot{\mathbf{r}} - \Omega^{\times 2}(t)\mathbf{r} - \frac{\mu}{r^3}\mathbf{r} + \bar{g}_2\hat{\boldsymbol{\Theta}}_2 \tag{4.22}$$

is the adaptive estimate of the unconstrained dynamics. The constraints, the reference system, and the additional feedback gain in the controller do not need to be altered at all. Hence, the dynamics of the altered system are now,

$$\dot{\mathbf{x}} = A\mathbf{x} + B\mathbf{u}_2 - B\frac{\mu}{r^3}\mathbf{r} + B\bar{g}_2\boldsymbol{\Theta}_2 \tag{4.23}$$

Applying Equation (4.22), the controller takes an identical form to that in Equation (4.11), i.e.,

$$\mathbf{u}_2 = A^+ \left(\mathbf{b} - A\hat{\mathbf{a}}_2\right) - K_r\mathbf{e} \tag{4.24}$$

Substituting the controller above into the dynamics in Equation (4.23) gives,

$$\dot{\mathbf{x}} = A_r \mathbf{x} - BK_r \mathbf{e} + BA^+ \mathbf{b} + B\mathbf{y}_2 \tag{4.25}$$

where $\mathbf{y}_2 = (\mathbf{a}_2 - A^+ A\hat{\mathbf{a}}_2)$. Similarly to $\mathbf{y}$, the minimum norm solution of $\mathbf{y}_2$ can be obtained analogous to that in Equation (4.13d) and hence Equation (4.25) can be rewritten as,

$$\dot{\mathbf{x}} = A_r \mathbf{x} - BK_r \mathbf{e} + BA^+ \mathbf{b} + BA^+ A\bar{g}_2 \tilde{\mathbf{\Theta}}_2 \tag{4.26}$$

where $\tilde{\mathbf{\Theta}}_2 = \mathbf{\Theta}_2 - \hat{\mathbf{\Theta}}_2$ is the difference between the actual unknown parameters and the new adaptive estimates. Thus, the error dynamics between the system and the reference system take the form:

$$\dot{\mathbf{e}} = A_c \mathbf{e} + BA^+ A\bar{g}_2 \tilde{\mathbf{\Theta}}_2 \tag{4.27}$$

Thus, similar to that in Section 4.2.4, Lyapunov's direct method is used to study the stability of the closed-loop dynamics obatained using the restructured controller. The Lyapunov function is defined as,

$$V_2 = \mathbf{e}^T S \mathbf{e} + \tilde{\mathbf{\Theta}}_2^T \sigma_{\Theta2}^{-1} \tilde{\mathbf{\Theta}}_2 \tag{4.28}$$

where $\sigma_{\Theta2} \in \mathbb{R}^{2\times2}$ and $\sigma_{\Theta2} = \sigma_{\Theta2}^T > 0$. By choosing the adaptation law for the new adaptive estimates to be,

$$\dot{\hat{\mathbf{\Theta}}}_2 = -\dot{\tilde{\mathbf{\Theta}}}_2 = \sigma_{\Theta2} \bar{g}_2^T A^+ A B^T S \mathbf{e} \tag{4.29}$$

the time derivative of the Lyapunov function becomes,

$$\dot{V} = -\mathbf{e}^T Q \mathbf{e} \tag{4.30}$$

which is negative definite. Therefore, as in Section 4.2.4, using Barbalat's lemma, asymptotic tracking of the reference states is guaranteed. However, the adaptive estimates are, again, not guaranteed to converge to the actual parameters. In order to guarantee the convergence of the estimator, instead of leaving the

adaptive estimates to naturally adapt over time, the finite-time estimation method introduced in Adetola and Guay (2008) is used, and sufficient conditions for PE required to estimate the unknown parameters within a finite time are studied.

4.4. Finite-Time Parameter Estimation

The method of finite-time parameter estimation is useful since once the parameters are estimated, they no longer need to be updated. Although this method still requires PE, it allows estimation to occur over a finite time. In addition, this method can also work if there is some temporary excitation in the system. Once the parameters are estimated, the excitation is no longer needed. Let $\hat{\mathbf{x}}$ be the state estimate with dynamics of (Adetola & Guay, 2008),

$$\dot{\hat{\mathbf{x}}} = A_0\mathbf{x} + B\mathbf{u}_2 + B\bar{g}_2\hat{\mathbf{\Theta}}_2 + k\boldsymbol{\epsilon} + w\dot{\hat{\mathbf{\Theta}}}_2 \tag{4.31}$$

where $k \in \mathbb{R}^{6\times6}$, $k = k_1 + k_2(t)$, $k_1 > 0$ and $k_2(t) \geq 0$, $\boldsymbol{\epsilon} = \mathbf{x} - \hat{\mathbf{x}}$ is the error of the estimated states, and $w \in \mathbb{R}^{6\times2}$ is a filter with dynamics of,

$$\dot{w} = B\bar{g}_2 - kw, \quad w(0) = 0 \tag{4.32}$$

Note that in Equation (4.31) the dynamics of the estimated states $\hat{\mathbf{x}}$ are estimates of how the actual states would propagate given the adaptive estimates. They are not estimated states based on an estimate of the actual state such as with an observer system. The error dynamics between the actual system and the estimated system are:

$$\dot{\boldsymbol{\epsilon}} = B\bar{g}_2\tilde{\mathbf{\Theta}}_2 - k\boldsymbol{\epsilon} - w\dot{\hat{\mathbf{\Theta}}}_2 \tag{4.33}$$

Let $\boldsymbol{\eta} = \boldsymbol{\epsilon} - w\tilde{\mathbf{\Theta}}_2$. Then, it follows that $\boldsymbol{\eta}$ has dynamics of,

$$\dot{\boldsymbol{\eta}} = -k\boldsymbol{\eta}, \quad \boldsymbol{\eta}(0) = \boldsymbol{\epsilon}(0) \tag{4.34}$$

Thus, for some $\bar{Q} \in \mathbb{R}^{2\times2}$ and $\mathbf{C} \in \mathbb{R}^2$ generated by,

$$\dot{\bar{Q}} = w^Tw, \quad \bar{Q}(0) = 0 \tag{4.35}$$

$$\dot{\mathbf{C}} = w^T(w\hat{\mathbf{\Theta}}_2 + \boldsymbol{\epsilon} - \boldsymbol{\eta}), \quad \mathbf{C}(0) = \mathbf{0} \tag{4.36}$$

if there exists a time t_c such that $\bar{Q}(t_c)$ is invertible and positive definite,

$$\bar{Q}(t_c) = \int_0^{t_c} w^T(\tau)w(\tau)d\tau > 0 \tag{4.37}$$

then the unknown vector $\mathbf{\Theta}_2$ can be found by,

$$\mathbf{\Theta}_2 = \bar{Q}^{-1}(t)\mathbf{C}(t), \quad t \geq t_c \tag{4.38}$$

Thus, the exact value of $\mathbf{\Theta}_2$ can be found if the matrix $\bar{Q}$ becomes positive definite. The inequality condition given in Equation (4.37) indicates whether the system has PE, i.e. if $\bar{Q}$ is always positive definite after the finite time t_c, then the system contains PE.

This finite-time estimation method and the reconstructed adaptive controller in Equation (4.24) are applied to the spacecraft hovering over the asteroid. However, since staying in the fixed hover position does not provide enough excitation in the system, artificial excitation is created by causing a disturbance in the hover. This is achieved by applying some disturbance control acceleration shortly to cause the spacecraft to have a nonzero velocity $\dot{\mathbf{r}}$. Once the inequality condition given in Equation (4.37) holds true for at least a temporary amount of time, the adaptive estimate of the system parameters is set to $\hat{\mathbf{\Theta}}_2 = \bar{Q}^{-1}\mathbf{C}$, feeding the correct parameters to the controller given in Equation (4.24). Since the controller in Equation (4.24) is designed based on the UK constrained motion analysis, the use of correct parameter estimates in the controller results in the minimum required accelerations needed to maintain the desired constraints, in this case the desired hover position.

4.5. Numerical Simulation Results and Discussion

The controllers developed above are applied in numerical simulations to control a spacecraft to hover over the asteroid Bennu. As discussed in Section 3.3, asteroid Bennu has a gravitational parameter of $\mu = 5.2\,\mathrm{m^3/s^2}$ with a density

of $\rho = 1.26\,\mathrm{g/cm^3}$ (Chesley et al., 2014). The shape of Bennu has major axes as $L_1 = 565\,\mathrm{m}$, $L_2 = 535\,\mathrm{m}$, and $L_3 = 508\,\mathrm{m}$, leading to $\beta = 0.9469$ and $\gamma = 0.8991$ (Nolan et al., 2013). It is assumed that the actual values of C_{20} and C_{22} are obtained using the relations given in Equation (2.24). From these relations, the actual spherical harmonic constants are found to be $C_{20} = -3.5061 \times 10^{-7}\,\mathrm{m^{-2}}$ and $C_{22} = 6.4766 \times 10^{-8}\,\mathrm{m^{-2}}$. The initial parameter estimates are chosen as 130% of the actual gravitational parameter ($6.76\,\mathrm{m^3/s^2}$) and assume the asteroids shape is a perfect sphere ($C_{20} = C_{22} = 0$). Bennu has an equatorial inclination of 175 degrees with a rotation period of 4.297 hours and rotates about the z axis, meaning Bennu rotates retrograde with respect to its orbit about the sun. The hover location is set as $\mathbf{r}^* = [400, 0, 0]^T\,\mathrm{m}$.

The first controller developed, as given in Equation (4.11), is applied first for the spacecraft to converge to the hover point and remain there. After μ has been estimated through the natural convergence of the adaptive estimate, the perturbing control is applied shortly to disturb the hover. Then, the restructured controller given in Equation (4.24) is applied to find the remaining unknown parameters to minimize the control accelerations for maintaining the hover position. Even if the parameters are not estimated, the controller still completes its objective of hovering. Additionally, the controller developed in Equation (4.11) is also applied for the under constrained scenario explored in Section 3.2.

4.5.1. Model Reference Adaptive UK Control Law

For the spacecraft to hover at the desired hover position, the spacecraft is fully constrained via the constraints in Equation (3.1a). The controller in Equation (4.11) is given the A matrix and $\mathbf{b}$ vector derived in Section 3.1:

$$A = I_3 \tag{3.3a}$$

$$\mathbf{b} = \left(\Omega^{\times^2}(t) + \dot{\Omega}^{\times}(t) + K_\alpha \Omega^{\times}(t) + K_\beta \right)(\mathbf{r}^* - \mathbf{r}) - \left(2\Omega^{\times}(t) + K_\alpha \right)\dot{\mathbf{r}} \tag{3.3b}$$

The spacecraft initial position and velocity with respect to the ACAF frame are set to be $\mathbf{r}(0) = [450, 75, -50]^T$ m and $\dot{\mathbf{r}}(0) = [0.5, 0.1, -0.2]^T$ m/s, respectively.

The control gain K_r in Equation (4.11) needs to be selected such that A_c becomes Hurwitz. Several methods, such as the linear quadratic regulator, could be applied to find an optimal gain. In this case, K_r is selected to be $K_r = [0.0001 I_3, 0.02 I_3]$, which turns A_c into that of a critically damped oscillator. Note that the relatively slow convergence values selected here help with the estimation of the unknown parameters as it allows more time while the spacecraft is still converging to the desired hover position. This means the spacecraft is moving relative to the asteroid and allows the controller to get more information from the dynamics for the estimation. The gains for Baumgarte's constraint stabilization method are also selected to be critically damped with the same values as given in K_r, $K_\alpha = 0.02 I_3$ and $K_\beta = K_\alpha^2 / 4 = 0.0001 I_3$.

The adaptation gain is chosen as $\sigma_\Theta = \text{diag}\{1, 100, 10\}$. The first element of the
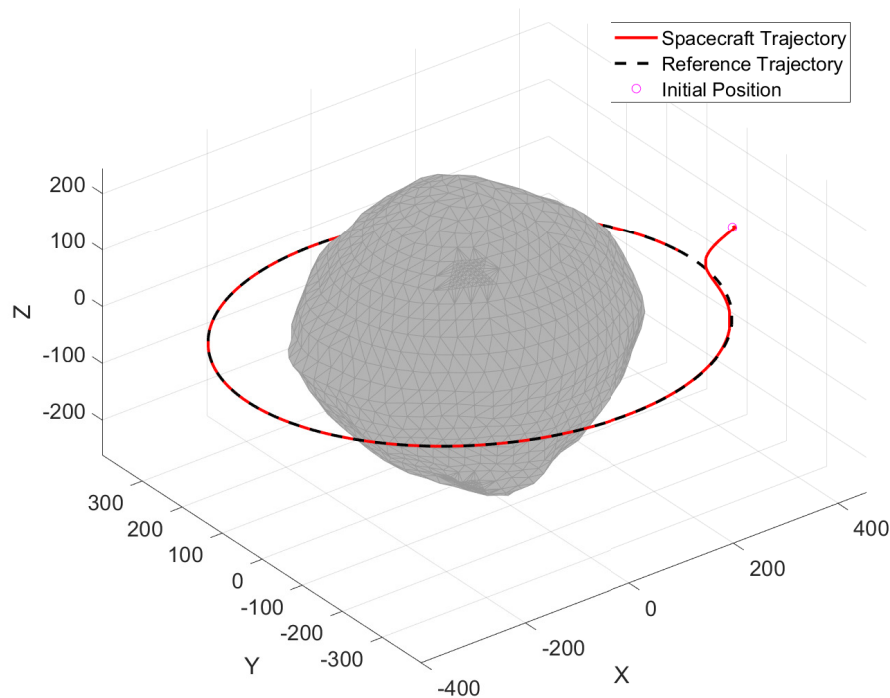
Figure 4.1 Spacecraft trajectory in the ACI frame using the adaptive control law in Equation (4.11).
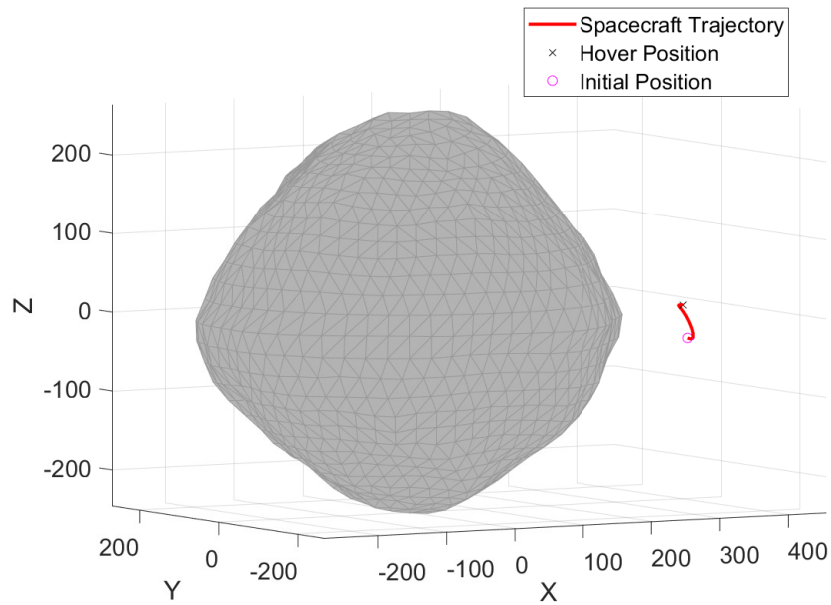
Figure 4.2 Spacecraft trajectory in the ACAF frame using the adaptive control law in Equation (4.11).
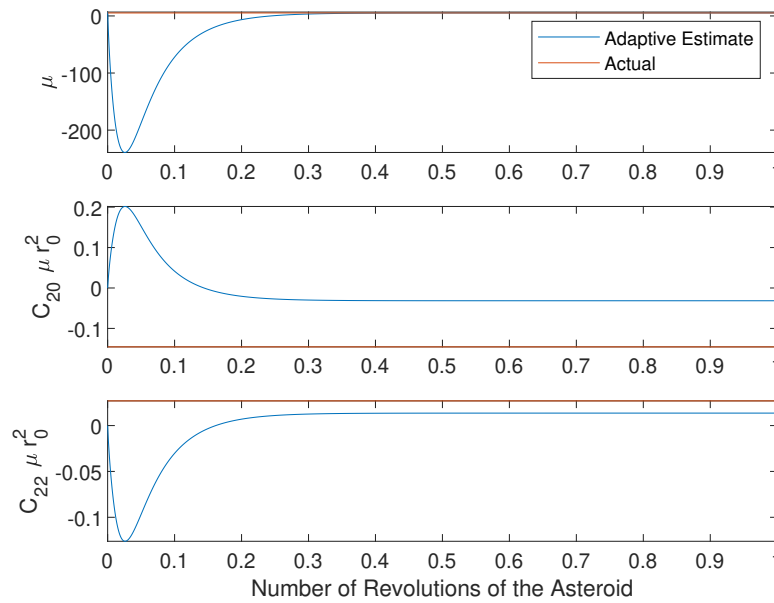
Figure 4.3 The adaptive estimates of the unknown parameters plotted over time.

adaptation gain σ_Θ controls how the estimated value of μ changes. The choice of a large value for that element will result in large jumps and oscillation. On the other hand, the choice of a small value for that element will result in less oscillation, but
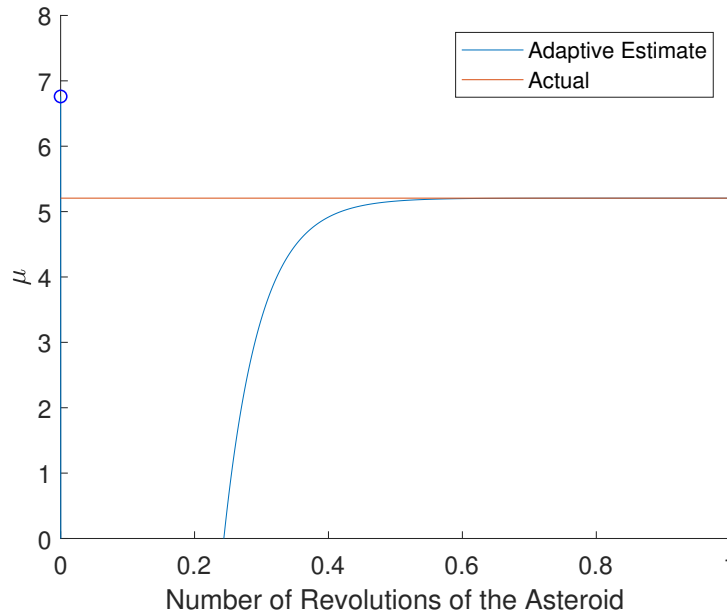
Figure 4.4 Magnified figure of the first adaptive estimate of the unknown parameters plotted over time.

it increases the settling time. In the Lyapunov stability analysis, the matrix Q in Equation (4.20) is selected as $Q = I_6$.

With these initial conditions and control settings, the controller was applied to hover over the surface of Bennu. Figure 4.1 shows the spacecraft trajectories in the ACI frame and Figure 4.2 is the trajectory in the ACAF frame. As can be seen, the controller causes the spacecraft to track the reference trajectory, despite only having an initial guess at the mass of the asteroid and not knowing the shape. This result is expected as the controller was proven to have asymptotic tracking of the reference system via the Lyapunov stability proof shown above starting at Equation (4.16).

However, the adaptive estimates were not guaranteed to converge to the correct values. In Figure 4.3, the adaptive estimates can be seen propagated over one full rotation of the asteroid Bennu. The first value, i.e. the estimate of μ, has a large jump, but then converges to the true value through the system dynamics' natural excitation. Figure 4.4 is a magnified picture of the convergence of the first adaptive estimate. The system provided enough excitation within that time to allow for the
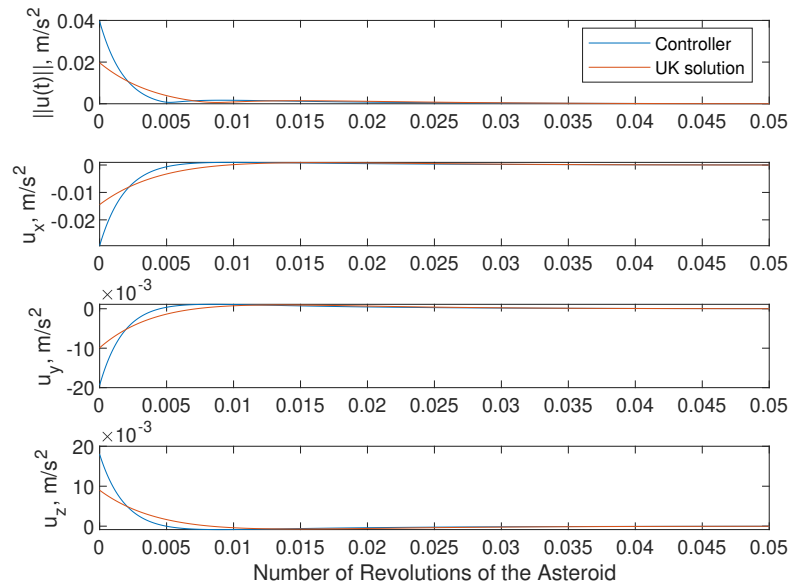
Figure 4.5 The transient control accelerations of the adaptive controller compared to the solution obtained by the UK equation.
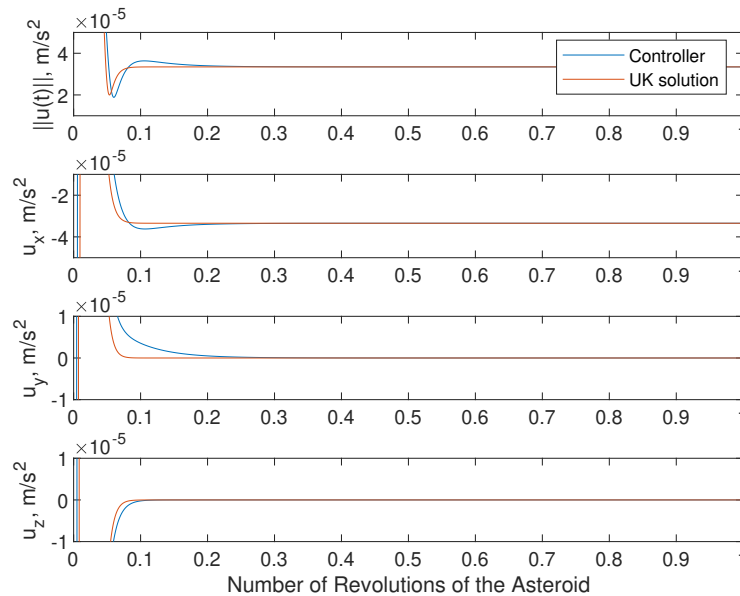
Figure 4.6 The steady state control accelerations of the adaptive controller compared to the solution obtained by the UK equation.

convergence of the adaptive estimate $\hat{\mu}$. The first value in σ_Θ determines the gain that propagates $\hat{\mu}$ in the adaptation law. As mentioned before, making this value larger causes an even larger jump, and causes oscillation of $\hat{\mu}$ before converging, and a smaller value reduces the initial jump, but increases the time required for the

parameter estimation to converge. The estimated values of second degree and order spherical harmonics $\hat{C}_{20}$ and $\hat{C}_{22}$, however, converge to constant values that are not necessarily the correct values of C_{20} and C_{22}.

The required control input accelerations to control the spacecraft are displayed in Figures 4.5 and 4.6. The controller given in Equation (4.11) is compared to the solutions given by the UK constraint equations with the correct dynamics. The transient response in Figure 4.5 is much larger in magnitude to start, to account for the initial conditions, but, as shown the response settles down quickly. Since the spacecraft is hovering in a body-fixed position relative to the asteroid, the steady state response of the control accelerations settle down to constant values, as the spacecraft is only accounting for the gravitational acceleration and the rotation of the asteroid. It can be seen that the control settles down in the negative $\hat{\mathbf{r}}^*$ direction, which shows that the asteroid's gravity is not enough to maintain the height of the hover and the spacecraft needs to accelerate inward toward the asteroid in order to stay in the desired hover position due to the rotation of the
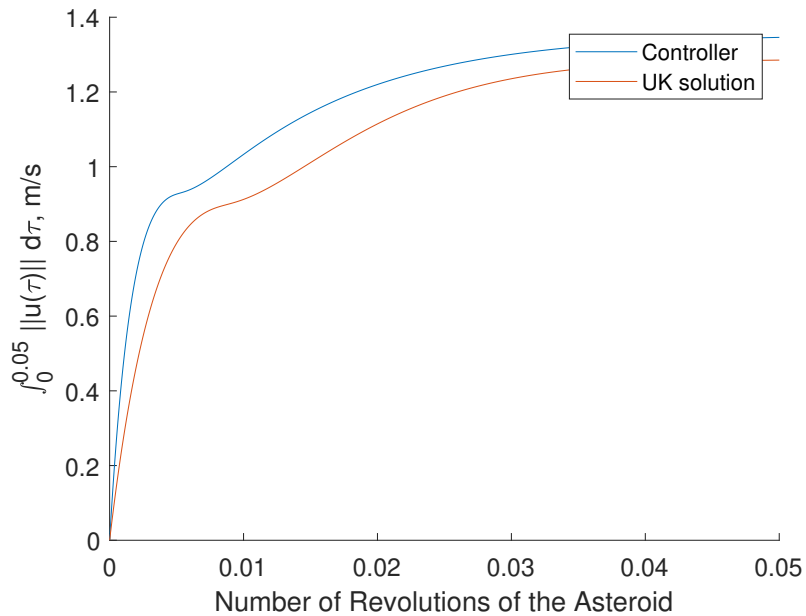
Figure 4.7 The transient integrated control effort required by the controller and the UK equation.
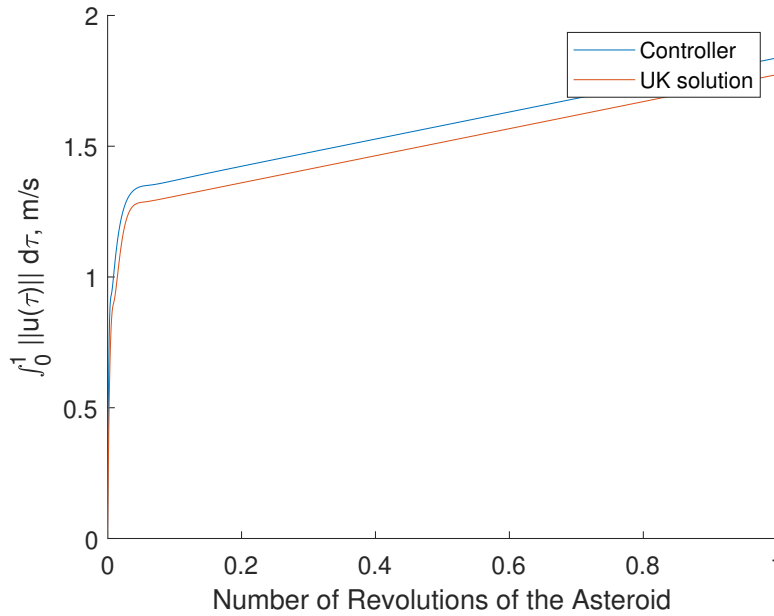
Figure 4.8 The steady state integrated control effort required by the controller and the UK equation.

asteroid. Both the controller and the UK solutions converge to the same value as they are both achieving the same result of hovering.

Figures 4.7 and 4.8 show the total integrated control effort over the full revolution of the asteroid for both the adaptive controller and the UK constraint equations. The adaptive controller requires more control effort in transient response, due to the unknown parameters and the estimation period. The steady state effort appears to have an identical slope for either method implemented. This can be explained, as the spacecraft is fully constrained, so there is only a single solution. However, since the natural propagation of the $\hat{\Theta}$ does not result in the convergence of C_{20} and C_{22}, the adaptive controller has a slightly higher slope during the maintenance of the desired hover as it has to account for the incorrect estimates and thus an incorrect solution.

Overall, the total control used by both the adaptive controller and the UK solutions are comparable and are within about $0.064\,\mathrm{m/s}$ of each other. The model reference feedback gain included in the controller accounts for the tracking control of the spacecraft, especially during the adaptive estimation period. Note that,
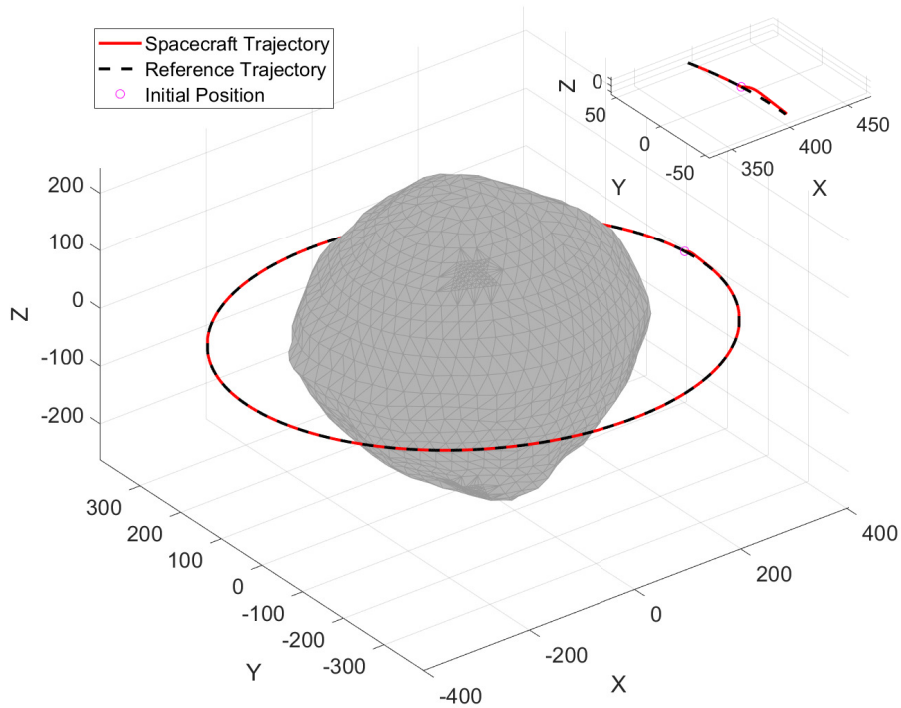
Figure 4.9 Spacecraft trajectory in the ACI frame using the restructured controller in Equation (4.24).

since μ is the largest factor in the gravitational acceleration of the asteroid, and since it is accurately estimated through the hovering dynamics, the remaining adaptive estimates will only account for a small perturbation to the gravitational acceleration. The secondary objective however, is to achieve the minimum control required, which requires the remaining parameter estimates to converge as well.

4.5.2. Restructured Controller and Remaining Parameter Estimation

Once the previous simulation ends, and μ is estimated correctly, the controller is restructured as in Section 4.3 to account for only two remaining unknowns. The next simulation represents the time immediately following the previous simulation, so the spacecraft is now hovering at the desired hover position. Since estimation of the unknown parameters is desired, the restructured controller in Section 4.3 and the finite-time estimation method discussed in Section 4.4 are implemented to accurately estimate the remaining two unknown parameters. However, the
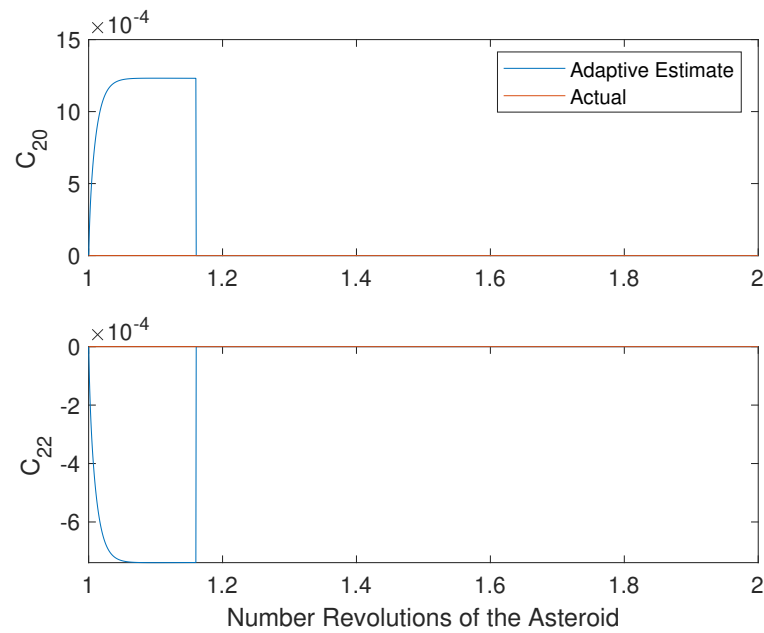
Figure 4.10 The remaining adaptive estimates of the unknown parameters plotted over time. The finite time estimation method is used in order to correctly estimate the remaining two parameters.
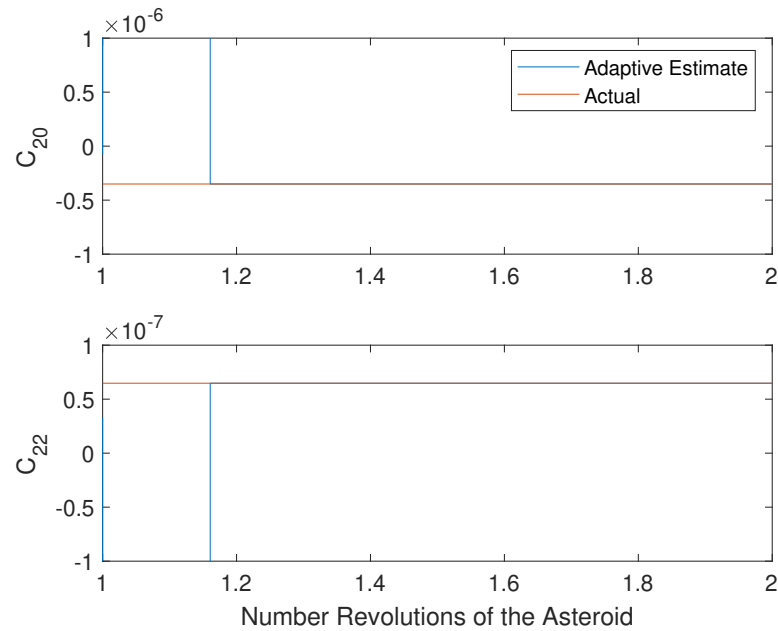
Figure 4.11 Magnified figure of the results of the finite time estimation method used to correctly estimate the remaining two parameters.

natural dynamics of the closed-loop system do not provide enough excitation

within the system for the parameters to naturally converge or for the excitation

condition given in Equation (4.37) to be satisfied. In order to introduce more excitation into the system, a disturbance control input is applied shortly to create a disturbance in the spacecraft's hover. The disturbance acceleration applied is $\mathbf{u}_d = [0.1, 0, 0]^T$ m/s^2 for 2 seconds. This initial disturbance introduces initial excitation
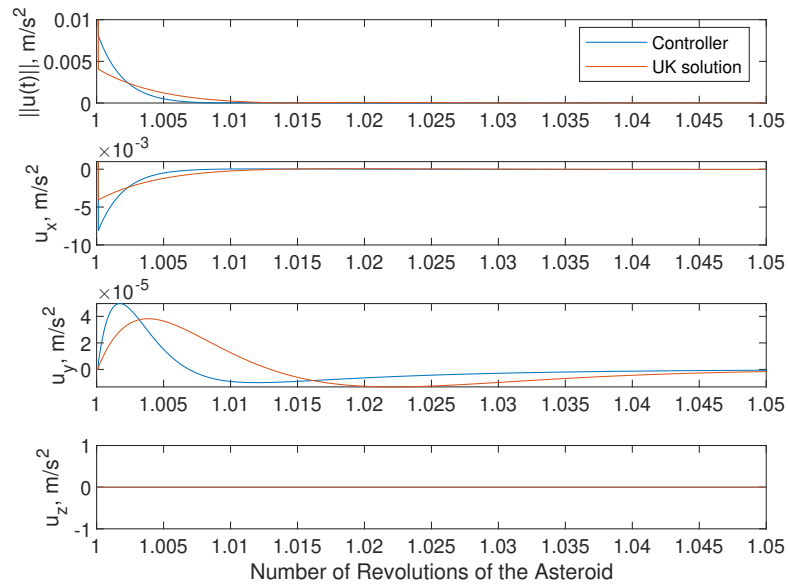
Figure 4.12 The transient control accelerations of the restructured adaptive controller compared to the solution obtained by the UK equation.
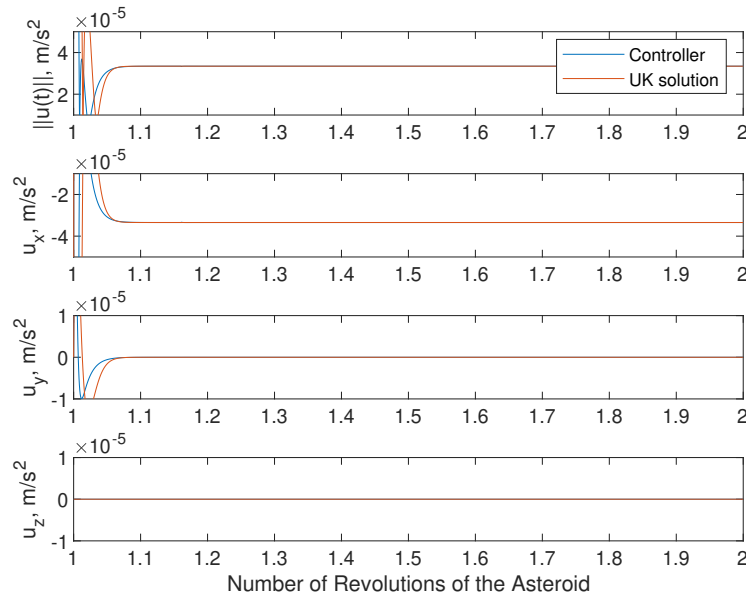
Figure 4.13 The steady state control accelerations of the restructured adaptive controller compared to the solution obtained by the UK equation.

into the system, causing Equation (4.37) to be satisfied, allowing the estimation of the remaining two parameters. This simulation starts after one revolution of the asteroid, T_p. The spacecraft is hovering, so it has an initial position and velocity of $\mathbf{r}(T_p) = [400, 0, 0]^T$ m and $\dot{\mathbf{r}}(T_p) = [0, 0, 0]^T$ m/s. The feedback gain K_r and the gains dictating Baumgarte's constraint stabilization method, K_α and K_β, remain the same as in the first controller. The new adaptation gain is chosen as $\sigma_{\Theta 2} = \text{diag}\{10, 1\} \times 10^{-6}$ with positive definite matrices Q and S the same as in the previous case. The initial states of the estimated system are $\hat{\mathbf{x}}(0) = [400, 0, 0, 0, 0, 0]^T$, which correspond to the desired hover position and velocity. The gain matrices for the finite-time estimation method are selected as $k_1 = I_6$ and

$$k_2 = \frac{1}{4} B \bar{g}_2 \sigma_{\Theta 2} \bar{g}_2^T B^T$$

The spacecraft is simulated for another rotation of the asteroid Bennu, using the restructured adaptive controller and the initial conditions given above. Figure 4.9 shows the spacecraft trajectory in the ACI frame. Again, it is seen that even with the initial disturbance control input to the spacecraft, the controller asymptotically tracks the reference system. The parameter estimates are again not guaranteed, which is shown in the first part of Figure 4.10. At around 1.17 periods, the finite-time parameter estimation occurs and the adaptation law for the estimated parameters used in the controller is overwritten. Figure 4.11 displays the accuracy of the finite-time estimation method. Due to the artificial excitation in the system, the last two unknown parameters are estimated accurately.

Now that the controller has all the correct parameters about the asteroid of Bennu, and it is already implementing the UK constraint equations as part of its control, it is using the minimum accelerations required to maintain the desired constraints, which in this case is hovering. Figures 4.12 and 4.13 show the input accelerations from the adaptive controller and the UK equations. Again, in Figure 4.12 there is a larger transient response to account for the disturbance
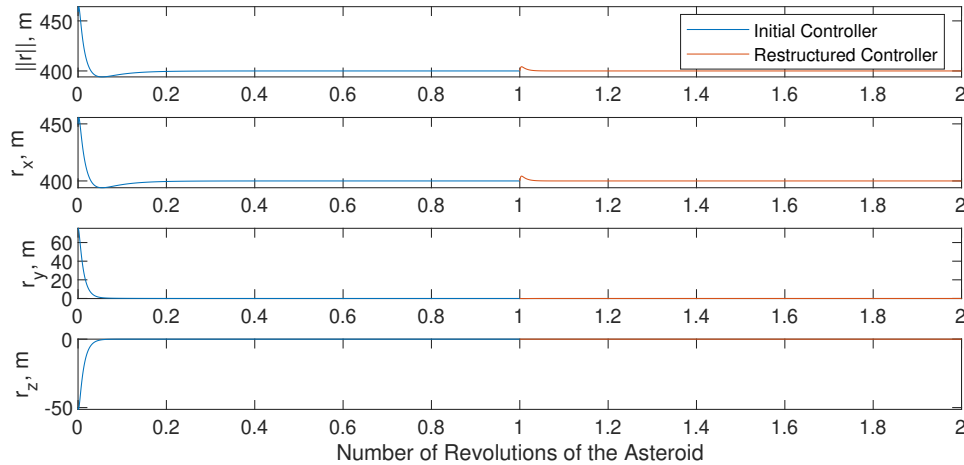
Figure 4.14   Spacecraft position components plotted over two revolutions of the asteroid.
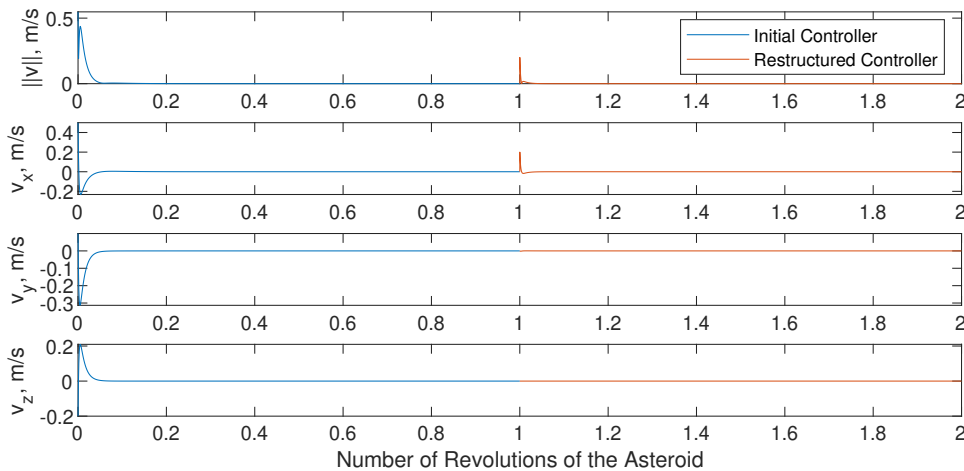
Figure 4.15   Spacecraft velocity components plotted over two revolutions of the asteroid.

introduced initially, but then in Figure 4.13 the control responses settle down to constant values for the steady state response, which is to maintain the desired hover position. The adaptive controller input accelerations will now match with the results obtained by the UK constrained motion analysis for maintenance of the desired hover. Using the parameters obtained, only the convergence of the constraints due to the controller will be different from the results obtained by the UK constrained motion analysis, due to the initial error of the estimates and the feedback gain included with the controller.

The full position and velocity components of the spacecraft over the two revolutions of the asteroid are shown in Figures 4.14 and 4.15. In the first half, the spacecraft tracks and converges to the reference trajectory while one of the adaptive estimates converges naturally. Then there is the external disturbance applied by the controller briefly, then the controller causes the spacecraft to converge again to the reference while also acquiring the remaining unknown parameters.

4.5.3. Application of the Adaptive Controller to an Under Constrained System

In this section it is assumed that the spacecraft is constrained to hover on the circular trajectory provided by the constraints in Equation (3.17). Recall the A matrix and $\mathbf{b}$ vector are obtained as,

$$A = \begin{bmatrix} \frac{\mathbf{r}_c^T}{r_c} \\ (\mathbf{r} - \mathbf{r}_c)^T \end{bmatrix} \tag{3.20a}$$

$$\mathbf{b} = \begin{bmatrix} 0 \\ -\dot{\mathbf{r}}^T\dot{\mathbf{r}} - (\mathbf{r} - \mathbf{r}_c)^T\dot{\Omega}^\times(t)(\mathbf{r} - \mathbf{r}_c) \end{bmatrix} - K_\alpha \begin{bmatrix} \dot{\Phi}_1 \\ \dot{\Phi}_2 \end{bmatrix} - K_\beta \begin{bmatrix} \Phi_1 \\ \Phi_2 \end{bmatrix} \tag{3.20b}$$

Thus the adaptive controller in Equation (4.11) can be applied with A and $\mathbf{b}$ above for the spacecraft to maintain the under constrained system despite the unknowns in the dynamics. The spacecraft is given the same initial conditions and control parameters as those specified in Section 4.5.1 above, i.e. the initial position and velocity of $\mathbf{r}(0) = [450, 75, -50]^T$ m and $\dot{\mathbf{r}}(0) = [0.5, 0.1, -0.2]^T$ m/s. The control matrices are set as $K_r = [0.0001I_3, 0.02I_3]$, $K_\alpha = 0.02I_3$, $K_\beta = K_\alpha^2/4 = 0.0001I_3$, $\sigma_\Theta = \text{diag}\{1, 100, 10\}$, and $Q = I_6$. However, two different initial conditions are explored for the reference system. First the reference system is also given the same initial condition as the spacecraft above, i.e. $\mathbf{r}_{r1}(0) = [450, 75, -50]^T$ m and $\dot{\mathbf{r}}_{r1}(0) = [0.5, 0.1, -0.2]^T$ m/s. The second reference's initial position and velocity are set to already be satisfying the constraints with $\mathbf{r}_{r2}(0) = [400, 50, 0]^T$ m and $\dot{\mathbf{r}}_{r2}(0) = [0, 0, 0.05]^T$ m/s.
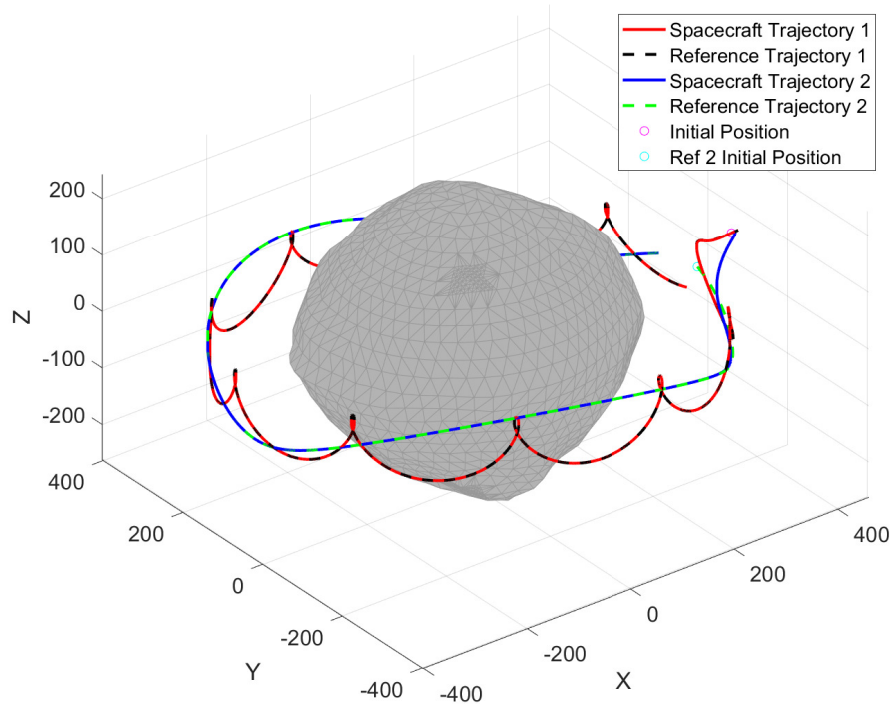
Figure 4.16 Under constrained spacecraft trajectory in the ACI frame using the adaptive control law in Equation (4.11).

The above initial conditions are applied to the spacecraft and it is simulated about the asteroid of Bennu. Figures 4.16 and 4.17 show the trajectories of the under constrained spacecraft in both the ACI and ACAF frames, respectively. Both figures show the trajectories of the spacecraft with the two different initial conditions for the reference system. In the first trajectory, the reference starts at the same position as the spacecraft, and thus it converges to the constraints via Baumgarte's stabilization method and keeps with the trajectory. The second trajectory starts with the reference already satisfying the constraints, so the spacecraft tracks that trajectory, which is different than if UK solutions were applied to the spacecraft. Despite the fact that the references and trajectories are different the controller causes both of them to satisfy the constraints despite having unknowns in the dynamics. Figure 4.18 shows the position components for each trajectory and reference over time. This figure, along with Figure 4.16, show
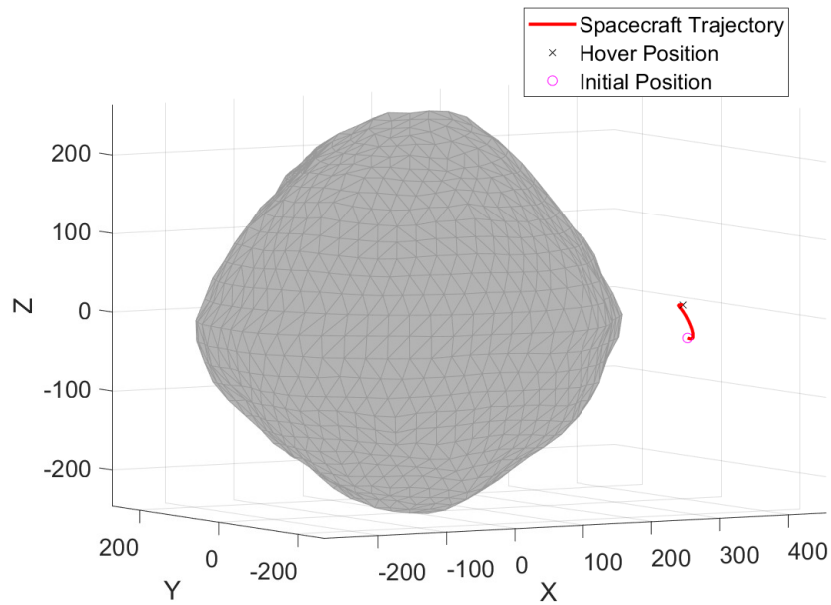
Figure 4.17 Under constrained spacecraft trajectory in the ACAF frame using the adaptive control law in Equation (4.11).
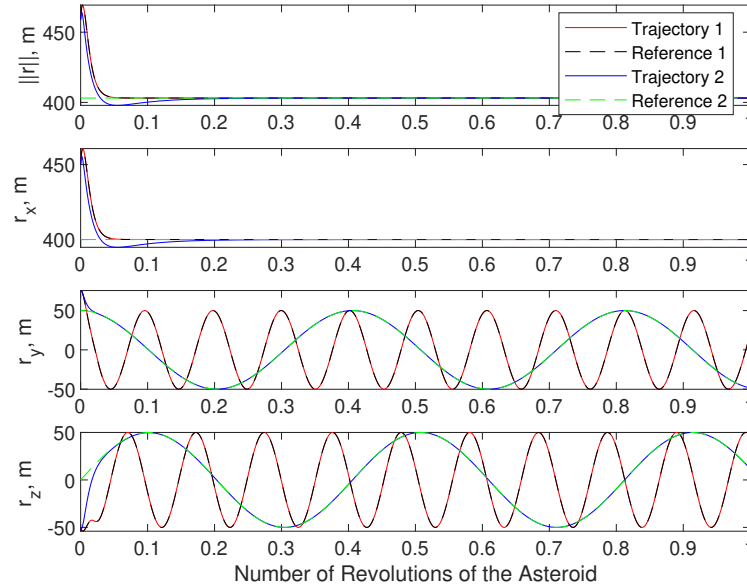
Figure 4.18 Under constrained spacecraft position components plotted over one revolution of the asteroid.
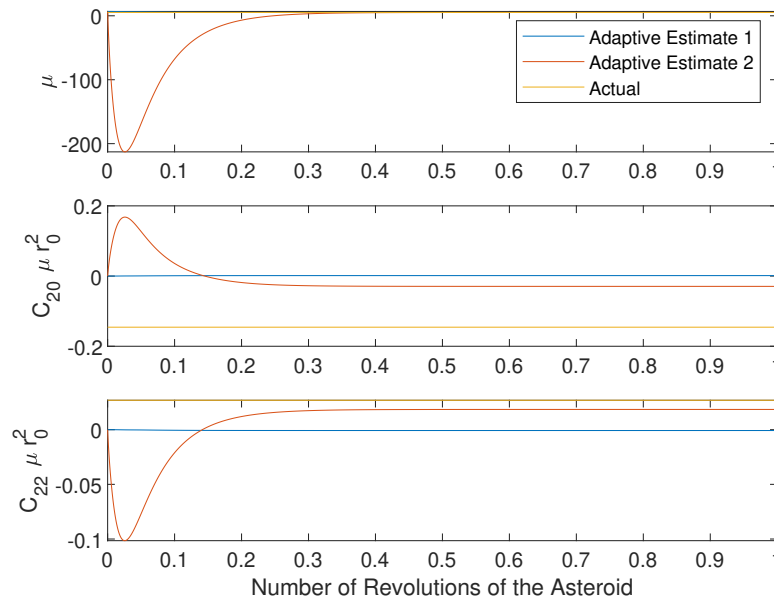
Figure 4.19 The adaptive estimates of the unknown parameters plotted over time.
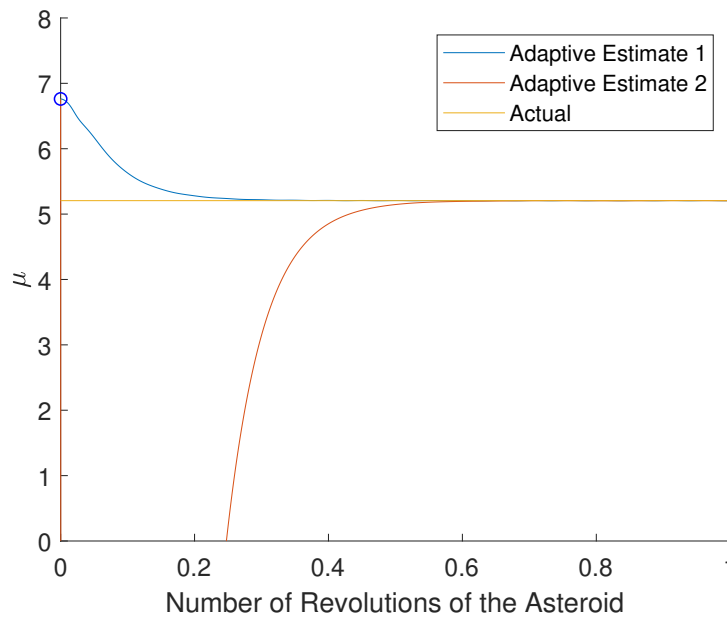
Figure 4.20 Magnified figure of the first adaptive estimate of the unknown parameters plotted over time.

the difference between the trajectories, even though they are satisfying the same constraints.

The adaptive parameters can be seen in Figures 4.19 and 4.20. Only the first
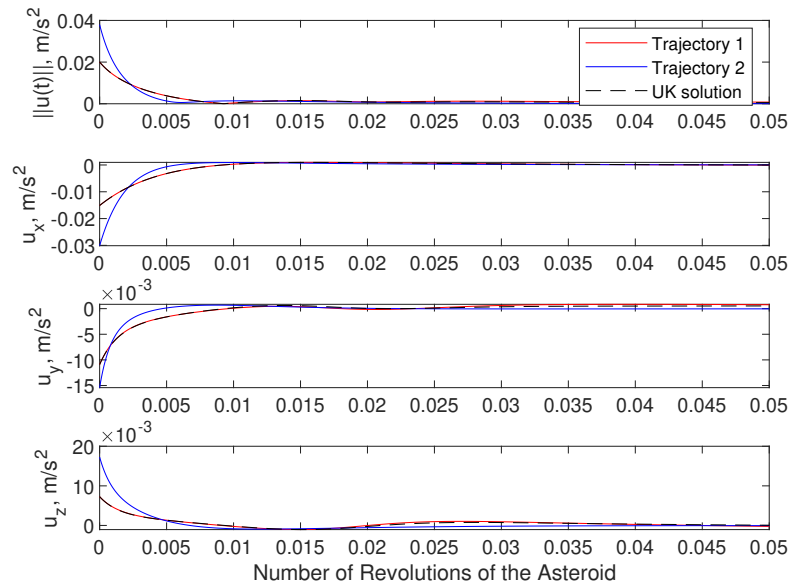
Figure 4.21 The transient control accelerations of the adaptive controller applied to the under constrained hover trajectory compared to the solution obtained by the UK equation.

adaptive parameter converges through the natural closed-loop dynamics. The other estimates do not converge to the actual unknown values. In the first trajectory, since the error between the system and its reference starts out as zero, the adaptive estimates propogate more slowly, avoiding the large jump and it converges to the actual value of the μ for Bennu. The second trajectory has an initial error between the system and the reference which causes the larger jump in the adaptation, but still converges to the actual value. The other adaptive estimates of the unknowns do not converge as expected.

Even though they satisfy the constraints, the solutions given by the controller do not exactly match that given by the UK equation. This is shown in Figures 4.21 and 4.22, which demonstrate the transient and steady state control accelerations, respectively. The solution given by the UK equations with the correct parameters is also shown in the figures as a comparison. The first trajectory's control matches the UK equation initially, but ends up drifting due to the unknowns, whereas the second trajectory's control is different from the beginning and throughout.
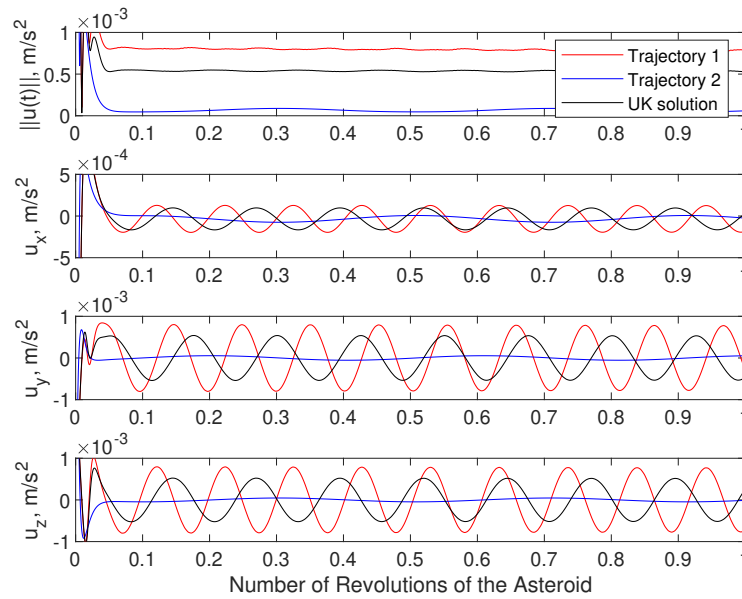
Figure 4.22   The steady state control accelerations of the adaptive controller applied to the under constrained hover trajectory compared to the solution obtained by the UK equation.
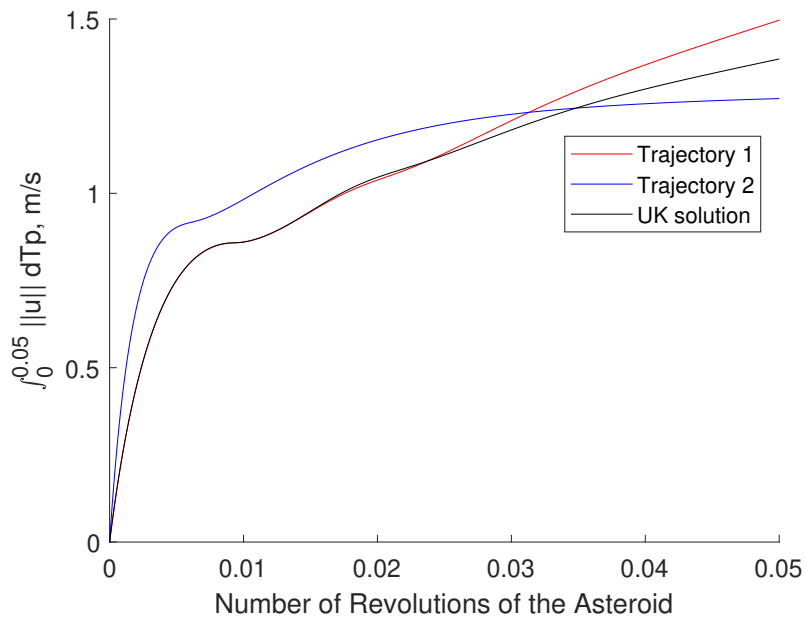
Figure 4.23   The transient integrated control effort required by the controller and the UK equation applied to the under constrained hover trajectory.

This happens because the second reference is already satisfying the constraints, it

continues to satisfy them in the same way, and thus the second trajectory tracks
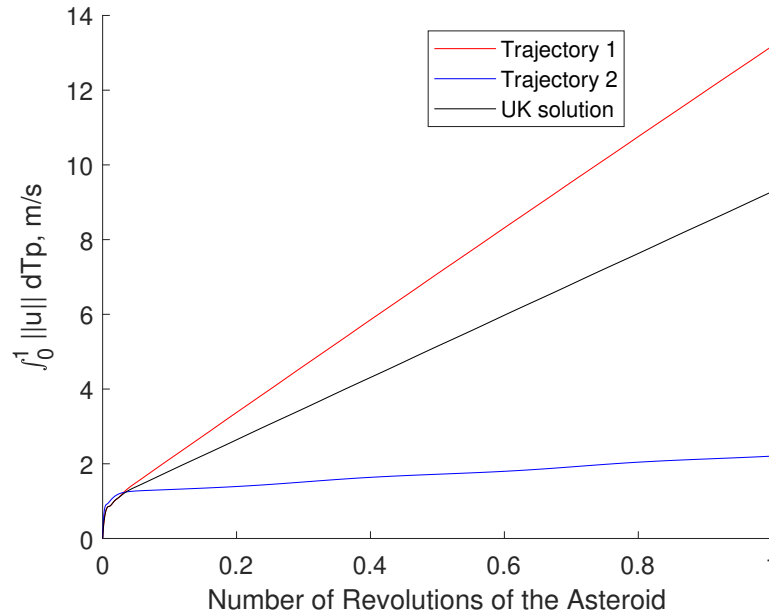
Figure 4.24 The steady state integrated control effort required by the controller and the UK equation applied to the under constrained hover trajectory.

that different solution of the constraints. Since the first adaptive estimate, which accounts for the largest portion of the gravitational force from the asteroid is obtained the control accelerations of the controllers at the end are only slightly different from the solutions obtained by the UK equation given the same positions and velocities. Note that the acceleration solutions given by the UK shown are those as if the UK solution was used from the initial conditions.

Figures 4.23 and 4.24 show the total integrated control effort of each trajectory and the UK solution over the revolution of the asteroid. The first trajectory control effort matches the UK solution initially, but has a slightly steeper slope and increases more quickly. The second trajectory has a greater transient required control effort as shown in Figure 4.23, but in Figure 4.24, the second trajectory requires much less control than the first trajectory of the UK solution. This is because that trajectory was chosen through the initial conditions of the second reference system. Although the system is under constrained, the end trajectory can be chosen through the reference trajectory because the controller asymptotically tracks the reference system.

4.6. Conclusions

In this chapter, the results of the UK constrained motion formalism have been implemented to control a spacecraft to hover over an asteroid with unknown gravitational parameters, μ, C_{20}, and C_{22}. Since the UK equations of constrained motion require for the exact dynamics to be known, indirect adaptive techniques have been applied to create adaptive estimates of the unknown parameters to use inside of the UK equations. This led to the design of an indirect model reference adaptive UK controller. The challenge then became accurate estimation of the unknown parameters of the asteroid, since the UK equations provide optimal solutions only when the correct dynamics are used. Using the natural dynamics of a spacecraft about an asteroid, along with a finite-time parameter estimation method, the gravitational parameters of the asteroid were able to be correctly estimated. Thus, the UK method was able to be successfully utilized for a system with unknowns in the dynamics.

Correct parameter estimation only increases the efficiency of the controller and is independent of the controller's ability to track a reference. Even without correct parameter estimation, the controller has been proven to asymptotically track a desired reference trajectory. If none of the adaptive estimates converge to the true values, this controller still achieves the desired hovering result with not much more control effort required than those obtained using the UK equations. Once the parameters are correctly estimated, the adaptive controller gains insight about the mass and shape of the asteroid, and the accelerations needed to achieve and maintain the desired hover are obtained through the use of the UK constrained motion analysis. Thus, the controller designed via the UK formulation was able to successfully maintain constraints in a fully constrained and an under constrained system with unknowns in the dynamics.

5. Rigid-Body Spacecraft Asteroid Hovering in Geometric Mechanics Framework

As opposed to the previous chapters where the spacecraft was considered as a point mass, in this chapter, it is considered as a rigid body with an orientation in addition to the position of its center of mass. Since the translational and rotational dynamics are often coupled through directional input and/or the external forces and torques, it is advantageous to consider the coupling between their dynamics using the geometric mechanics framework. Furthermore, geometric mechanics uses rotation matrices for orientation, which avoids the singularities, discontinuities, and non-uniqueness of the other attitude parameterization sets. The UK formulation discussed in Section 2.1.1 is extended for rigid body constrained motion in the geometric mechanics framework.

5.1. Geometric Mechanics Formulation Development

In the geometric mechanics framework, the configuration (orientation and position) of a rigid body is expressed in Special Euclidean group $\mathsf{SE}(3) = \mathsf{SO}(3) \times \mathbb{R}^3$, where $\mathsf{SO}(3)$ is special orthogonal group. The Lie group of $\mathsf{SE}(3)$, similar to $\mathsf{SO}(3)$, is a group in multiplication, but not in addition, i.e. for $g_1, g_2 \in \mathsf{SE}(3)$, $(g_1 g_2) \in \mathsf{SE}(3)$ and $g_1^{-1} \in \mathsf{SE}(3)$, $g_1 g_1^{-1} = I_4$, but $(g_1 + g_2) \notin \mathsf{SE}(3)$. The orientation and position of a rigid body is described by,

$$g = \begin{bmatrix} R & \mathbf{r} \\ \mathbf{0}_{1\times 3} & 1 \end{bmatrix} \in \mathsf{SE}(3) \tag{5.1a}$$

where $R \in \mathsf{SO}(3)$ is the rotation matrix from the body frame of the rigid body to the inertial frame, and $\mathbf{r} \in \mathbb{R}^3$ is the position of the rigid body's center of mass relative to and expressed in the inertial frame. The rigid body's augmented velocity vector is,

$$\mathbb{V} = \begin{bmatrix} \boldsymbol{\omega} \\ \mathbf{v} \end{bmatrix} \in \mathbb{R}^6 \tag{5.1b}$$

where $\boldsymbol{\omega} \in \mathbb{R}^3$ is the angular velocity and $\mathbf{v} \in \mathbb{R}^3$ is the translational velocity of the center of mass, both relative to the inertial frame, but expressed in the body frame of the rigid body. Thus a rigid-body spacecraft can be compactly defined in space by its orientation and position through g and its velocities in $\mathbb{V}$. This state space with state variables $(g, \mathbb{V})$ is the tangent bundle $\mathsf{TSE}(3) = \mathsf{SE}(3) \times \mathbb{R}^6$ (Lang, 1999; Sastry, 1999).

Before discussing the dynamics of $\mathsf{TSE}(3)$, some mappings are discussed. The wedge map $\mathbb{V}^\vee : \mathbb{R}^6 \to \mathfrak{se}(3)$, where $\mathfrak{se}(3)$ is the Lie algebra of the Lie group $\mathsf{SE}(3)$, is defined as,

$$\mathbb{V}^\vee = \begin{bmatrix} \omega^\times & \mathbf{v} \\ \mathbf{0}_{1\times 3} & 0 \end{bmatrix} \tag{5.2}$$

The unwedge map is the inverse of the wedge map such that $(\cdot)^\lvert : \mathfrak{se}(3) \to \mathbb{R}^6$. The adjoint action map $\mathrm{Ad}_g : \mathsf{SE}(3) \to \mathbb{R}^{6\times 6}$ is defined as,

$$\mathrm{Ad}_g = \begin{bmatrix} R & 0_{3\times 3} \\ r^\times R & R \end{bmatrix} \tag{5.3}$$

The adjoint operator $\mathrm{ad}_{\mathbb{V}} : \mathbb{R}^6 \to \mathbb{R}^{6\times 6}$ is defined as,

$$\mathrm{ad}_{\mathbb{V}} = \begin{bmatrix} \omega^\times & 0_{3\times 3} \\ v^\times & \omega^\times \end{bmatrix} \tag{5.4}$$

The co-adjoint operator $\mathrm{ad}_{\mathbb{V}}^* : \mathbb{R}^6 \to \mathbb{R}^{6\times 6}$ is defined as,

$$\mathrm{ad}_{\mathbb{V}}^* = \mathrm{ad}_{\mathbb{V}}^T = \begin{bmatrix} -\omega^\times & -v^\times \\ 0_{3\times 3} & -\omega^\times \end{bmatrix} \tag{5.5}$$

The dynamics of a rigid body in $\mathsf{SE}(3)$ are described by the kinematic and kinetic equations of motion (Bullo & Murray, 1995; Nazari et al., 2018):

$$\dot{g} = g\mathbb{V}^\vee \tag{5.6a}$$

$$\dot{\mathbb{V}} = \mathbb{I}^{-1}\mathrm{ad}_{\mathbb{V}}^* \mathbb{I}\mathbb{V} + \mathbb{I}^{-1}\boldsymbol{\tau} + \mathbb{I}^{-1}\mathbf{u} \tag{5.6b}$$

where $\mathbb{I}$ is inertia tensor of the rigid body given by,

$$\mathbb{I} = \begin{bmatrix} J & 0_{3\times3} \\ 0_{3\times3} & m_b I_3 \end{bmatrix} \tag{5.7}$$

where $J \in \mathbb{R}^{3\times3}$ is the moment of inertia matrix, m_b is the mass of the rigid body, $\boldsymbol{\tau} \in \mathbb{R}^6$ is the external torques and forces applied on the rigid body expressed in its body frame, and $\mathbf{u} \in \mathbb{R}^6$ is the control input torques and forces also expressed in the body frame of the rigid body.

5.2. Dynamics of a Rigid-Body Spacecraft Hovering About an Asteroid

As can be seen from Section 5.1, the spacecraft body (SCB) frame is added to the set of coordinate frames previously established when the spacecraft was considered a point mass. The SCB frame is oriented along the principle axes of the spacecraft, with the x, y, and z axes being the major, intermediate, and minor axes, respectively. The orientation of the SCB frame relative to the ACI frame is expressed by the rotation matrix R. In this chapter, the position vector of the spacecraft $\mathbf{r}$ is expressed in the ACI frame, instead of the ACAF frame, due to the definition in g in Equation (5.1a).

With the new dynamics defined by Equation (5.6), the external forces need to be defined. As opposed to the previous chapters where the spacecraft was considered a point mass, both external forces and torques need to be expressed in the SCB frame. The external forces and moments in Equation (5.6b) are expressed by,

$$\boldsymbol{\tau} = \begin{bmatrix} \mathbf{L}_G \\ \mathbf{F}_G \end{bmatrix} \tag{5.8}$$

where $\mathbf{L}_G \in \mathbb{R}^3$ is the external torques acting on the spacecraft and $\mathbf{F}_G \in \mathbb{R}^3$ is the external forces.

5.2.1. External Forces Acting on the Spacecraft

For the gravitational forces acting on the spacecraft, the asteroid is still modeled as a tri-axial ellipsoid as in Section 2.2.2. However, in addition, MacCullagh's approximation is used in lieu of spherical harmonics. Thus the gravitational potential of the rigid-body asteroid becomes (Schaub & Junkins, 2018):

$$U = \frac{\mu}{r} + \frac{\mu}{2m_{\mathcal{A}} r^3} \left[\text{tr}(J_{\mathcal{A}}) - 3 {}^{\mathcal{A}}\hat{\mathbf{r}}^T J_{\mathcal{A}} {}^{\mathcal{A}}\hat{\mathbf{r}} \right] \tag{5.9}$$

where $r = ||\mathbf{r}||$ is the magnitude of the position vector, $m_{\mathcal{A}}$ is the mass of the asteroid, $J_{\mathcal{A}} \in \mathbb{R}^{3\times3}$ is the moment of inertia of the asteroid expressed in the ACAF frame, and ${}^{\mathcal{A}}\hat{\mathbf{r}} = {}^{\mathcal{A}}\mathbf{r}/r$ is the unit vector of the spacecraft position expressed in the ACAF frame. The moment of inertia of the asteroid is,

$$J_{\mathcal{A}} = \frac{m_{\mathcal{A}} r_0^2}{5} \begin{bmatrix} \beta^2 + \gamma^2 & 0 & 0 \\ 0 & \alpha^2 + \gamma^2 & 0 \\ 0 & 0 & \alpha^2 + \beta^2 \end{bmatrix} \tag{5.10}$$

Let $R_{\mathcal{A}} \in \mathsf{SO}(3)$ be the rotation matrix from the ACAF frame to the ACI frame. Applying the relation ${}^{\mathcal{A}}\hat{\mathbf{r}} = R_{\mathcal{A}}^T \hat{\mathbf{r}}$ into Equation (5.9) and using Equation (2.29), the force applied to the spacecraft due to the gravitational field of the asteroid expressed in the SCB frame is obtained as,

$$\begin{aligned} \mathbf{F_G} &= m_b R^T \left(\nabla_{\mathbf{r}} U \right) \\ &= -\frac{\mu m_b}{r^3} R^T \left[I_3 + \frac{3}{m_{\mathcal{A}} r^2} \left(R_{\mathcal{A}} J_{\mathcal{A}} R_{\mathcal{A}}^T + \frac{1}{2} \left(\text{tr}(J_{\mathcal{A}}) - 5 \hat{\mathbf{r}}^T R_{\mathcal{A}} J_{\mathcal{A}} R_{\mathcal{A}}^T \hat{\mathbf{r}} \right) I_3 \right) \right] \mathbf{r} \end{aligned} \tag{5.11}$$

where m_b is the mass of the spacecraft. Note that the approximation of the gravity force in Equation (5.11) only accounts for the perturbations due to the rigid body properties of the asteroid and treats the spacecraft as a point mass. In this work, the errors due to this approximation are neglected.

5.2.2. External Torques Acting on the Spacecraft

In addition to the external forces acting on the spacecraft, there also exist external torques. The asteroid applies a gravity gradient torque on the spacecraft due to the spacecraft being a rigid body. The gravity gradient torque applied on the spacecraft and expressed in the SCB frame is (Schaub & Junkins, 2018):

$$\mathbf{L}_G = \frac{3\mu}{r^5}{}^{\mathcal{S}}r^{\times}J{}^{\mathcal{S}}\mathbf{r} \tag{5.12}$$

where ${}^{\mathcal{S}}\mathbf{r}$ is the position of the spacecraft expressed in the SCB frame and J is the principle moment of inertia matrix of the spacecraft. Substituting the relations ${}^{\mathcal{S}}\mathbf{r} = R^T\mathbf{r}$ and $\left(R^T\mathbf{r}\right)^{\times} = R^T r^{\times} R$ into Equation (5.12) gives,

$$\mathbf{L}_G = \frac{3\mu}{r^5}R^T r^{\times} R J R^T \mathbf{r} \tag{5.13}$$

Note that this approximation of the gravity gradient torque in Equation (5.13) assumes that the asteroid is a point mass and the errors due to this assumption are neglected.

5.3. Udwadia-Kalaba Formulation in Geometric Mechanics Framework

With the geometric mechanics framework modeled, the UK formulation discussed in Section 2.1.1 is extended from constrained particle motion to constrained rigid body motion. In this case, instead of having particles position vectors of $3n$ dimensions, there will be an attitude and position vector per rigid-body resulting in a g and V per rigid body in geometric mechanics. This results in $6n$ degrees of freedom. From Equation (5.6b) the equation of motion of the unconstrained system is,

$$\dot{\bar{\mathbb{V}}} = \bar{\mathbb{I}}^{-1}\mathrm{a}\bar{\mathrm{d}}_{\bar{\mathbb{V}}}^{*}\bar{\mathbb{I}}\bar{\mathbb{V}} + \bar{\mathbb{I}}^{-1}\bar{\boldsymbol{\tau}} = \bar{\mathbf{a}}$$

where the augmented velocity vector of the rigid bodies is,

$$
\bar{\mathbb{V}} = \begin{bmatrix} \mathbb{V}_1 \\ \mathbb{V}_2 \\ \vdots \\ \mathbb{V}_n \end{bmatrix} \in \mathbb{R}^{6n} \tag{5.14}
$$

and the extended inertia tensor matrix becomes,

$$
\bar{\bar{\mathbb{I}}} = \begin{bmatrix} \mathbb{I}_1 & 0_{6\times6} & \cdots & 0_{6\times6} \\ 0_{6\times6} & \mathbb{I}_2 & \ddots & \vdots \\ \vdots & \ddots & \ddots & 0_{6\times6} \\ 0_{6\times6} & \cdots & 0_{6\times6} & \mathbb{I}_n \end{bmatrix} \in \mathbb{R}^{6n\times6n} \tag{5.15}
$$

Both $\bar{\boldsymbol{\tau}}$ and $\bar{\mathrm{ad}}_{\mathbb{V}}^*$ follow the same as $\bar{\mathbb{V}}$ and $\bar{\bar{\mathbb{I}}}$ respectively so that the unconstrained accelerations of the system of rigid bodies is,

$$
\bar{\mathbf{a}} = \begin{bmatrix} \mathbb{I}_1^{-1}\mathrm{ad}_{\mathbb{V}_1}^*\mathbb{I}_1\mathbb{V}_1 + \mathbb{I}_1^{-1}\boldsymbol{\tau}_1 \\ \mathbb{I}_2^{-1}\mathrm{ad}_{\mathbb{V}_2}^*\mathbb{I}_2\mathbb{V}_2 + \mathbb{I}_2^{-1}\boldsymbol{\tau}_2 \\ \vdots \\ \mathbb{I}_n^{-1}\mathrm{ad}_{\mathbb{V}_n}^*\mathbb{I}_n\mathbb{V}_n + \mathbb{I}_n^{-1}\boldsymbol{\tau}_n \end{bmatrix} \tag{5.16}
$$

The orientation and the position of each rigid body is represented within their respective g matrices. Note that the dynamics on $\mathsf{SE}(3)$ do not change for each rigid body and remain as in Equation (5.6a). Thus when m constraints are applied to the system of rigid bodies, the equations of motion become,

$$
\dot{\bar{\mathbb{V}}} = \bar{\mathbf{a}} + \bar{\mathbf{a}}_c \tag{5.17}
$$

where $\bar{\mathbf{a}}_c$ is angular and translational constraint acceleration applied on the system. Note that the equation above mimics Equation (2.2) for a system of particles. Most equality constraints are applicable, except that they need to be linear in terms of $\dot{\bar{\mathbb{V}}}$. Hence, any consistent equality constraints of the form:

$$
\boldsymbol{\Phi}\left(g_1, g_2, \ldots, g_n, \mathbb{V}_1, \mathbb{V}_2, \ldots, \mathbb{V}_n, t\right) = \mathbf{0} \tag{5.18}
$$

can be expressed after differentiation with respect to time as,

$$A\dot{\bar{\mathbb{V}}} = \mathbf{b} \tag{5.19}$$

where $A \in \mathbb{R}^{m \times 6n}$ and $\mathbf{b} \in \mathbb{R}^m$ are the resulting matrix and vector from differentiation of the constraints. Thus identically to the system of particles, the geometric mechanics Udwadia-Kalaba (GMUK) equation is:

$$\mathbf{\mathfrak{a}}_c = \bar{\mathbb{I}}^{-1/2} \left(A\bar{\mathbb{I}}^{-1/2} \right)^+ (\mathbf{b} - A\mathbf{\mathfrak{a}}) \tag{5.20}$$

Since Equation (5.20) mimics the original UK equation given by Equation (2.5), so it can be shown to similarly minimize the Gaussian, guaranteeing that Equation (5.20) gives the minimum accelerations required to satisfy the constraints set on n rigid-body spacecraft. Alternatively, the symmetric form of the GMUK equation given in Equation (5.20) is:

$$\mathbf{\mathfrak{a}}_c = \bar{\mathbb{I}}^{-1} A^T \left(A\bar{\mathbb{I}}^{-1} A^T \right)^+ (\mathbf{b} - A\mathbf{\mathfrak{a}}) \tag{5.21}$$

Since the particles are now being considered as rigid bodies, the case where there is $n = 1$ rigid body does not reduce the UK equation as it did with particles.

5.4. Rigid-Body Spacecraft Asteroid Hovering Using the Geometric Mechanics UK Formulation

The extension above for the GMUK formulation can be applied for the case of a rigid body hovering over an asteroid. First, the constraints must be chosen. The desired position can be expressed by $\mathbf{r}_d = R_\mathcal{A}\mathbf{r}^*$, where $\mathbf{r}_d$ is the desired position expressed in the ACI frame and $\mathbf{r}^*$ is the desired hover position expressed in the ACAF frame as in the previous chapters. Now the desired orientation of the spacecraft needs to be set. The spacecraft attitude is constrained such that the x axis of the SCB frame points towards the center of the asteroid, its y axis is in the x-y plane of the ACAF frame, and its z axis is oriented appropriately to obey the right hand rule. Thus the desired rotation matrix from the SCB frame to the

ACAF frame is defined as,

$$R_{d/\mathcal{A}} = \begin{bmatrix} -\dfrac{R_{\mathcal{A}}^T \mathbf{r}}{r} & -\dfrac{A_z^\times R_{\mathcal{A}}^T \mathbf{r}}{\left(\mathbf{r}^T R_{\mathcal{A}} T_{xy} R_{\mathcal{A}}^T \mathbf{r}\right)^{1/2}} & \dfrac{R_{\mathcal{A}}^T r^\times R_{\mathcal{A}} A_z^\times R_{\mathcal{A}}^T \mathbf{r}}{r \left(\mathbf{r}^T R_{\mathcal{A}} T_{xy} R_{\mathcal{A}}^T \mathbf{r}\right)^{1/2}} \end{bmatrix} \qquad (5.22)$$

where $\mathbf{A}_z = [0,0,1]^T$ is the z axis of the ACAF frame, and,

$$T_{xy} = \begin{bmatrix} 1 & 0 & 0 \\ 0 & 1 & 0 \\ 0 & 0 & 0 \end{bmatrix}$$

With the desired position and orientation defined, the desired configuration relative to the ACAF frame in $\mathsf{SE}(3)$ can be defined by,

$$g_{d/\mathcal{A}} = \begin{bmatrix} R_{d/\mathcal{A}} & \mathbf{r}^* \\ \mathbf{0}_{1\times 3} & 1 \end{bmatrix} \qquad (5.23)$$

The equation above defines the desired configuration of the spacecraft relative to the ACAF frame. So the desired configuration relative to the ACI frame is obtained by,

$$g_d = \begin{bmatrix} R_{\mathcal{A}} R_{d/\mathcal{A}} & \mathbf{r}_d \\ \mathbf{0}_{1\times 3} & 1 \end{bmatrix} \qquad (5.24)$$

Then the desired augmented velocity vector can be obtained from the desired configuration given in Equation (5.24). Relative to the ACAF frame, the SCB frame should remain constant such that $\mathbb{V}_{d/\mathcal{A}} = \mathbf{0}_{6\times 1}$. The desired velocity relative to the ACI frame is obtained from,

$$\mathbb{V}_d = \mathbb{V}_{d/\mathcal{A}} + \mathrm{Ad}_{g_{d/\mathcal{A}}^{-1}} \mathbb{V}_{\mathcal{A}} \qquad (5.25)$$

where,

$$g_{d/\mathcal{A}}^{-1} = \begin{bmatrix} R_{d/\mathcal{A}}^T & -R_{d/\mathcal{A}}^T \mathbf{r}^* \\ \mathbf{0}_{1\times 3} & 1 \end{bmatrix}, \quad \mathbb{V}_{\mathcal{A}} = \begin{bmatrix} \mathbf{\Omega}(t) \\ \mathbf{0}_{3\times 1} \end{bmatrix}$$

The desired inertial velocity and the desired accelerations expressed in the desired reference frame are:

$$\mathbb{V}_d = \begin{bmatrix} R_{d/\mathcal{A}}^T \boldsymbol{\Omega}(t) \\ R_{d/\mathcal{A}}^T \Omega^\times(t)\mathbf{r}^* \end{bmatrix}, \quad \dot{\mathbb{V}}_d = \begin{bmatrix} R_{d/\mathcal{A}}^T \dot{\boldsymbol{\Omega}}(t) \\ R_{d/\mathcal{A}}^T \dot{\Omega}^\times(t)\mathbf{r}^* \end{bmatrix} \tag{5.26}$$

The constraints are defined in $\mathsf{SE}(3)$ for the spacecraft's configuration to match the desired configuration, i.e.,

$$g = g_d \tag{5.27a}$$

Using the Lie algebra, Equation (5.27a) can be converted into a vector equation since $g = \exp(\xi^\vee)$, where $\xi^\vee \in \mathfrak{se}(3)$ (Sastry, 1999). Pre-multiplying both sides of Equation (5.27a) by g_d^{-1}, taking the matrix logarithm, and using the unwedge mapping defined below Equation (5.2) results in,

$$\left[\log_{\mathsf{SE}(3)}\left(g_d^{-1}g\right)\right]^| = \mathbf{0}_{6\times 1} \tag{5.27b}$$

Since the constraints in Equation (5.27a) are holonomic constraints, they are differentiated with respect to time twice. The first derivative results in,

$$g\mathbb{V}^\vee = g_d\mathbb{V}_d^\vee \tag{5.28a}$$

Pre-multiplying both sides of Equation (5.28a) by g^{-1} and using the unwedge mapping gives the vector expression:

$$\mathbb{V} - \left(g^{-1}g_d\mathbb{V}_d^\vee\right)^| = \mathbf{0}_{6\times 1} \tag{5.28b}$$

Now, taking the derivative again yields,

$$g\mathbb{V}^{\vee 2} + g\dot{\mathbb{V}}^\vee = g_d\mathbb{V}_d^{\vee 2} + g_d\dot{\mathbb{V}}_d^\vee \tag{5.29}$$

Applying Baumgarte's constraint stabilization method and putting the equations

into the form of Equation (5.19) gives,

$$I_6\dot{\mathbb{V}} = \left[g^{-1}g_d\left(\mathbb{V}_d^{\vee 2} + \dot{\mathbb{V}}_d^\vee\right) - \mathbb{V}^{\vee 2}\right]^| - K_\alpha\left[\mathbb{V} - \left(g^{-1}g_d\mathbb{V}_d^\vee\right)^|\right]$$
$$- K_\beta\left[\log_{\mathsf{SE}(3)}\left(g_d^{-1}g\right)\right]^| \tag{5.30a}$$

where,

$$A = I_6 \tag{5.30b}$$

$$\mathbf{b} = \left[g^{-1}g_d\left(\mathbb{V}_d^{\vee 2} + \dot{\mathbb{V}}_d^\vee\right) - \mathbb{V}^{\vee 2}\right]^| - K_\alpha\left[\mathbb{V} - \left(g^{-1}g_d\mathbb{V}_d^\vee\right)^|\right]$$
$$- K_\beta\left[\log_{\mathsf{SE}(3)}\left(g_d^{-1}g\right)\right]^| \tag{5.30c}$$

Since the position and orientation of the spacecraft are explicitly defined in Equation (5.27a), $A = I_6$, similar to the case where the spacecraft was modeled as a point mass in Equation (3.3a). Applying this to the GMUK equation given by Equation (5.21) yields the simple result of,

$$\mathfrak{a}_c = \mathbf{b} - \mathfrak{a} \tag{5.31}$$

This equation gives the translational and rotational accelerations required to converge to and maintain the desired configuration of the spacecraft.

5.5. Numerical Simulation Results and Discussions

The GMUK formulation developed above is applied for a rigid-body spacecraft to hover over the asteroid of Bennu. As in the previous chapters, Bennu has a gravitational parameter of $\mu = 5.2\,\mathrm{m^3/s^2}$, a mass of $m_\mathcal{A} = 7.8 \times 10^{10}$ kg, and a density of $\rho = 1.26\,\mathrm{g/cm^3}$ (Chesley et al., 2014). Bennu was determined to have major axes of $L_1 = 565$ m, $L_2 = 535$ m, and $L_3 = 508$ m, leading to $\beta = 0.9469$ and $\gamma = 0.8991$ (Nolan et al., 2013). The moment of inertia matrix can be found using Equation (5.10) and is $J_A = \mathrm{diag}([2.1227, 2.2514, 2.3613]) \times 10^{15}$ kg m^2. Bennu has an equatorial inclination of 175 degrees with a rotation period of 4.297 hours and rotates about the z axis of the ACAF frame.
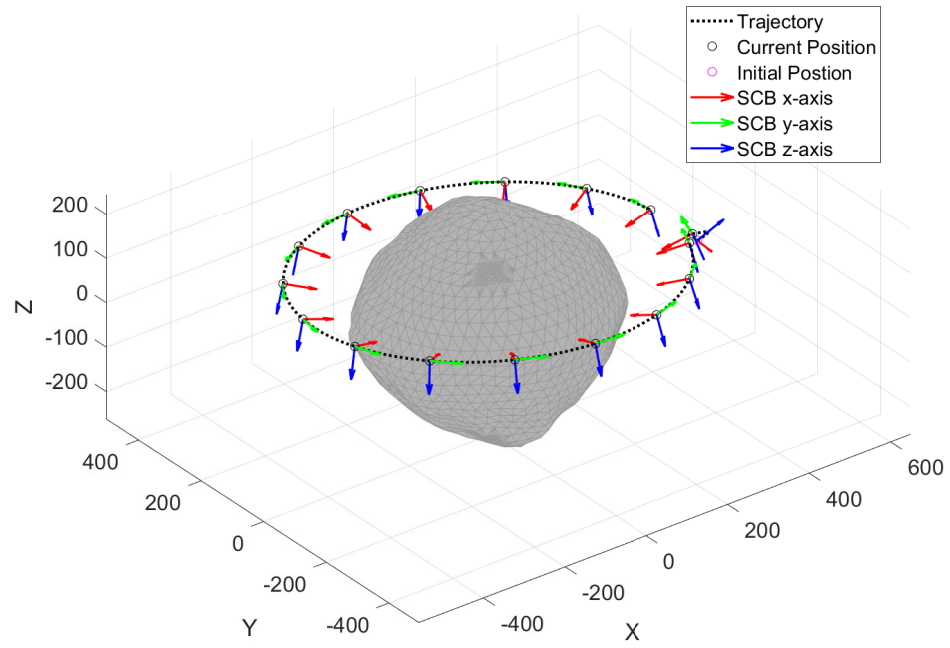
Figure 5.1   Spacecraft trajectory in the ACI frame.
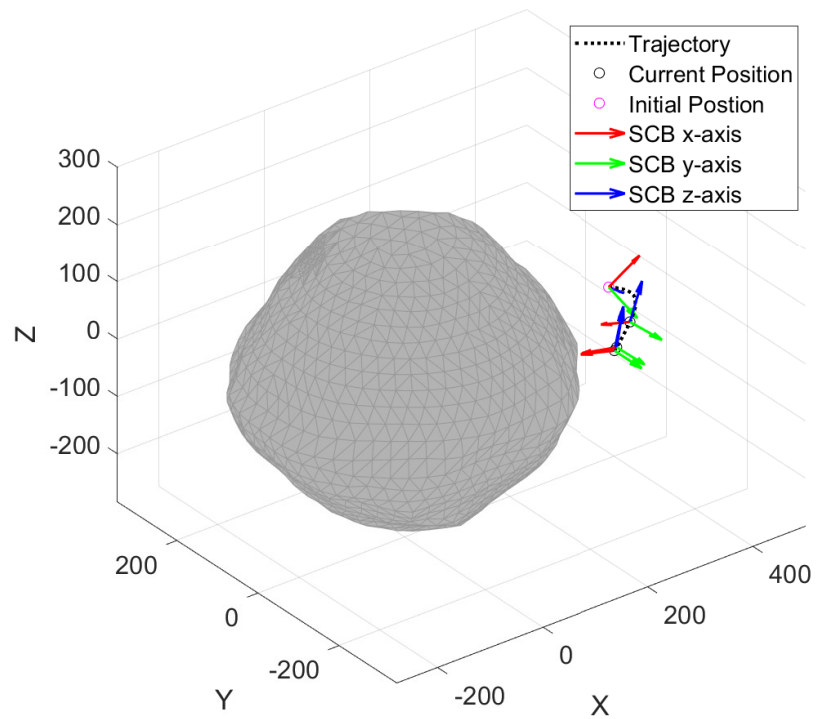
Figure 5.2   Spacecraft trajectory in the ACAF frame.
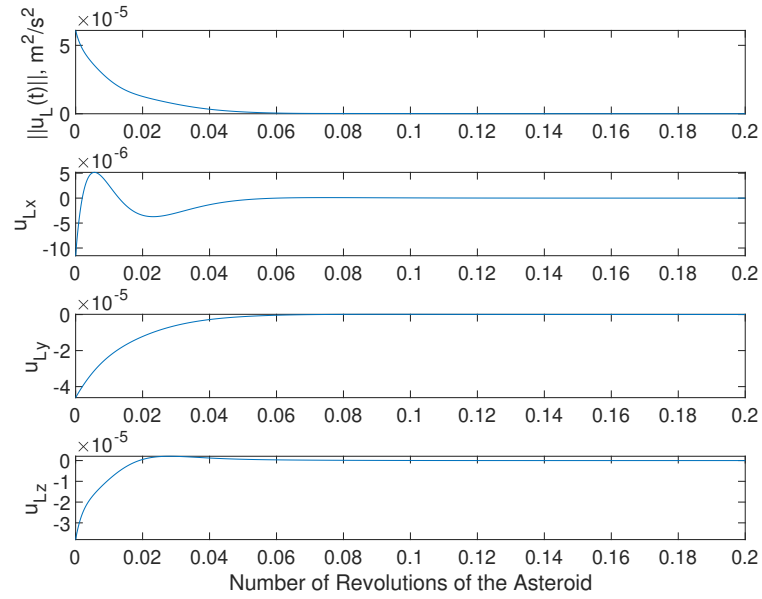
Figure 5.3 The angular acceleration control inputs required for achieving and maintaining the desired orientation.
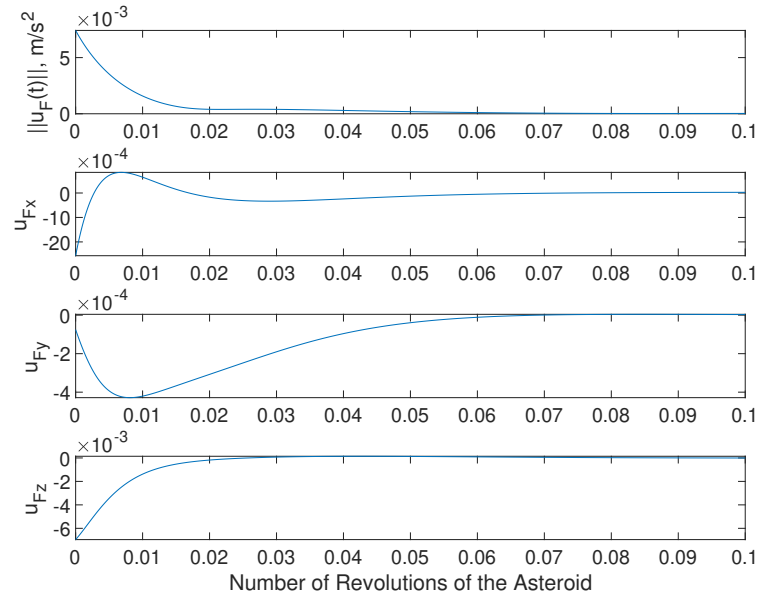
Figure 5.4 The transient translational control accelerations obtained by the GMUK equation.

The rigid-body spacecraft is given a mass $m = 250$ kg, with the moment of inertia given as $J = \text{diag}([175, 100, 75])$ kg m^2. The desired hover position expressed in the ACAF frame is set as $\mathbf{r}^* = [400, 0, 100]^T$ m, with the orientation given by Equation (5.22). The initial position and velocity of the spacecraft are set as
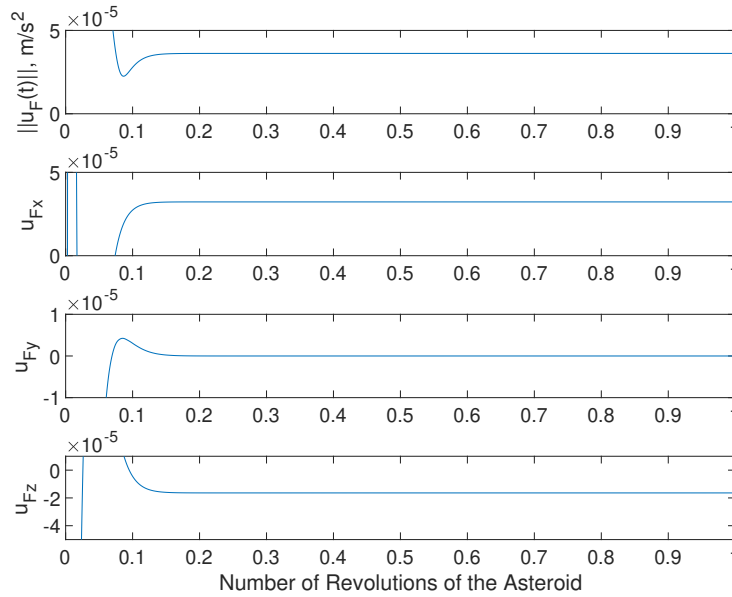
Figure 5.5   The steady state translational control accelerations obtained by the GMUK equation.

$\mathbf{r}(0) = [450, -75, 50]^T$ m and $\mathbf{v}(0) = [0.1818, 0.0366, 0.5154]^T$ m/s. The initial orientation of the spacecraft is set as a 3-2-1 sequence rotation matrix with angles of $\theta_3 = 0.2618$ rad, $\theta_2 = 0.7854$ rad, and $\theta_1 = 0.5236$ rad respectively. The initial angular velocity of the spacecraft is given as $\boldsymbol{\omega}(0) = [0.0990, 0.9901, 0.0990]^T \times 10^{-3}$ rad/s. The matrices for Baumgarte's constraint stabilization method are set to be critically damped with $K_\alpha = 0.01 I_6$ and $K_\beta = K_\alpha^2/4 = 0.25 \times 10^{-4} I_6$.

Applying the GMUK formulation to the spacecraft results in the spacecraft hovering over the asteroid with the desired orientation. Figure 5.1 shows the spacecraft trajectory and orientations in the ACI frame, while Figure 5.2 shows the trajectory in the ACAF frame. As shown in both figures, the spacecraft begins with the initial conditions specified above, but converges to the correct position and orientation, then maintains the desired state relative to the asteroid. Figure 5.3 shows the angular control accelerations expressed in the SCB frame. Since the position vector of the spacecraft is oriented along one of the principal axes of the spacecraft, the gravity gradient torque reduces to zero, so the required torque to maintain the orientation is zero. Figures 5.4 and 5.5 show the transient and steady

state control accelerations, respectively, required to maintain the hover. The control is initially high to account for the initial conditions, but drops down to a constant value to maintain the hovering position. The results of this numerical simulation show that the UK constrained motion equations have been successfully applied in the geometric mechanics framework for a spacecraft hovering over the surface of the asteroid with a desired orientation.

5.6. Conclusions

The current Udwadia-Kalaba formulation is a simple and powerful tool. The extension of the UK formulation into the geometric mechanics framework allows the UK method to be used for constrained motion analysis of rigid bodies more easily as well as accounting for any coupling between the translational and rotational dynamics. The Geometric Mechanics Udwadia-Kalaba equations developed in this chapter are a successful implementation of the UK formulation into the geometric mechanics framework. However, there is still more testing that needs to be done in order to extend this formulation to allow any quantity and/or types of constraints. This chapter only simulated the fully constrained case hovering of a rigid body. This new formulation would be useful in all cases of constrained motion analysis. Despite the single use displayed here, the application of this formulation goes well beyond that of asteroid hovering, opening pathways for more optimal rigid-body controllers in the future.

6. Conclusions and Future Work

Throughout this thesis, the constrained motion of a spacecraft about an asteroid was studied. The Udwadia-Kalaba (UK) formulation was introduced to analyze the constrained motion of a spacecraft over an asteroid. The first objective was completed by applying the UK formulation to constrain the spacecraft to hover over the asteroid, in both the fully constrained and under constrained cases. The UK formulation provided the explicit solutions to both cases, allowing minimum control input for maintaining the constraints.

The next objective was to develop an adaptive controller based on the UK equation in order to apply the UK formulation despite unknowns in the dynamics. The controller developed was proven to have asymptotic tracking of the constraints despite the unknowns. Without estimation of the unknowns the controller still provided close control responses to the minimum required. The controller paired with persistence of excitation and/or other parameter estimation methods guaranteed the minimum control input to maintain the desired constraints due to its basis in the UK fundamental equation.

The last objective was to extend the UK formulation for the use of rigid-body systems using geometric mechanics instead of particles. The geometric mechanics UK (GMUK) formulation was developed and applied for a fully constrained asteroid hovering case. The simulation proved the results successful. Although the extension to under constrained cases was not explored and simulated, the theory for it was provided through the generality of the extension.

Future research areas include; a) under constrained geometric mechanics UK constrained motion analysis application; b) extending the UK formulation to the case of inequality constraints; c) creating an adaptive controller for a rigid-body spacecraft based on the GMUK formulation; and d) implementation of the adaptive controller developed in this research to the case of space problems/missions other than asteroid hovering.

REFERENCES

Adetola, V., & Guay, M. (2008). Finite-time parameter estimation in adaptive control of nonlinear systems. *IEEE Transactions on Automatic Control, 53*(3), 807–811.

Baumgarte, J. (1972). Stabilization of constraints and integrals of motion in dynamical systems. *Computer Methods in Applied Mechanics and Engineering, 1*, 1–16.

Bullo, F., & Murray, R. M. (1995). *Proportional derivative (PD) control on the Euclidean Group* (tech. rep.). Pasadena, CA, California Institute of Technology.

Chesley, S. R., Farnocchia, D., Nolan, M. C., Vokrouhlicky, D., Chodas, P. W., Milani, A., Spoto, F., Rozitis, B., Benner, L. A. M., Bottke, W. F., Busch, M. W., Emery, J. P., Howell, E. S., Lauretta, D., Margot, J. L., & Taylor, P. A. (2014). Orbit and bulk density of the OSIRIS-REx target asteroid (101955) Bennu. *Icarus, 235*, 5–22.

Cho, H., & Udwadia, F. E. (2010). Explicit solution to the full nonlinear problem for satellite formation-keeping. *Acta Astronautica, 67*, 369–387.

Furfaro, R. (2015). Hovering in asteroid dynamical environments using higher-order sliding control. *Journal of Guidance, Control, and Dynamics, 38*(2), 263–279.

Gui, H., & de Ruiter, A. H. J. (2017). Control of asteroid-hovering spacecraft with disturbance rejection using position-only measurements. *Journal of Guidance, Control, and Dynamics, 40*(10), 2401–2416.

Kaufman, H., Barkana, I., & Sobel, K. (1998). *Direct Adaptive Control Algorithms: Theory and Applications.* New York, Springer.

Kikuchi, S., Terui, F., Ogawa, N., Saiki, T., Ono, G., Yoshikawa, K., Takei, Y., Mimasu, Y., Ikeda, H., Sawada, H., Morota, T., Hirata, N., Hirata, N., Kouyama, T., Kameda, S., & Tsuda, Y. (2019). Design and reconstruction of the Hayabusa 2 precision landing on Ryugu [AAS 19-762]. *AAS/AIAA Astrodynamics Specialist Conference.* Portland, ME. August 11-15.

Lam, T. (2006). A new approach to mission design based on the fundamental equations of motion. *Journal of Aerospace Engineering, 19*(2), 59–67.

Lang, S. (1999). *Fundamentals of Differential Geometry.* New York, Springer.

Lauretta, D., Balram-Knutson, S., Beshore, E., Boynton, W., d'Aubigny, C. D., DellaGiustina, D., Enos, H., Golish, D., Hergenrother, C., Howell, E., Bennett, C., Morton, E., Nolan, M., Rizk, B., Roper, H., Bartels, A.,

Bos, B., Dworkin, J., Highsmith, D., ... Sandford, S. (2017). OSIRIS-REx: Sample return from asteroid (101955) Bennu. *Space Science Reviews*, *212*, 925–984.

Lee, D., & Vukovich, G. (2015). Adaptive sliding mode control for spacecraft body-fixed hovering in the proximity of an asteroid. *Aerospace Science and Technology*, *46*, 471–483.

Memon, M. W., Nazari, M., Seo, D., & Prazenica, R. (2019). Constrained motion analysis and nonlinear optimal tracking control of two-craft coulomb formation in elliptic chief orbits [AAS 19-706]. *AAS/AIAA Astrodynamics Specialist Conference.* Portland, ME. August 11-15.

Müller, A., & Terze, Z. (2014a). On the choice of configuration space for numerical lie group integration of constrained rigid body systems. *Journal of Computational and Applied Mathematics*, *262*, 3–13.

Müller, A., & Terze, Z. (2014b). The significance of the configuration space lie group for the constraint satisfaction in numerical time integration of multibody systems. *Mechanism and Machine Theory*, *82*, 173–202.

Nazari, M., Maadani, M., Butcher, E. A., & Yucelen, T. (2018). Morse-lyapunov-based control of rigid body motion on $\mathsf{TSE}(3)$ via backstepping. *AIAA Guidance, Navigation, and Control Conference.* Kissimmee, Florida. January 8-12.

Nazari, M., Wauson, R., Critz, T., Butcher, E. A., & Scheeres, D. J. (2014). Observer-based body frame hovering control over a tumbling asteroid. *Acta Astronautica*, *102*, 124–139.

Nguyen, N. T. (2018). *Model-Reference Adaptive Control: A Primer.* New York, Springer.

Nolan, M. C., Magri, C., Howell, E. S., Benner, L. A. M., Giorgini, J. D., Hergenrother, C. W., Hudson, R. S., Lauretta, D. S., Margot, J. L., Ostro, S. J., & Scheeres, D. J. (2013). Shape model and surface properties of the OSIRIS-REx target asteroid (101955) Bennu from radar and lightcurve observations. *Icarus*, *226*, 629–640.

Patel, H., Henderson, T. A., & Nazari, M. (2019). Application of Udwadia-Kalaba formulation to three-body problem [AAS 19-805]. *AAS/AIAA Astrodynamics Specialist Conference.* Portland, ME. August 11-15.

Sastry, S. (1999). *Nonlinear Systems: Analysis, Stability, and Control.* New York, Springer.

Schaub, H., & Junkins, J. L. (2018). *Analytical Mechanics of Space Systems* (4th ed.). Reston, VA, American Institute of Aeronautics; Astronautics, Inc.

Scheeres, D. J. (2012). *Orbital Motion in Strongly Perturbed Environments: Applications to Asteroid, Comet and Planetary Satellite Orbiters.* Berlin, Heidelberg, Springer.

Seo, D., & Nazari, M. (2019). Rigid body adaptive stabilization on the tangent bundle of the lie groups. *AIAA Guidance, Navigation, and Control Conference.* San Diego, CA. January 7-11.

Seo, D. (2015). Fast adaptive pose tracking control for satellites via dual quaternion upon non-certainty equivalence principle. *Acta Astronautica, 115*, 32–39.

Stackhouse, W., Nazari, M., Henderson, T., & Prazenica, R. (2020). Adaptive control design using the Udwadia-Kalaba formulation for hovering over an asteroid with unknown gravitational parameters. *AIAA Guidance, Navigation, and Control Conference.* Orlando, FL. January 6-10.

Stackhouse, W., Nazari, M., Henderson, T., & Yucelen, T. (2019). Spacecraft asteroid hovering using Udwadia-Kalaba formualation with time-varying coefficients [AAS 19-641]. *AAS/AIAA Astrodynamics Specialist Conference.* Portland, ME. August 11-15.

Tiwari, M., Prazenica, R. J., & Henderson, T. (2020). Tracking reference orbits around asteroids with unknown gravitational parameters using a nonlinear adaptive controller. *AIAA Guidance, Navigation, and Control Conference.* Orlando, FL. January 6-10.

Udwadia, F. E., & Kalaba, R. E. (1992). A new perspective on constrained motion. *Proceedings of the Royal Society of London. Series A: Mathematical and Physical Sciences, 439*, 407–410.

Udwadia, F. E., & Kalaba, R. E. (2008). *Analytical Dynamics: A New Approach.* New York, Cambridge University Press.

Udwadia, F. E., & Schutte, A. D. (2012). A unified approach to rigid body rotational dynamics and control. *Proceedings of the Royal Society A, 468*, 395–414.

Vukovich, G., & Gui, H. (2017). Robust adaptive tracking of rigid-body motion with applications to asteroid proximity operations. *IEEE Transactions on Aerospace and Electronic Systems, 53*(1), 419–430.

Wibben, D. R., Levine, A., Rieger, S., McAdams, J. V., Antreasian, P. G., Leonard, J. M., Moreau, M. C., & Lauretta, D. S. (2019). OSIRIS-REx frozen orbit design and flight experience [AAS 19-677]. *AAS/AIAA Astrodynamics Specialist Conference.* Portland, ME. August 11-15.

Zhang, B., Cai, Y., & Li, F. (2019). Adaptive double-saturated control for hovering over an asteroid. *Advances in Space Research, 63*(7), 2035–2051.

APPENDIX A.   Satisfaction of Gauss's Principle

In order to show that Equation (2.19) minimizes the Gaussian in Equation (2.18), it is first shown to satisfy the constraints. Equation (2.4) discussed in the main text:

$$A\ddot{\mathbf{q}} = \mathbf{b} \tag{2.4}$$

is assumed to be consistent and can be rewritten as (Udwadia & Kalaba, 2008),

$$\left(AM^{-1/2}\right) M^{1/2}\ddot{\mathbf{q}} = \mathbf{b} \tag{A.1}$$

Pre-multiplying both sides of Equation (A.1) by $\left(AM^{-1/2}\right) \left(AM^{-1/2}\right)^{+}$ results in,

$$\left(AM^{-1/2}\right) \left(AM^{-1/2}\right)^{+} \left(AM^{-1/2}\right) M^{1/2}\ddot{\mathbf{q}} = \left(AM^{-1/2}\right) \left(AM^{-1/2}\right)^{+} \mathbf{b} \tag{A.2}$$

Since $\left(AM^{-1/2}\right)^{+}$ is a MP inverse, it satisfies the first MP condition in Equation (2.7a),

$$\left(AM^{-1/2}\right) M^{1/2}\ddot{\mathbf{q}} = \left(AM^{-1/2}\right) \left(AM^{-1/2}\right)^{+} \mathbf{b} \tag{A.3}$$

The left hand side above matches the left hand side of Equation (A.1) so,

$$\mathbf{b} = \left(AM^{-1/2}\right) \left(AM^{-1/2}\right)^{+} \mathbf{b} \tag{A.4}$$

Therefore, if Equation (2.4) is consistent, then Equation (A.4) is true.

In the second part of the proof, it is shown that the resulting equations of motion in Equation (2.19) satisfy the constraint equations in Equation (2.4):

$$\begin{aligned} A\ddot{\mathbf{q}} &= A\mathbf{a} + AM^{-1/2} \left(AM^{-1/2}\right)^{+} (\mathbf{b} - A\mathbf{a}) \\ &= \left[I - AM^{-1/2} \left(AM^{-1/2}\right)^{+}\right] A\mathbf{a} + AM^{-1/2} \left(AM^{-1/2}\right)^{+} \mathbf{b} \end{aligned} \tag{A.5}$$

The second term on the right hand side of the equation above can be simplified

using Equation (A.4) since the constraints are consistent:

$$
\begin{aligned}
A\ddot{\mathbf{q}} &= \left[I - AM^{-1/2}\left(AM^{-1/2}\right)^{+}\right]AM^{-1/2}M^{1/2}\mathbf{a} + \mathbf{b} \\
&= \left[AM^{-1/2} - AM^{-1/2}\left(AM^{-1/2}\right)^{+}AM^{-1/2}\right]M^{1/2}\mathbf{a} + \mathbf{b} \\
&= \mathbf{b} \tag{A.6}
\end{aligned}
$$

where the first term on the right hand side of the above equation is eliminated due to the first MP condition in Equation (2.7a). Thus the resulting accelerations given by the UK equation in Equation (2.19) satisfies Equation (2.4).

Lastly, assume that there is another solution $\ddot{\mathbf{y}}$ that satisfies the constraints and represents the resulting accelerations of the system. This solution can be written $\ddot{\mathbf{y}} = \ddot{\mathbf{q}} + \mathbf{z}$, where $\mathbf{z}$ is the difference between $\ddot{\mathbf{y}}$ and $\ddot{\mathbf{q}}$ obtained by the UK equation. This solution must satisfy the constraints so,

$$
A\ddot{\mathbf{y}} = \mathbf{b} \tag{A.7}
$$

$$
A\ddot{\mathbf{q}} + A\mathbf{z} = \mathbf{b} \tag{A.8}
$$

Since $\ddot{\mathbf{q}}$ satisfies the constraints, the first term on the left hand side can be replaced by the results of Equation (A.6) giving,

$$
\mathbf{b} + A\mathbf{z} = \mathbf{b} \tag{A.9}
$$

$$
A\mathbf{z} = \mathbf{0} \tag{A.10}
$$

Pre-multiplying and post-multiplying by A^{+} and $\mathbf{z}^{+}$ respectively,

$$
A^{+}A\mathbf{z}\mathbf{z}^{+} = \mathbf{0} \tag{A.11}
$$

$$
\left(A^{+}A\mathbf{z}\mathbf{z}^{+}\right)^{T} = \mathbf{0}^{T} \tag{A.12}
$$

$$
\mathbf{z}\mathbf{z}^{+}A^{+}A = \mathbf{0}^{T} \tag{A.13}
$$

The third and fourth MP conditions in Equations (2.7c) and (2.7d) are used to obtain the last equation. Pre-multiplying and post-multiplying by $\mathbf{z}^{+}$ and A^{+} respectively and using the second MP condition given in Equation (2.7b), results

in,

$$\mathbf{z}^+\mathbf{z}\mathbf{z}^+A^+AA^+ = \mathbf{0}^T \tag{A.14}$$

$$\mathbf{z}^+A^+ = \mathbf{0}^T \tag{A.15}$$

$$\mathbf{z}^TA^+ = \mathbf{0}^T \tag{A.16}$$

The last result follows since for an $n \times 1$ vector $\mathbf{z}$, $\mathbf{z}^+ = 1/(\mathbf{z}^T\mathbf{z})\,\mathbf{z}^T$. Therefore if Equation (A.10) is expressed as,

$$\left(AM^{-1/2}\right)\left(M^{1/2}\mathbf{z}\right) = \mathbf{0} \tag{A.17}$$

then the result from Equation (A.16) becomes,

$$\left(M^{1/2}\mathbf{z}\right)^T\left(AM^{-1/2}\right)^+ = \mathbf{0} \tag{A.18}$$

This last expression is true if $\ddot{\mathbf{y}}$ is a solution to the constraints in Equation (2.4).

The Gaussian of the solution $\ddot{\mathbf{y}}$ becomes,

$$G(\ddot{\mathbf{y}}) = \left[M^{1/2}\left(\ddot{\mathbf{q}}+\mathbf{z}\right) - M^{1/2}\mathbf{a}\right]^T\left[M^{1/2}\left(\ddot{\mathbf{q}}+\mathbf{z}\right) - M^{1/2}\mathbf{a}\right] \tag{A.19}$$

$$= \left[\left(AM^{-1/2}\right)^+(\mathbf{b}-A\mathbf{a}) + M^{1/2}\mathbf{z}\right]^T\left[\left(AM^{-1/2}\right)^+(\mathbf{b}-A\mathbf{a}) + M^{1/2}\mathbf{z}\right] \tag{A.20}$$

$$= \left[\left(AM^{-1/2}\right)^+(\mathbf{b}-A\mathbf{a})\right]^T\left[\left(AM^{-1/2}\right)^+(\mathbf{b}-A\mathbf{a})\right]$$

$$+ \left[\left(AM^{-1/2}\right)^+(\mathbf{b}-A\mathbf{a})\right]^T\left(M^{1/2}\mathbf{z}\right) + \left(M^{1/2}\mathbf{z}\right)^T\left(AM^{-1/2}\right)^+(\mathbf{b}-A\mathbf{a})$$

$$+ \left(M^{1/2}\mathbf{z}\right)^T\left(M^{1/2}\mathbf{z}\right) \tag{A.21}$$

Equation (A.18) eliminates the third term, and since the second and third terms are the transpose of each other, the second is also elminated. This yields,

$$G(\ddot{\mathbf{y}}) = \left[\left(AM^{-1/2}\right)^+(\mathbf{b}-A\mathbf{a})\right]^T\left[\left(AM^{-1/2}\right)^+(\mathbf{b}-A\mathbf{a})\right]$$

$$+ \left(M^{1/2}\mathbf{z}\right)^T\left(M^{1/2}\mathbf{z}\right) \tag{A.22}$$

$$= G(\ddot{\mathbf{q}}) + \mathbf{z}^TM\mathbf{z} \tag{A.23}$$

$$\geq G(\ddot{\mathbf{q}}) \tag{A.24}$$

Therefore, $G(\ddot{\mathbf{y}}) > G(\ddot{\mathbf{q}})$ for all $\mathbf{z} \neq \mathbf{0}$. This shows that the solution $\ddot{\mathbf{y}}$ is only minimized when $\mathbf{z} = \mathbf{0}$ and $\ddot{\mathbf{y}} = \ddot{\mathbf{q}}$, meaning the solution provided by the UK equations minimizes the Gaussian from Gauss's principle of least constraint.